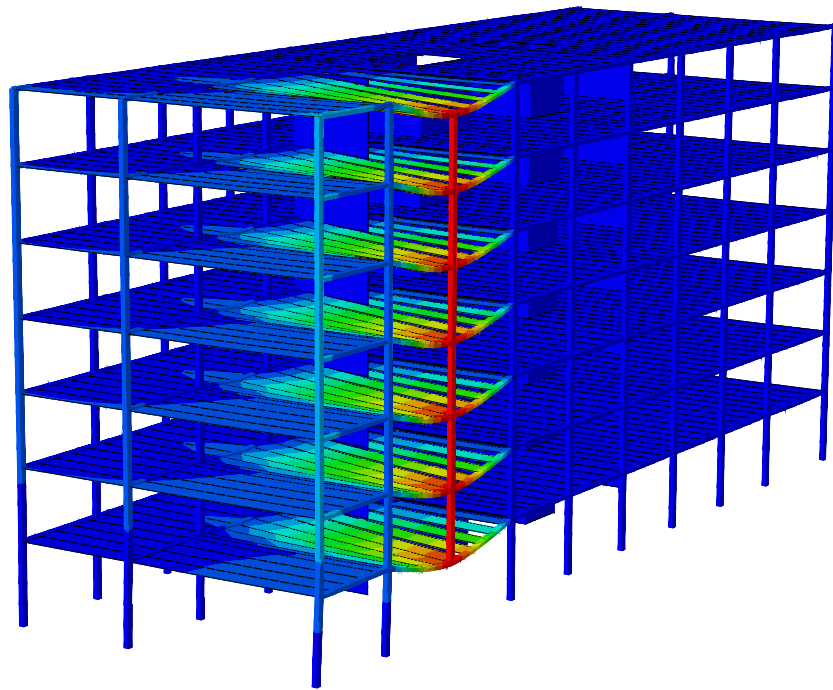




LUND
UNIVERSITY



STRUCTURAL ROBUSTNESS

FE methodology for analysing alternate load paths in buildings

AXEL KJELLMAN

Structural
Mechanics

Master's Dissertation

DEPARTMENT OF CONSTRUCTION SCIENCES
DIVISION OF STRUCTURAL MECHANICS

ISRN LUTVDG/TVSM--17/5223--SE (1-135) | ISSN 0281-6679

MASTER'S DISSERTATION

STRUCTURAL ROBUSTNESS

FE methodology for analysing
alternate load paths in buildings

AXEL KJELLMAN

Supervisors: Professor **KENT PERSSON** and **PETER PERSSON**, PhD, Div. of Structural Mechanics, LTH, together with **JESPER AHLQUIST**, MSc, Sweco AB.

Examiner: Professor **PER-ERIK AUSTRELL**, Div. of Structural Mechanics, LTH.

Copyright © 2017 Division of Structural Mechanics,
Faculty of Engineering LTH, Lund University, Sweden.

Printed by Media-Tryck LU, Lund, Sweden, June 2017 (*PI*).

For information, address:

Division of Structural Mechanics,
Faculty of Engineering LTH, Lund University, Box 118, SE-221 00 Lund, Sweden.

Homepage: www.byggmek.lth.se

Preface

My journey towards a master's degree in structural engineering ends with the completion of this thesis. The thesis has been made in a collaboration between the division of structural mechanics at Lund University, Faculty of Engineering (LTH) and Sweco structures.

I would like to thank prof. Kent Persson and PhD Peter Persson at LTH, and Jesper Ahlquist at Sweco structures for supporting me during my work. I would also like to thank Wilhelm Jakobsson at Sweco structures for helping me with practical matters and thank you Bo Zadig at LTH for your help with graphics and figures.

A handwritten signature in blue ink, reading "Axel Kjellman". The signature is fluid and cursive, with the first name "Axel" and the last name "Kjellman" clearly distinguishable.

Axel Kjellman

Lund, June 2017

Abstract

Robust structures are necessary in order to avoid a progressive collapse if a local failure occurs, for instance, failure of a column. Robustness is achieved in structures by designing them for so-called accidental actions, such as an explosion or a vehicle impact. These actions are often unexpected, sudden and local as they act on a limited part of the structure. It should be emphasised that progressive collapse design is about avoiding a collapse due to a local failure and not due to an abnormal load on the entire structure.

There are two main strategies often used in progressive collapse design. One strategy is to use a general method that aims to provide enough robustness and continuity in the structure. Another strategy for the designer is to show, by notional removal of elements, for instance, a column, that the structure can enable alternate load paths and therefore remains stable.

Even though no assurance is made that the structure is robust using the general method, it is the most commonly used method, partially due to an absence of guidance in regulations of how the notional removal strategy should be performed. The advantage of the notional removal strategy is that it provides an understanding of the actual performance of the structure.

In the USA, the Department of Defence has developed guidance on how numerical analysis using the finite element method should be used to validate the structure's robustness. In the thesis, progressive collapse analysis of a structure has been performed, inspired by the methods used in the USA, to provide knowledge of how numerical models can be used to validate robustness. The main focus of the thesis has been to examine if linear, non-linear or dynamic effects are needed in the analysis and how detailed the models need to be.

By comparing results from 2D and 3D analyses, it is questionable if a 2D model is accurate enough to represent all load carrying mechanisms that are present in the event of a column failure. When only linear effects were included in the analysis, it resulted in conservative results. Progressive collapse design is based on the advantage of large deformations and displacements, which are effects that could not be utilised in a linear analysis. However, with non-linear analyses, these effects are included which lead to an essential capacity increase due to a development of cable action in the beams. Results from the analyses showed that a non-linear static analysis could replace a dynamic analysis by adding an extra load on the structure to account for the dynamic effects. It is beneficial if the dynamic analysis could be avoided due to its high computational cost.

Keywords: accidental action, robustness, finite element method, FE, dynamics, progressive collapse, redundancy, alternate path, notional removal, precast

Abbreviations

LS	Geometrical linear static
NLS	Geometrical non-linear static
NLD	Geometrical non-linear dynamic
DLF	Dynamic load factor
FE	Finite Element
2D	Two-dimensional
3D	Three-dimensional

Contents

1	Introduction	1
1.1	Background	1
1.2	Aim and objective	2
1.3	Disposition	3
1.4	The studied building	3
2	Robustness in structures	7
2.1	Accidental actions	7
2.2	Dynamic effects	7
2.3	Redundancy	8
2.3.1	Ties	9
2.3.2	Fractures in structures	10
2.4	Load transferring mechanisms in a structure	11
2.4.1	Facade column loss – failure mode	13
2.4.2	Corner column loss – failure mode	15
2.5	Robustness of the studied building	16
3	Progressive collapse – regulations	17
3.1	Eurocode	17
3.1.1	General	17
3.1.2	Building classes	18
3.1.3	Measures suggested to prevent progressive collapse	19
3.2	Unified Facilities Criteria	22
3.2.1	Building classes and specified measures	22
3.2.2	Alternate path method	23
4	The finite element method	31
4.1	Linear static problems	31
4.2	Non-linear material	33
4.3	Non-linear geometry	37
4.4	Dynamic problems	38
5	Non-linear analysis of beams	43
5.1	Method	43
5.2	Modelling and results	44
5.2.1	Rectangular-/quadratic cross-sections	44
5.2.2	HSQ-profiles	53

5.3	Summary and discussion	61
6	2D progressive collapse analysis	63
6.1	Method	63
6.2	FE-model of the 2D structure	64
6.2.1	Geometry	64
6.2.2	Material model	65
6.2.3	Boundary conditions and loading	65
6.2.4	Mass and damping	66
6.3	Column 5 removal	67
6.3.1	LS analysis	68
6.3.2	NLS analysis	69
6.3.3	NLD analysis	72
6.4	Column 1 removal	77
6.4.1	LS analysis	77
6.4.2	NLS analysis	77
6.4.3	NLD analysis	79
6.5	Summary and discussion	79
7	3D progressive collapse analysis	81
7.1	Method	81
7.2	FE-model of the 3D structure	81
7.2.1	Geometry	81
7.2.2	Walls/elevator shafts	82
7.2.3	Facade	83
7.2.4	Inner columns and beams	83
7.2.5	Slab	84
7.2.6	Mass and damping	85
7.2.7	Loading and boundary conditions	85
7.3	Column 3 removal	87
7.3.1	NLS analysis	88
7.3.2	NLD analysis	95
7.4	Column 1 removal	99
7.4.1	NLS analysis	100
7.4.2	NLD analysis	105
7.5	Column 12 removal	109
7.5.1	NLS analysis	110
7.5.2	NLD analysis	115
7.6	Summary and discussion	119
8	Concluding remarks	121
8.1	Conclusions	121
8.2	Further studies	123
	References	125
	Appendices	I

A VKR profile	I
B Example of a column-to-beam connection	III
C Example of a hollow-core beam	V
D Strain limits for different steel classes	VII
E UFC – risk category of buildings and other structures	IX

1 Introduction

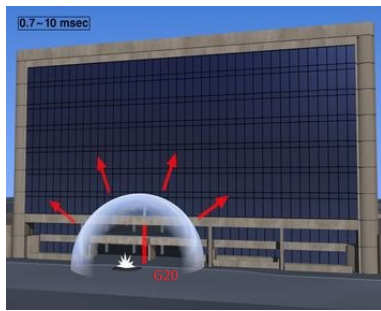
1.1 Background

There are several types of actions, such as wind, dead load and snow that will act on a structure during its life. It is impossible, and certainly not economical, to design a structure for every possible event. However, if the risk for it to occur is high enough and it leads to severe consequences, it needs to be considered by the designer.

Progressive collapse was first recognised after the well-known Ronan Point accident in the UK. A gas explosion on the top floor led to a partial collapse of the building which can be seen in Figure 1.1. Another example is the Oklahoma City bombing in 1995 which led to several injuries and casualties. It was a terrorist attack on the Murrah federal building, an explosion led to the failure of a column and a collapse of the building. Figure 1.2a illustrates the explosion close to column G20 which failed due to it. Figure 1.2b shows the collapsed building.



Figure 1.1: Ronan Point after an explosion in 1968, retrieved from [1].



(a) Explosion close to column G20, retrieved from [2].



(b) After collapse, retrieved from [3].

Figure 1.2: Terrorist attack on the Murray building.

What these two events have in common, is that a local failure, caused by an explosion, resulted in a collapse which was a disproportionately large compared to the initial damage. Designing structures against progressive collapse implies preventing the spreading of a local failure to other parts of the structure and not to prevent failure due to an abnormal load on the entire structure. Robustness in structures is more relevant than ever, even if events as Ronan Point or the Oklahoma City bombing are rare, as terrorist threats to our society have increased.

When designing structures against progressive collapse according to regulations in Europe, there are two strategies that are often used. One strategy is to use the indirect method, it is a general method which aims to provide enough robustness and continuity by for instance adding continuous reinforcement throughout the entire structure.

Another strategy for the designer is to show, by notional removal of elements, for instance, a column, that the structure can enable alternate load paths and therefore remains stable. The notional removal strategy is not often used due to an absence of guidance in the European regulations on how it should be performed. An advantage using notional removal is that the design is based on understanding and performance of the actual structure. The difficulty is to actually perform correct analyses when using notional removal. It usually implies complicated dynamic events and large deformations which are issues that are not often dealt with when designing structures. On the other hand, with the use of the indirect method, no assurance is made that the structure is robust.

However, the Department of Defence in the USA has developed guidelines for how to perform advanced progressive collapse analysis by using the finite element method. For larger structures the designer must show, by following these guidelines, that the structure can enable alternate load paths if some elements are notionally removed.

1.2 Aim and objective

The aim of the thesis is to provide knowledge of how numerical models can be used to validate robustness by performing progressive collapse analysis. Details in the numerical model, type of analysis and how these factors affect the load carrying mechanisms within the model and its resistance to progressive collapse are the main focus of the thesis. The

objective is to investigate a fictional building's ability to develop alternate load paths by using different models and types of analyses.

The method used is inspired by the guidelines provided by the Department of Defence in the USA. Finite element models are created of the building and analyses performed when columns are removed. The level of details needed in the models are investigated, as well as the need for considering dynamics, non-linear material and geometrical effects.

1.3 Disposition

Chapter 1	Introduction and description of the investigated building.
Chapter 2	Theory of progressive collapse design.
Chapter 3	Progressive collapse design according to regulations.
Chapter 4	The finite element method.
Chapter 5	Non-linear analysis of beams.
Chapter 6	2D progressive collapse analysis.
Chapter 7	3D progressive collapse analysis.
Chapter 8	Concluding remarks and further studies.

1.4 The studied building

The studied building is inspired by a real building in Malmö, Sweden, which also was investigated, with respect to progressive collapse design, by Niklewski and Nygårdh [4]. In the present study, some modifications of the building have been done. For instance, the number of columns is reduced and another type of beam profile is used in the facade. A sketch of the fictive building is presented in Figures 1.3, 1.4 and 1.5. A 3D model is shown in Figure 1.6. Robustness of the building is discussed in Section 2.5.

The columns consist of VKR-profiles shown in Appendix A. The facade beams consist of asymmetrical HSQ-profiles and inner beams of symmetrical HSQ-profiles, both types are shown in Figure 1.7. Every column-to-beam connection, column-to-ground connection, beam-to-wall connection is considered as moment stiff. A typical beam-to-column connection for this type of a structure is shown in Appendix B.

Horizontal stabilisation of the building is achieved through transferring of load from the facade, to slabs, to concrete walls and elevator shafts in the centre of the building. The walls and elevator shafts consist of concrete and their connection to the ground is considered as moment stiff. The slabs consist of hollow-core concrete beams, shown in Appendix C, which are lined up between facade beams, inner beams and walls. A layer of concrete is placed on top of the hollow-core beams.

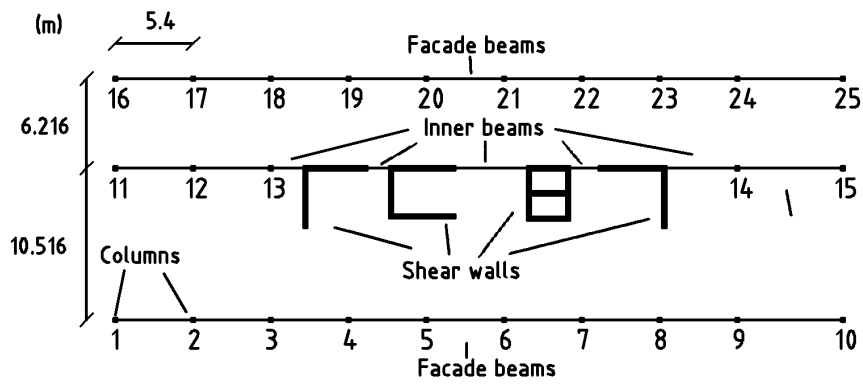


Figure 1.3: Plan view of the building.

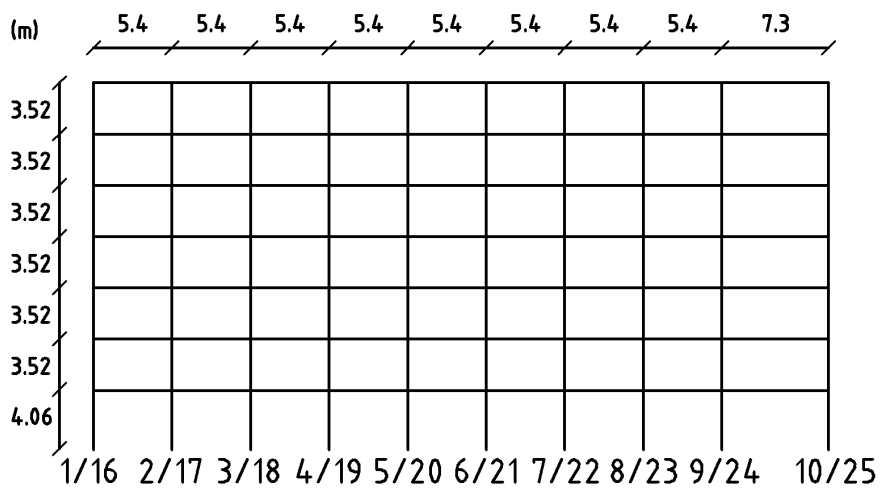


Figure 1.4: Columns 1-10, 16-25 and beams in the facade.

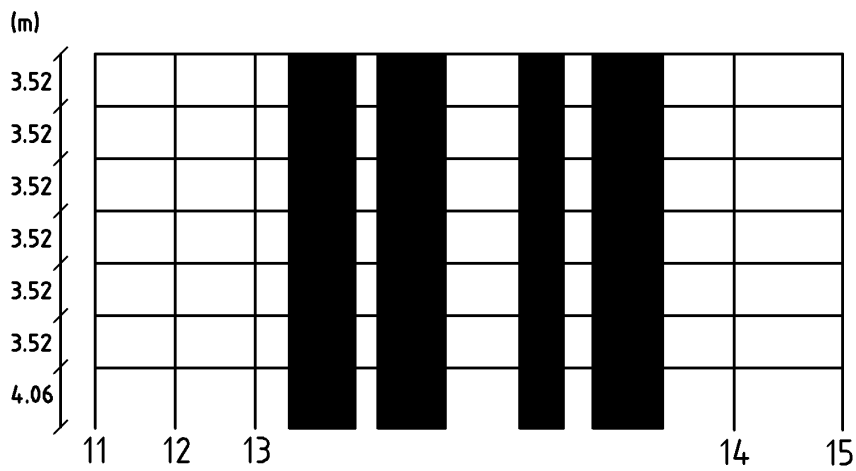


Figure 1.5: Inner columns 11-15, beams, and walls.

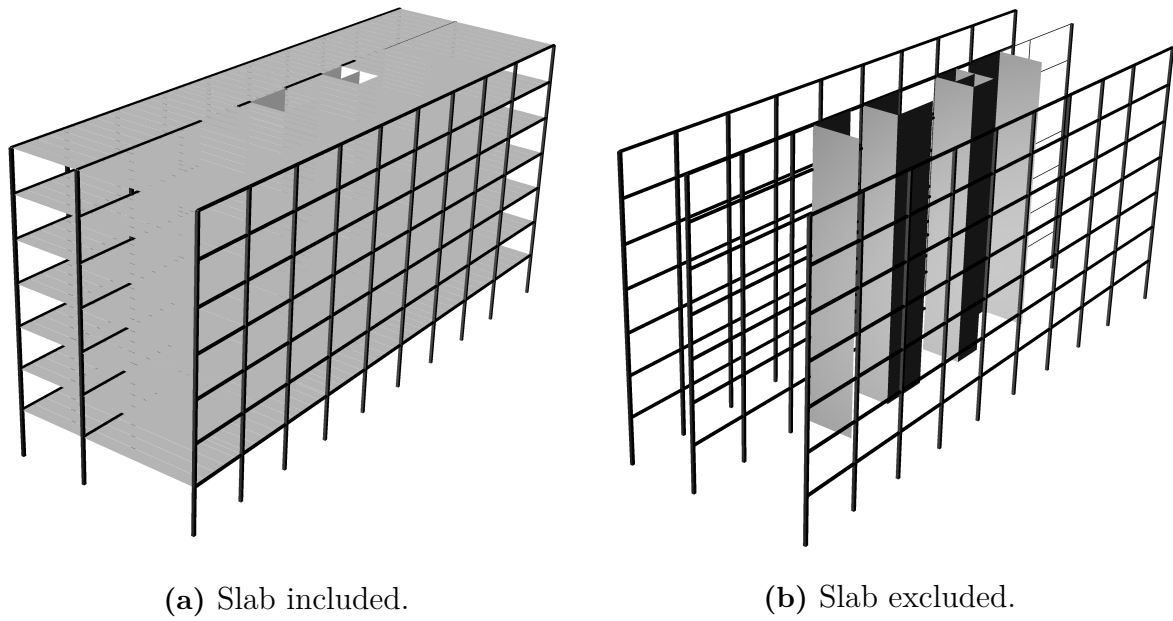
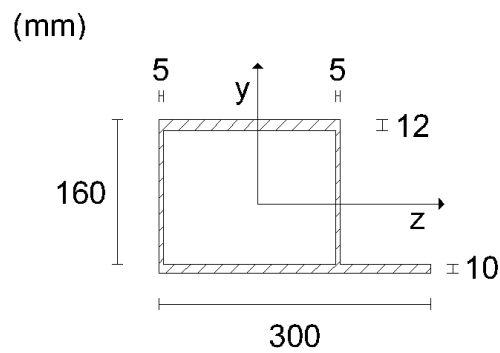
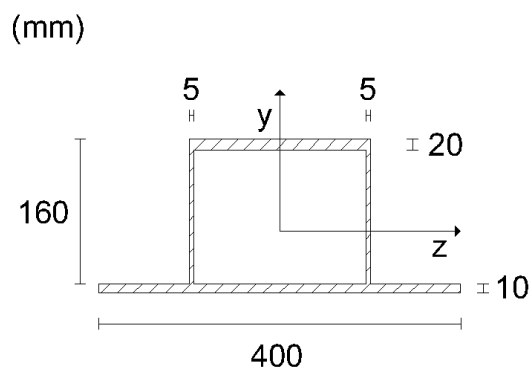


Figure 1.6: 3D model of the building.



(a) Asymmetrical cross-section for the facade beams



(b) Symmetrical cross-section for the inner beams

Figure 1.7: Cross-sections of the beams in the studied building.

2 Robustness in structures

This chapter is an introduction to the methods used in progressive collapse design for precast concrete structures. For more detailed information about progressive collapse design, the reader is referred to [5].

2.1 Accidental actions

Vehicle impacts or explosions are examples of events that are rare, but frequent enough so that there are rules for how to design structures to withstand them. These type of actions are called accidental actions and are often unexpected, sudden and local as they act on a limited part of the structure. Therefore, it should not be associated with a load acting on the entire structure, from for instance extreme weather. Examples of accidental actions are

- Dynamic pressure due to explosions.
- Vehicle impact.
- Static overload.
- Settlements in the foundation.
- Ground movements.
- Design and construction errors.

Vehicle impacts and explosions are the most common accidental actions and therefore the most studied. After the well-known Ronan Point collapse (Figure 1.1), several studies investigated the pressure from explosions and it was rarely more than 17 kN/m^2 . This is a large load compared to the static load cases used when designing buildings, for instance a live load of 2.5 kN/m^2 in offices. Although, it is well below the static load 34 kN/m^2 , which is a value that is often used when designing elements to be able to resist accidental actions.

To estimate the developed load in case of a vehicle impact is complicated. It depends on a number of things, such as velocity, mass and how the kinetic energy is dissipated into the structure and the colliding vehicle [5]. It is therefore questionable if a static load of 34 kN/m^2 can resemble the complicated load distribution due to vehicle impacts.

2.2 Dynamic effects

A sudden column failure will result in a loss of the static equilibrium which leads to acceleration of masses. The kinetic energy due to the moving masses needs to be absorbed

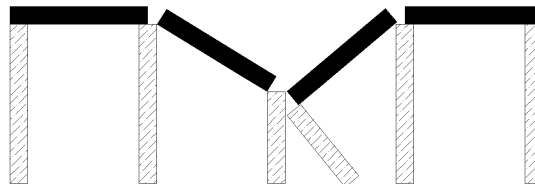
in the structural elements. In progressive collapse design, the designer must consider, due to the kinetic energy, that internal forces in the elements will be higher than in the same static load situation.

Elements exposed to an impact or explosion respond differently compared to the same static load condition due to a high strain rate in the materials. A uniformly distributed load might give a flexural failure mode in static conditions, while the same load distribution in a dynamic situation, might lead to a failure in shear near the supports [5].

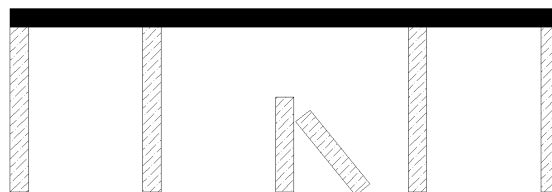
2.3 Redundancy

A building must if an incident occurs and a column collapses, be able to redistribute the load carried by that column to other elements. A column failure leads to extra load on the adjacent elements and might result in their failure. If the structure is unable to find equilibrium, it will lead to an entire, or partial collapse depending on the continuity in the load-bearing system.

Figure 2.1a illustrates a load-bearing system which does not have any redundancy, in the case of a column loss the supported beam will fail. However, since it is not continuous, the collapse will be local and not distributed to the rest of the structure. Figure 2.1b illustrates a redundant system which has the capability of redistributing forces in the case of a column failure. Because of the column failure, the adjacent columns are subjected to an extra load, if they are unable to carry the extra load, the whole structure is in risk of a progressive collapse.



(a) Non-redundant structure.



(b) Redundant structure.

Figure 2.1: The concept of redundancy in structures with simply supported elements (a) and continuous elements (b).

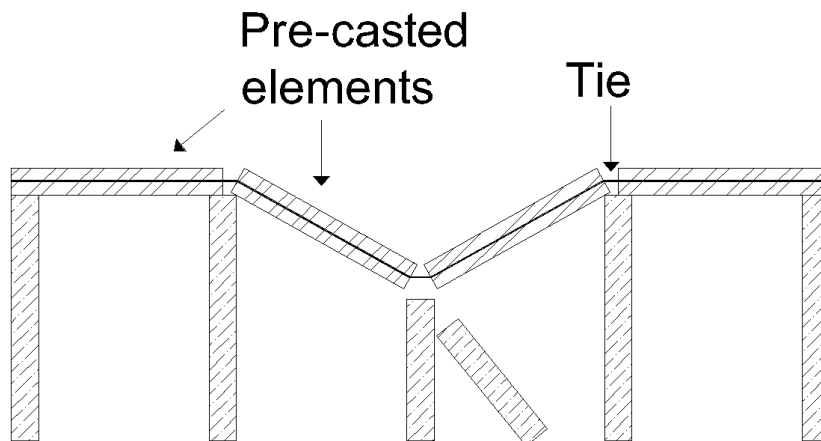


Figure 2.2: Principle functioning of the tying system.

2.3.1 Ties

In [5], the authors describe the interaction between elements as more important for the redundancy than the strength of single elements. Another important aspect mentioned is the building layout which affects the stability and ability to change load paths. The ability to enable alternate load paths is particularly a problem in precast structures due to lack of continuity. To add continuity and increase the redundancy in precast structures, elements are usually connected by ties. Figure 2.2 illustrates the principle functioning of the ties which ensure continuity within the structure.

The ties consist of rebars, tendons or continuous beams and are placed in a transverse, longitudinal and vertical direction throughout the whole structure. Transverse and longitudinal ties are referred to as horizontal ties which could be either peripheral ties around the structure or internal ties across the structure. Vertical ties are often placed in vertical elements, for instance, columns, and are continuous from the lowest to the highest level in the structure [6]. By connecting every element, the structural stability and capability of redistributing loads increases. The principle layout of the tying system can be seen in Figure 2.3.

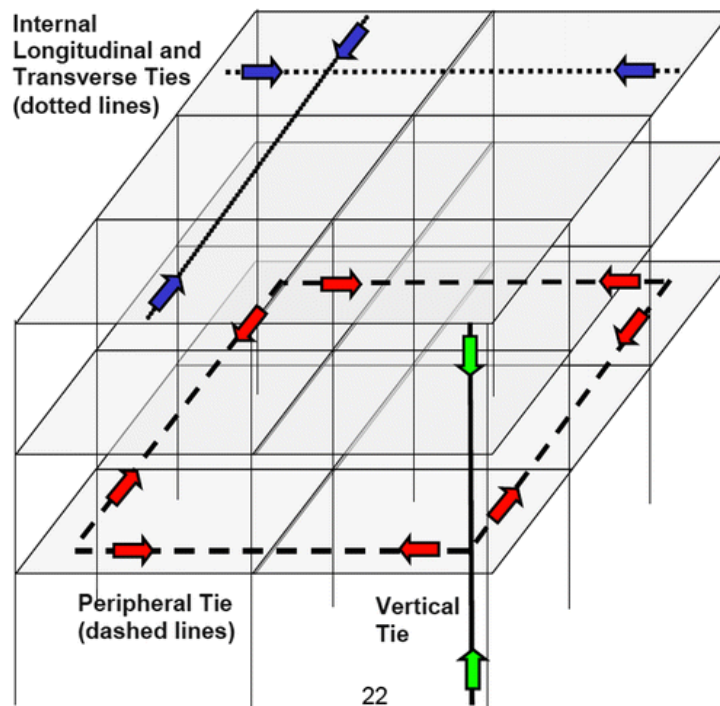


Figure 2.3: Typical layout of the tying system in a structure, retrieved from [5].

2.3.2 Fractures in structures

Ductility is the structure's ability to develop large deformations without failing. It is a very important structural property, because, for the ties to function, the advantage of large deformations and displacements must be allowed [5]. A not so ductile structure will give a brittle failure which loses all its loading capacity very sudden.

To achieve a ductile structure, it requires a material with the ability of large plastic deformations, for instance, steel. Concrete is a material with a low capability of plastic deformations which is why concrete elements, in precast structures, must be tied together with steel rebars, steel tendons or continuous steel beams.

A typical rebar connection between concrete elements is shown in Figure 2.4. For a ductile structure with large deformability, it is beneficial if plasticity can develop along the whole bar. However, it is not the case with rebar ties because they are embedded in concrete. It limits the deformation to single cracks in the interface between the tied elements and plasticity of the rebars can only develop within these cracks [5], see Figure 2.5. It will result in a very high strain of the ties in these cracks and might lead to a fracture in the material and failure of the connection.

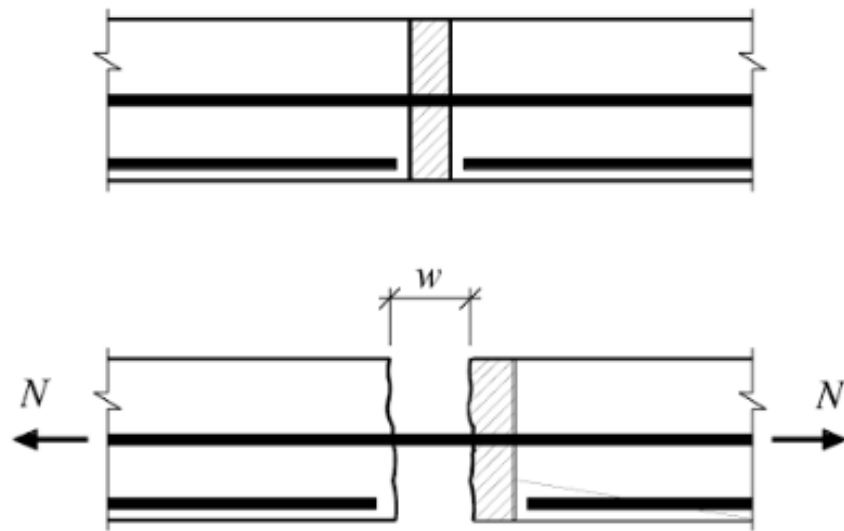


Figure 2.4: Typical connection between elements using rebars as ties, retrieved from [5].

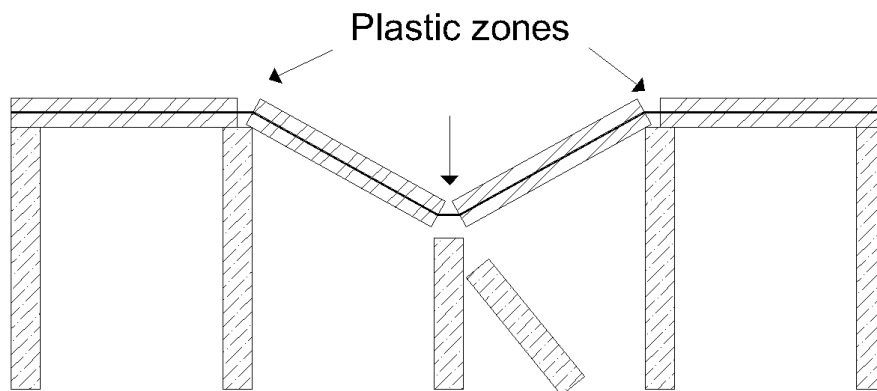


Figure 2.5: Plasticity concentrated to the cracks between the connected elements.

2.4 Load transferring mechanisms in a structure

The concept of bridging over a failed column is essential in progressive collapse design. If a support to a beam suddenly fails, the span length is doubled and the beam will in most cases not be able to transfer the load to adjacent columns through bending action. Instead, cable action can be the main load bearing action, it implies that vertical load resistance is achieved through the development of tensile force in the beam which is beneficial due to the absence of bending and buckling. It requires, on the other hand, large deformations to be efficient.

Rebars, tendons or continuous beams are not ideal cables and there will be a combina-

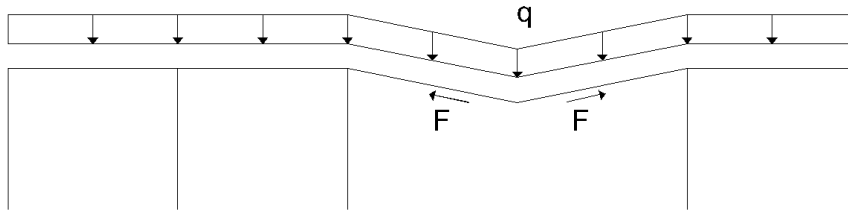


Figure 2.6: Cable action used for bridging over a failed column.

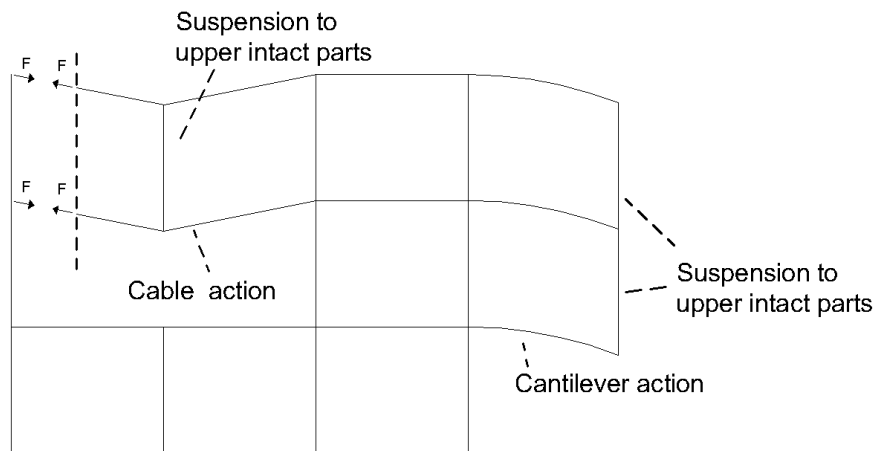


Figure 2.7: Example of alternative load paths in a structure.

tion of a tensile force and bending moment, but with increased deformation it will carry more load through cable action. The principles of how cable action bridges over a failed column are illustrated in Figure 2.6.

The authors of [5] point out that there is an issue with the use of cable action in the ties, it results in a large horizontal force that has to be transferred to the rest of the structure. Good anchoring of the rebars or beams and an ability for adjacent columns to transfer the horizontal force to other stable parts of the structure is essential for the cable action to work. The horizontal force is, in particular, a problem for loss of a column close to an edge because the horizontal force needs to be supported by a limited part of the structure. In Figure 2.7, loss of the column at storey 2 will result in a horizontal force due to cable action of the beam, it is in particular a problem to the left of the structure, where the entire horizontal force is supported by the edge column. To the right of the structure, the horizontal force is transferred to several columns and it is supported by a larger part of the structure.

In the case of a corner column loss, cantilever action is supposed to transfer the load which is possible if continuous beams are used. If simply supported beams are used, it could be achieved by horizontal ties placed in the top of the beams. Figure 2.8 illustrates the intended cantilever mechanism, where tension in the tie and compression in the lower

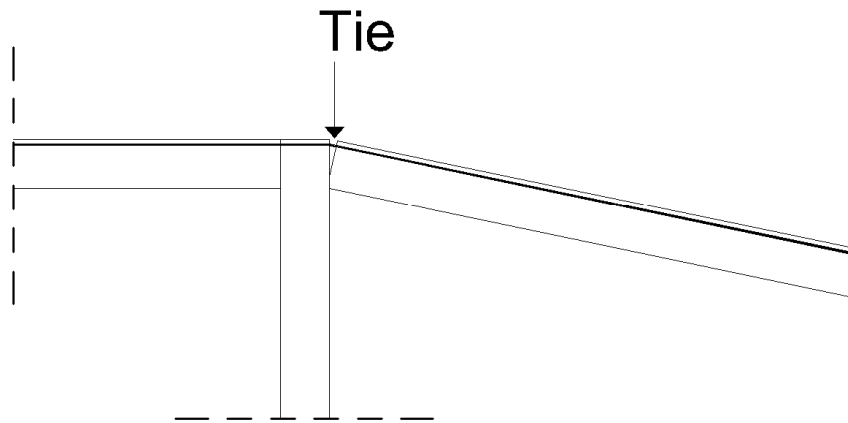


Figure 2.8: Cantilever action in a simply supported beam.

part of the beam creates a force couple and a moment which prevent rotation at the support.

Vertical ties provided in columns through all storeys should also improve the capacity of load redistribution. The purpose of using vertical ties is that the elements are suspended to the upper, intact parts of the structure, see Figure 2.7. For the suspension mechanism, illustrated in Figure 2.7, to work, a good anchorage between vertical and horizontal ties should be provided.

Membrane action of floors and roofs is also a strategy used to bridge over removed columns. It is a mechanism that is more relevant for in-situ cast structures and difficult to achieve in precast structures due to the lack of tensile strength in the transverse direction of the elements.

2.4.1 Facade column loss – failure mode

In the case of a failed perimeter column, a transition to a load-bearing system with cable action should occur. The authors of [5] present one possible failure mode, for a precast structure, which is shown in Figure 2.9.

Because of large deformations occurring, the concrete topping will most probably detach and its contribution can be neglected. The deformation caused by the column failure results in a deflection of the facade beam. Because of the stiff hollow-core units, the deformation will be concentrated to the longitudinal joints and will result in splitting of the elements in these joints.

During the deformation, the hollow-core units can fall off the facade beam, but through rebars, which are usually placed inside the cores, they will remain attached to the beam [5]. A typical facade beam, consisting of a continuous HSQ-profile as the one in the studied building, is connected to the hollow-core units with ties as shown in Figure 2.10.

For the failure mode described above it is a risk that the horizontal continuous beams, rebars or tendons along the edge have to take most of the load by normal force and cable action. For it to work, it is essential that large deformation is possible which

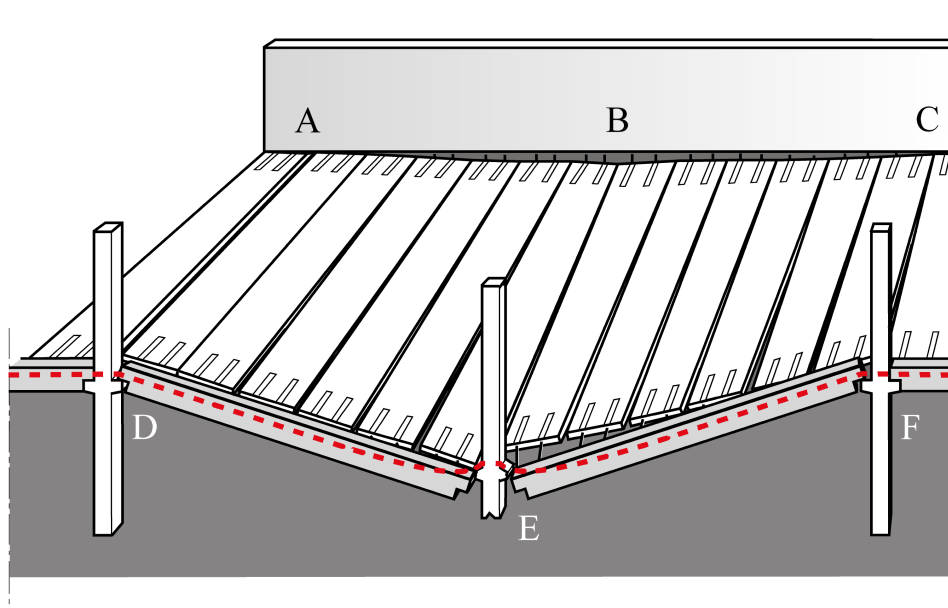


Figure 2.9: Possible failure mode in case of a facade-column loss.

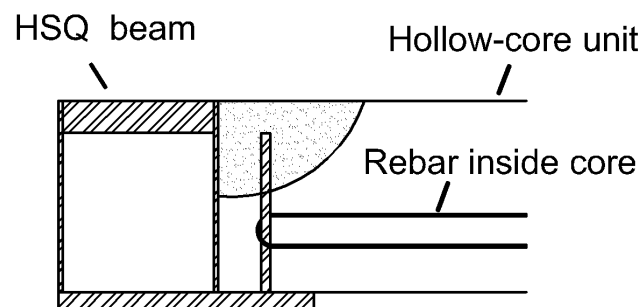


Figure 2.10: Embedded rebar tying a hollow-core unit to an HSQ-profile in the facade.

is a major issue using rebars or tendons. Due to their embedment in concrete, their plastic deformation is concentrated to connections D, E and F shown in Figure 2.9. A concentration of plasticity in the tendons and rebars will cause very high strain and might lead to a fracture in the material before the tie has deformed as much as needed to reach equilibrium. An example computation performed by Niklewski and Nygårdh [4], showed that the possible deflection before the rebars breaks was too low if plasticity was assumed to only develop in connections D, E and F in Figure 2.9.

With continuous HSQ-profiles in the facade instead of rebars, plasticity will most likely be able to develop unhindered along the beam and the problem with concentration of plasticity because of embedment in concrete is not present in the studied building.

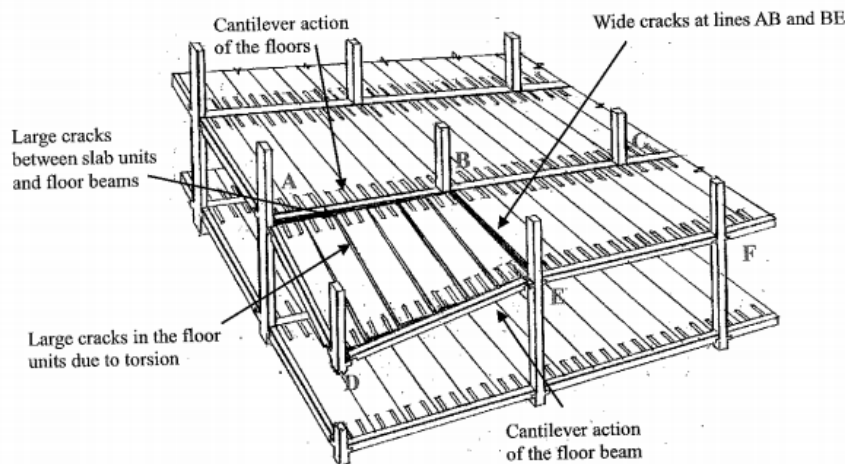


Figure 2.11: Possible failure mode due to the failure of a corner column, retrieved from [5].

2.4.2 Corner column loss – failure mode

A cast in-situ structure is described by the authors of [5], as better to resist progressive collapse. The whole slab will, due to reinforcement in both a transverse and longitudinal direction, transfer load through cantilever action. It is not possible in a precast structure where cantilever action by the slab is limited and contribution of the top concrete layer can be neglected because it will most probably detach. If upper storeys are subjected to a similar load, they will probably deflect in the same way and the suspension function to upper intact parts will not work. It is not difficult to realise that a precast structure is extra sensitive to a corner column loss because the only remaining load carrying mechanism is through cantilever action by the facade beam, illustrated in Figure 2.11.

One strengthening measure could be to add an edge beam which would also contribute by cantilever action. Although, it is doubtful whether this cantilever effect is strong enough [5]. Especially for the type of beam shown in Figure 2.8, because the distance between the force couple usually is limited.

Another possible mechanism, discussed by Westerberg [7], is membrane action if continuous perimeter ties are provided around corners. This mechanism is explained in Figure 2.12, the ties will be subjected to a tensile force and a diagonal compression force, shown in red, will arise in the slab.

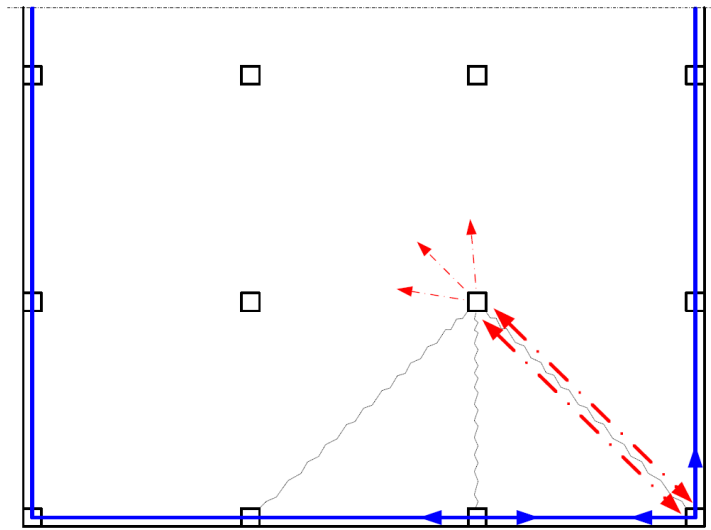


Figure 2.12: Possible membrane action in case of a corner column failure, retrieved from [7].

2.5 Robustness of the studied building

The following section describes how robustness is achieved in the studied building. The continuous beams will act as peripheral and internal ties and ensure load transferring to other parts of the structure if a column fails. The issue with concentration of plasticity is assumed to not be present because the beams are not embedded in concrete and plasticity will develop freely along the beams.

Embedded rebars, one per hollow-core unit, connect the hollow-core units with the facade and inner beams.

The columns are assumed to be tied together through the continuous beams, which will enable a suspension function to upper intact parts if a column would fail.

3 Progressive collapse – regulations

The following chapter describes the approach to progressive collapse design as given in Eurocode [8] and in regulations from The Department of Defence in the USA [9].

3.1 Eurocode

How to design concrete structures for accidental actions is described in SS-EN 1992-1-1 [10] and Annex A of SS-EN 1991-1-7 [8]. The use of two regulations has caused some confusion in Sweden in what actually applies, it was investigated by Niklewski and Nygårdh in [4]. Annex A of SS-EN 1991-1-7 is only informative but has been made normative in Sweden by Boverket, it is usually stricter than SS-EN 1992-1-1 and will be decisive in most cases [7]. In the following chapter, the approach in Annex A of SS-EN 1991-1-7 is summarised.

3.1.1 General

Two different design situations are presented in SS-EN 1991-1-7, which one to be used depends on if it is a known action or unknown action. They require different measures to be performed by the designer. The alternative measures are given as described.

For **unknown actions**, three design strategies can be used, these are

- Use notional removal and perform analyses to ensure that the structure is capable of load redistribution.
- Design the vertical load bearing elements as key elements.
- Use the indirect method, this implies the use of prescriptive rules which should ensure that the structure is robust enough.

known actions, it could, for instance, be a vehicle impact if a column is placed close to a road. The strategies presented in SS-EN-1991-1-7 to design building against known actions are

- Use notional removal and perform analyses to ensure that the structure is capable of load redistribution.
- Design the vertical load bearing elements as key elements for the known action.
- Use protective measures.

Table 3.1: Consequence classes in Eurocode, retrieved from [8].

Consequence class	Example of categorisation of building type and occupancy
1	Single occupancy houses not exceeding 4 storeys. Agricultural buildings. Buildings into which people rarely go, provided no part of the building is closer to another building, or area where people do go, than a distance of $1\frac{1}{2}$ times the building height.
2a Lower Risk Group	5 storey single occupancy houses. Hotels not exceeding 4 storeys. Flats, apartments and other residential buildings not exceeding 4 storeys. Offices not exceeding 4 storeys. Industrial buildings not exceeding 3 storeys. Retailing premises not exceeding 3 storeys of less than 1 000 m ² floor area in each storey. Single storey educational buildings All buildings not exceeding two storeys to which the public are admitted and which contain floor areas not exceeding 2000 m ² at each storey.
2b Upper Risk Group	Hotels, flats, apartments and other residential buildings greater than 4 storeys but not exceeding 15 storeys. Educational buildings greater than single storey but not exceeding 15 storeys. Retailing premises greater than 3 storeys but not exceeding 15 storeys. Hospitals not exceeding 3 storeys. Offices greater than 4 storeys but not exceeding 15 storeys. All buildings to which the public are admitted and which contain floor areas exceeding 2000 m ² but not exceeding 5000 m ² at each storey. Car parking not exceeding 6 storeys.
3	All buildings defined above as Class 2 Lower and Upper Consequences Class that exceed the limits on area and number of storeys. All buildings to which members of the public are admitted in significant numbers. Stadia accommodating more than 5 000 spectators Buildings containing hazardous substances and /or processes

3.1.2 Building classes

The measures described in Section 3.1.1 are not needed for all type of buildings. Eurocode divides buildings into different consequence classes depending on their characteristics. For each class, different measures need to be considered by the designer. The classes are presented in Table 3.1.

For the classes in Table 3.1, suggested measures are:

- In consequence class 1 there is no need to consider local failure.
- In consequence class 2a, provide horizontal ties.
- In consequence class 2b, provide horizontal ties and perform one of the following measures.
 - Provide vertical ties in every column. This is the indirect method.
 - Use notional removal. It implies that the designer has to verify that the structure remains stable if a load bearing element fails.

- Design the column or load-bearing wall as a key element. It implies that the element should resist the accidental action which results in an oversized element.
- In consequence class 3, perform a risk analysis for both foreseeable and unforeseeable hazards.

The studied building described in Section 1.4 belongs to consequence class 2b and the notional removal method is appropriate to use. There is, however, no guidelines of how to perform such an analysis in Eurocode. Note that no verification has to be made if ties are used.

3.1.3 Measures suggested to prevent progressive collapse

Horizontal ties

The concept of ties has already been introduced in Section 2.3.1. The following Section describes how these ties should be designed according to SS-EN 1991-1-7.

As mentioned in Section 3.1.2, horizontal ties are required, for all building types except those in consequence class 1. The ties could be rolled steel sections, as is the case for the studied building, or reinforcement in concrete slabs. Two types of horizontal ties are defined in SS-EN 1991-1-7 with different requirements, these are:

Horizontal ties along the building perimeter, they should be continuous and within 1.2 meters of the floor edge on each storey and be continuous around corners [11], which would require additional reinforcement or an extra beam for the studied building. SS-EN 1991-1-7 require that these ties can sustain a tensile force which is determined by the largest of

$$\begin{aligned} T_p &= 0.4(g_k + \psi q_k)a_1L \\ T_p &= 75\mu \text{ [kN]} \end{aligned} \tag{3.1}$$

where

g_k , is the characteristic permanent load.

q_k , is the characteristic live load.

ψ_1 , is the relevant load combination factor. For instance the frequent factor for live load, ψ_1 [11].

a_1 , is the distance to the inner tie, see Figure 3.1.

L , is the distance presented in Figure 3.1.

μ , a factor usually equal to 1 [11].

Horizontal inner ties should be provided in each storey and placed in two perpendicular directions as illustrated in Figure 3.1. They should be anchored to, either ties along the building perimeter, or to beams or walls supporting the floor. If they are distributed evenly in the floor, they must sustain an evenly distributed load given by the maximum of

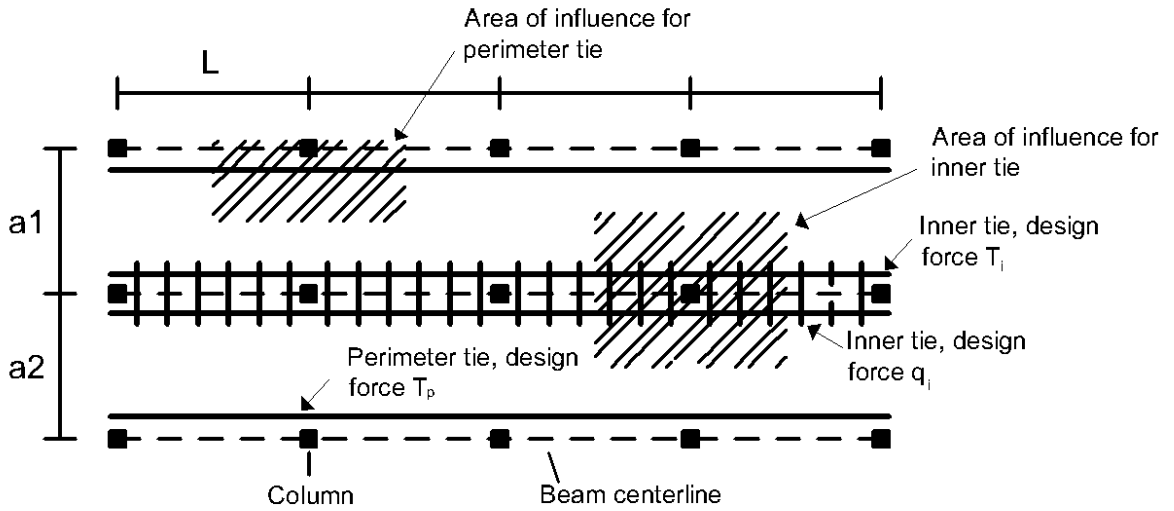


Figure 3.1: Design forces for the horizontal ties.

$$\begin{aligned} q_i &= 0.8(g_k + \psi_1 q_k) a_m \\ q_i &= 20\mu \quad [\text{kN/m}] \end{aligned} \quad (3.2)$$

where

$$a_m = \frac{(a_1 + a_2)}{2}.$$

If instead the tie is concentrated to beam lines, as Figure 3.1 illustrates, it must sustain a load that is given by the maximum of

$$\begin{aligned} T_i &= 0.8(g_k + \psi_1 q_k) a_m L \\ T_i &= 75\mu \quad [\text{kN/m}]. \end{aligned} \quad (3.3)$$

For Columns that are placed with different centre-to-centre distance between them, a distance L should be chosen which gives the maximum design load according to Equation 3.1 or 3.3 [11].

Vertical ties

As mentioned in Section 3.1.2, in consequence class 2b, SS-EN 1991-1-7 gives an option to achieve sufficient robustness by using the indirect method. It implies continuous vertical ties in every load bearing column and wall, from the foundation to the roof.

Vertical ties should be able to sustain a reaction force on a column or wall which acts as a support to the floor. The largest reaction force along the column's length should be used, but only from one floor. This is illustrated in Figure 3.2.

The design force is determined with an accidental load combination acting on the supported floor. For columns in the perimeter and a simply supported floor, this implies

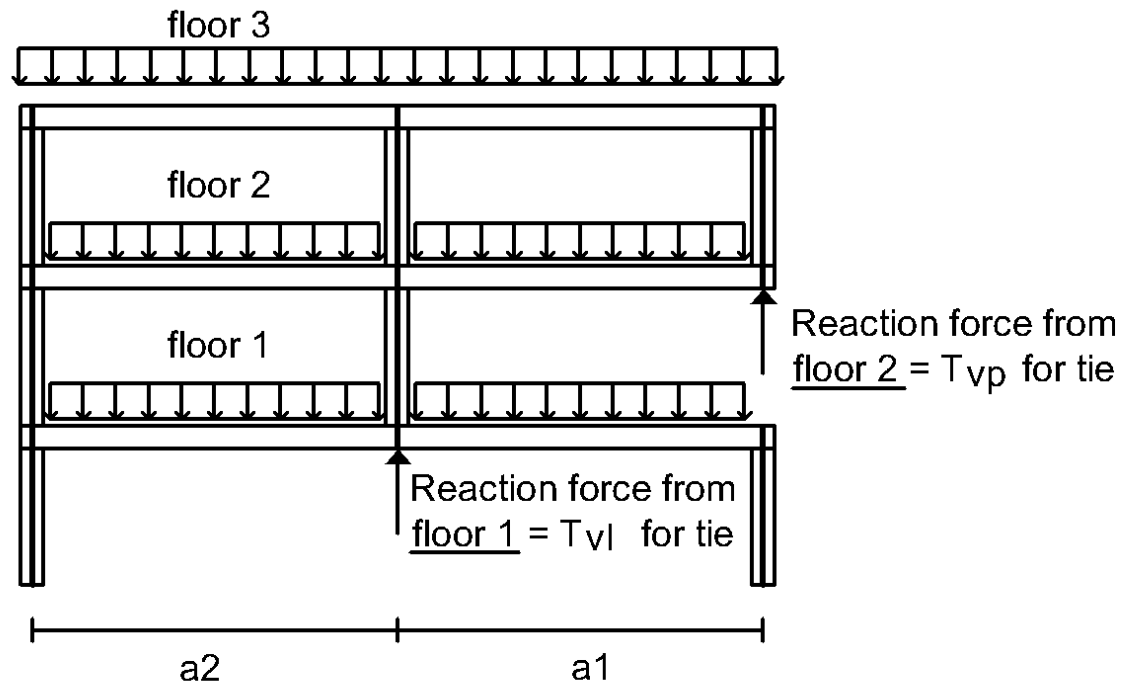


Figure 3.2: Design forces for the vertical ties.

a load given by the evenly distributed load multiplied with the area of influence for the column [11], see Figure 3.1.

$$T_{vP} = (g_k + \psi_1 q_k) \frac{1}{2} a_i L. \quad (3.4)$$

For centre line columns, the design load for the tie is determined by multiplying the area of influence shown in Figure 3.1 with the load that acts on the floor

$$T_{vP} = (g_k + \psi_1 q_k) a_m L \quad (3.5)$$

where a_m is explained in Equation 3.2 [11].

Notional removal

An accidental action that results in a failure of an element is accepted if the overall structural stability and load bearing capacity are maintained. This applies to both unknown and known accidental actions.

In SS-EN 1991-1-7, there is an option for the designer to validate the stability of the structure, if vertical load bearing elements fail. It can be done by doing a notional removal of load-bearing elements and verify that it does not result in a progressive collapse. In the case of an unknown accidental action, every column or load-bearing wall should be removed one at a time in each storey. For a known accidental action, the designer can verify that the building remains stable without the affected element, this is one of the strategies described under known actions in Section 3.1.1.

A recommended limit of the extent of the damaged area is given in SS-EN 1991-1-7, but it depends on the type of building. It should not be more than 15% of the floor or 100 m², in adjacent storeys.

There is no further detailed description in SS-EN 1991-1-7 of how the analysis of notional removal should be performed.

Key element

If for instance, a redistribution of load can not be ensured when a column is removed, the column could be designed as a key element. A key element is designed to resist a specific load, SS-EN 1991-1-7 recommends a value of 34 kN/m², the load should be applied in both horizontal and vertical direction, one at a time. This load is applicable for walls and slabs [11]. For columns, it is recommended that a value of 100 kN/m is used [12].

Protective measures

Protective measures are used for a known accidental action and are supposed to remove or reduce the risk of damage to the structure [8]. It could, for instance, be vehicles stopped by barriers.

3.2 Unified Facilities Criteria

A standard for how to design buildings against progressive collapse in the US has been produced by the Department of Defence. The standard is a part of the Unified Facilities Criteria (UFC) which provides planning, design, construction, sustainment, restoration and modernisation criteria and applies to US military departments, defence agencies etc [9]. The following chapter summarises the approach used in the UFC document *Design of Buildings to Resist Progressive Collapse* [9], with a focus on the alternate path method described in the document.

In a progressive collapse design, a distinction is made, as in Eurocode, between known and unknown accidental loads. For known accidental loads, there is a design method on how to harden the building which is not discussed any further. For unknown threats, which could be a terrorist attack but no event is defined, the objective is to reduce the risk of mass casualties. It is achieved, by not limiting the initial damage, but by designing robust enough structures.

3.2.1 Building classes and specified measures

As in Eurocode, a direct or indirect design approach is used. The direct design approach is a method in which the structure is designed explicitly to resist progressive collapse. It implies the use of the alternate path method which is similar to the notional removal method used in Eurocode, see Section 3.1.3.

Specified Load Resistance (SLR) is also used and it is a method where elements in the building are designed to resist a specified load or threat. SLR could be compared with designing key elements according to Eurocode, see Section 3.1.3.

The indirect method uses a more implicit approach to achieve robustness. It is done by providing a minimum level of strength, continuity and ductility in the whole structure by following general guidelines for improving structural redundancy. In the UFC, it is achieved by use of ties similar to the ones in Eurocode.

Dependent on the structural characteristics, different measures need to be considered. As in Eurocode, buildings are divided into risk categories from 1 to 4, See Appendix E, dependent on their importance or the risk to human life in the event of a collapse. For instance, a minor storage facility belongs to category 1, schools category 3 and an air traffic control centre is a category 4 building [13]. Category 2 includes buildings not listed in category 1,3 or 4. For each risk category, a combination of indirect and direct methods are used to achieve robustness.

In category 1 no consideration of progressive collapse is needed. For category 2 the indirect method or alternate path method could be used. The main difference to Eurocode is for category 3 and 4 where the alternate path method is required in combination with other measures such as enhanced local resistance in category 3 and tie forces in category 4.

As mentioned in Section 2.2, the failure mode can be different in a dynamic event than a static event for the same load case. Enhanced local resistance implies that perimeter columns and walls can use its maximum flexural strength without failing in shear. The purpose of enhanced local resistance is to achieve a ductile failure mechanism when a wall or column is loaded laterally to failure [9]. A ductile failure mechanism limits the dynamic effects because the time of removal is longer and some energy is absorbed in the column.

In category 3 and 4, a requirement of the alternate path method implies that the structure should be able to bridge over a notional removed vertical load bearing element, which should be removed one at a time at specific locations. If the designer is unable to prove that bridging over the removed element is possible, the building should be re-designed.

The design approach used in the UFC is summarised in Figure 3.3.

3.2.2 Alternate path method

Three different approaches using numerical models are described in [9], the linear static, non-linear static and non-linear dynamic. The UFC points out that advanced simulations should not prevent the use of simplified analytic methods or hand calculations which could be more efficient for some type of buildings.

When creating numerical models, elements are classified as either primary or secondary where primary elements are defined as elements that contribute to the resistance to progressive collapse. An example of a secondary element is a steel beam, pinned to girders, but it could be a primary element if the connection is partially restrained and contributes to the resistance to a progressive collapse.

Figure 3.4 shows the correct approach on how to remove the vertical load bearing elements. A length equal to the height of the storeys, for both columns and walls, should be removed so that adjacent beams remain continuous. For walls, a width twice this height should be removed.

In the analysis, columns and walls should be removed once at a time, as a minimum, near the middle of the short side, long side and at corners. This should be done at the

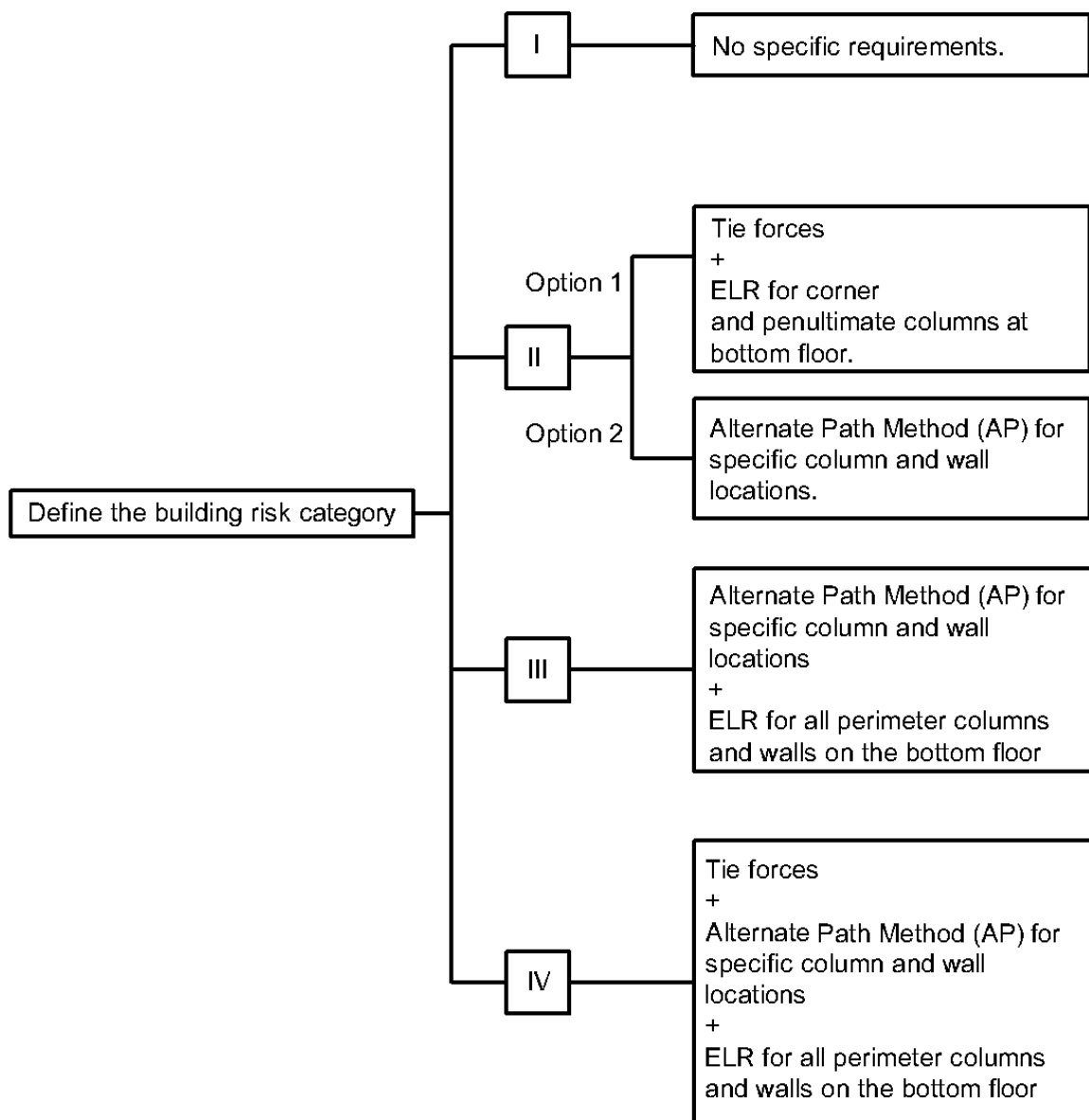


Figure 3.3: The design approach following the guidelines specified in the UFC.

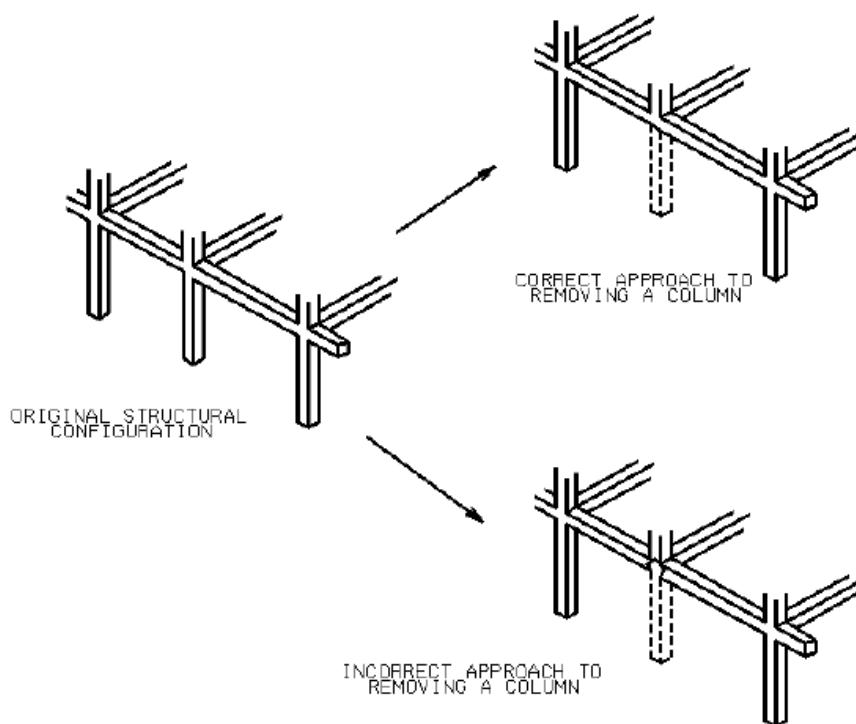


Figure 3.4: Correct removal of columns, retrieved from [9].

ground level, top level, mid level and levels above a column splice or where the column changes in size. Removal should also be done where there is a distinctive change in the plan geometry, for example, a decrease in bay size. Examples of external column removal locations are presented in Figure 3.5.

Internal columns and walls should be removed in the middle of the long side, short side, and at corners of an uncontrolled public access area. Within this area, other columns or walls might also need to be removed, this is determined by engineering judgement. Examples of internal column removal locations are presented in Figure 3.6.

Numerical models – procedures

Linear static

In the linear static procedure, only linear geometrical and static effects are regarded in the model. It implies that the geometry of the structure does not change during the analysis which results in, for instance, that cable action of the beams is not possible.

There are some limitations, listed in [9], for using the linear static method. One example is that the structure must not have distinctive irregularities in the vertical or lateral load bearing system. The modelling is done with a 3D model where only stiffness of primary elements, see Section 3.2.2, should be included. It should be detailed enough so that a correct transfer of vertical load from floor and roof to the primary elements is achieved.

The applied load of the structure is dependent on which type of action that is to be determined. Actions are divided into either force controlled or deformation controlled

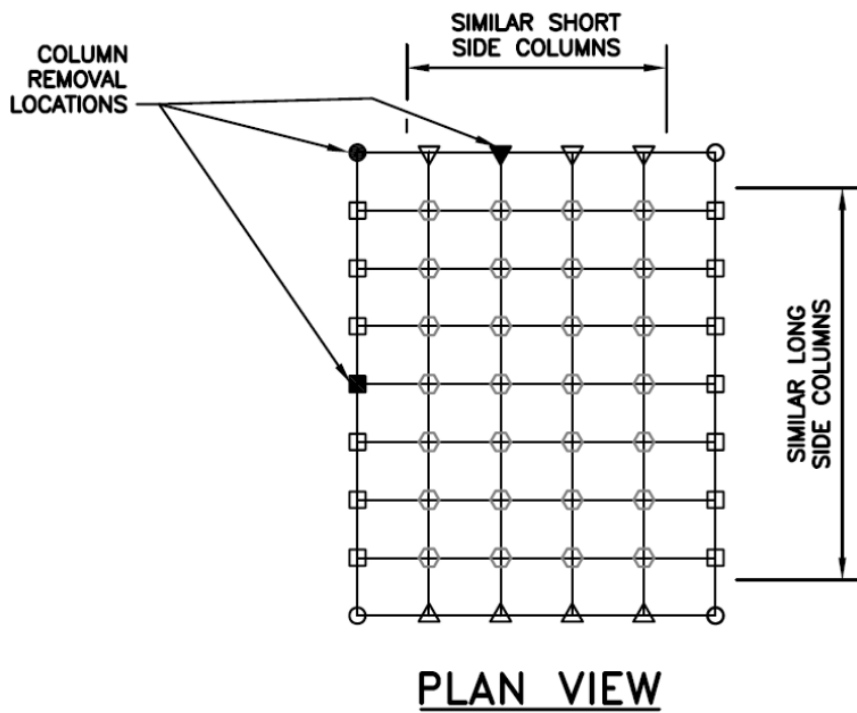


Figure 3.5: External column removal locations, retrieved from [9].

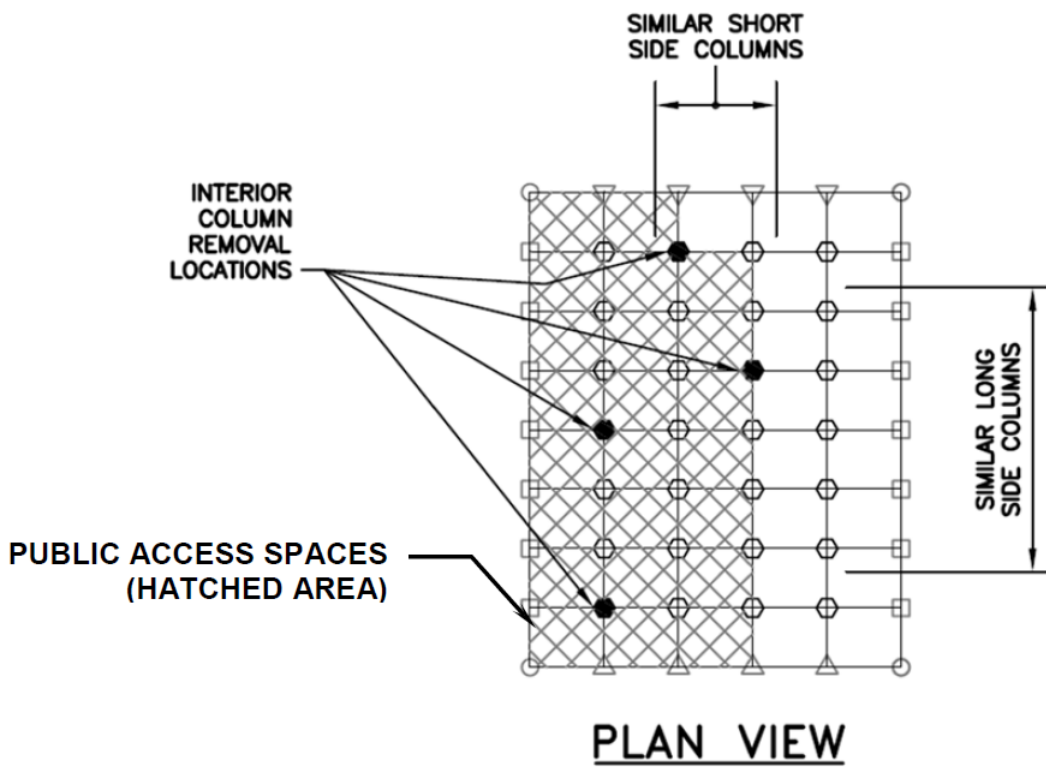


Figure 3.6: Internal column removal locations, retrieved from [9].

actions. For instance, in a moment frame, the moment is considered as a deformation controlled action while shear or axial force is a force controlled action. The load combinations used when designing for the different actions are

$$\begin{aligned} G_{LD} &= \Omega_{LD}(1.2D + (0.5L \text{ or } 0.2S)) \\ G_{LF} &= \Omega_{LF}(1.2D + (0.5L \text{ or } 0.2S)) \\ G &= 1.2D + (0.5L \text{ or } 0.2S) \end{aligned} \tag{3.6}$$

where

- G_{LD} = Increased gravity loads
for deformation controlled actions
- G_{LF} = Increased gravity loads
for force controlled actions
- G = Gravity load
- D = Dead load
- L = Live load
- S = Snow load
- Ω_{LD} = Dynamic load factor for deformation controlled actions
- Ω_{LF} = Dynamic load factor for force controlled actions.

The increased load, G_{LD} and G_{LF} , should only be applied to the affected areas, see Figure 3.7. The remaining structure is loaded with G according to equation 3.6. The magnitude of the dynamic load factors, Ω_{LF} and Ω_{LD} , is dependent on material and type of structural element but is usually a value between 1–2.

Non-linear static

Including non-linear geometrical behaviour enables cable action of the beams. Plastic hinges are also allowed to form along the elements.

The non-linear static method has, unlike the linear static method, no limitations due to irregular geometry. Both primary and secondary elements can be included in the model but the stiffness of secondary elements must be set to zero. Secondary elements must, if they are not included, be checked after the analysis is performed so that they can withstand the displacements and rotations obtained. Stability issues, such as lateral torsional buckling, or buckling of columns must be considered.

The load combination is the same as for the linear static method but with a dynamic load factor that is computed according to the next section.

$$G_N = \Omega_N(1.2D + (0.5L \text{ or } 0.2S)) \tag{3.7}$$

where

G_N = Increased gravity load
 D = Dead load
 L = Live load
 S = Snow load
 Ω_N = Dynamic load factor.

As for the linear static method, the increased load is only applied to affected areas. Remaining parts of the structure is loaded with G , which is computed according to Equation 3.6. This is described in Figure 3.7.

Dynamic load factor using the non-linear static analysis

Load that is applied to the areas affected by a column removal must, because of dynamic effects which are not considered in static procedures, be increased to account for the dynamic effects occurring due to a sudden failure. It is achieved by multiplying the applied load by a dynamic load factor Ω_N (see equation 3.7). The magnitude of Ω_N depends on the ductility of the structural elements. A factor 2 is considered appropriate if the structure should remain elastic, although it could be less if damage and plasticity are allowed to develop in the structure.

A study performed by McKay, Marchand, and Stevens [14], investigated how the dynamic load factors should be determined to better match the static results to the results obtained by performing a dynamic analysis. The study was performed by modelling a structure and perform a non-linear dynamic analysis to determine plastic rotations and deformations. A linear static and non-linear static analysis were performed with different dynamic load factors until a good match between the dynamic models and static models was achieved. The study was performed with different column removal locations and using structures with different characteristics, such as building height and bay spacing.

The result was an equation depending on the allowable plastic rotation of the section divided by the rotation at which the section yields. For steel structures, the recommended value of the dynamic load factor should be computed according to

$$\Omega_N = 1.08 + \frac{0.76}{\frac{\theta_{pra}}{\theta_y} + 0.83} \quad (3.8)$$

where

θ_{pra} = Allowable plastic rotation
 θ_y = Rotation at which the section yields.

For connections, θ_{pra} should be computed for the connection and θ_y is for the connected elements, such as beams and slabs.

Figure 3.8 illustrates how the dynamic load factor depends on the ratio between θ_{pra} and θ_y . A high ductility in the element implies a high ratio which gives a low value for Ω_N . When the ratio approaches zero, which occurs for low ductility in the element, Ω_N reaches a value of two.

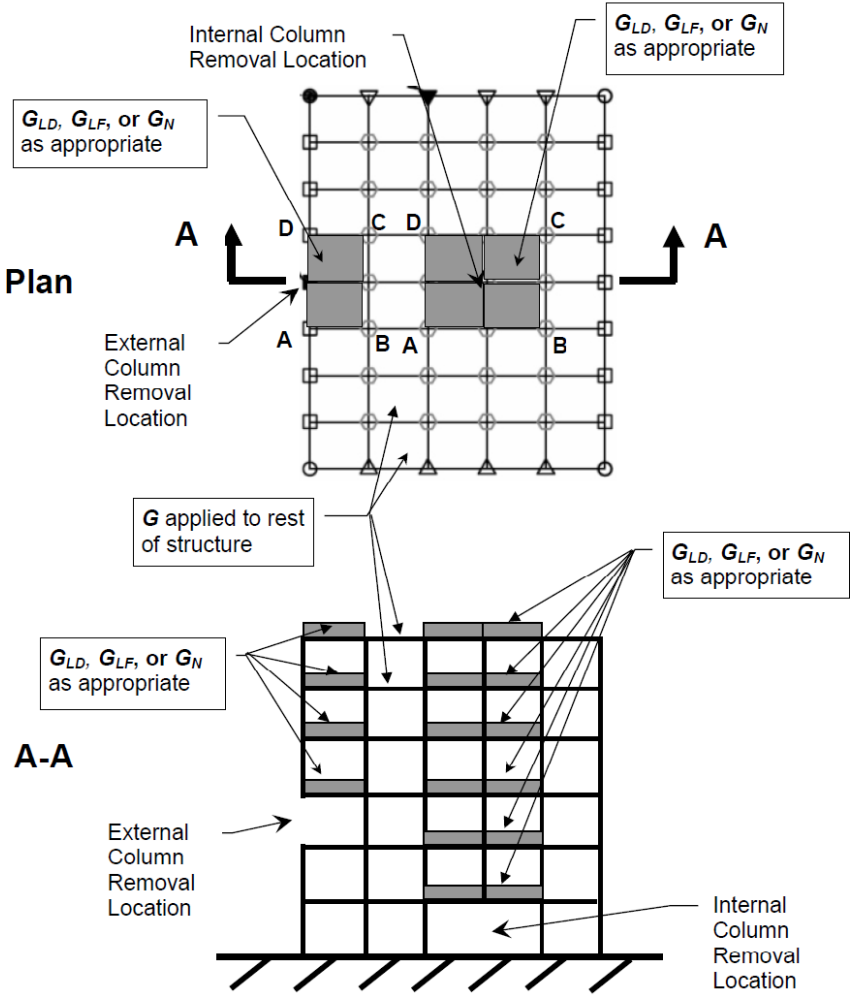


Figure 3.7: The application of a dynamic load factor in the static analysis, retrieved from [9].

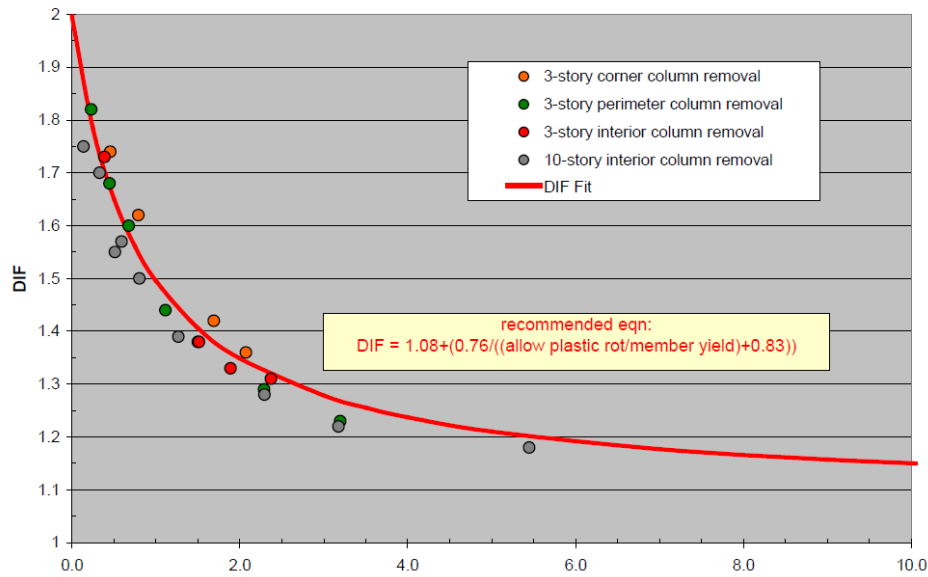


Figure 3.8: Dynamic load factor as a function of $\frac{\theta_{pra}}{\theta_y}$, used for structural steel, retrieved from [9].

The used Ω_N for an entire structure should be the one computed with the lowest ratio between θ_{pra} and θ_y for any primary element, component or connection touching the area defined in Figure 3.7.

Non-linear dynamic

In the non-linear dynamic procedure, the effect of non-linear geometry and dynamics is included and plastic hinges are allowed along the elements.

The procedure is similar to the non-linear static approach but dynamic loading results in that no dynamic load factors are used and loading is computed according to equation 3.7 with $\Omega_N = 1$. The starting condition of the dynamic analysis is when gravity load has been applied to the model and static equilibrium is reached without any removal of elements.

Removal of elements is preferred to be done instantaneously. Otherwise, the time could be determined by computing the period of the structural response mode due to a removal of the element. The removal should then be done in one tenth of that period. The analysis should be performed for a time period equivalent to when a maximum vertical displacement is reached or a full cycle of vertical motion has occurred.

4 The finite element method

In the present chapter, a summary is given of the finite element method and how it is implemented in continuum mechanics. For the reader unfamiliar with the finite element method, it will serve as a short introduction. For derivations and more information about the finite element method, the reader is referred to Ottosen and Petersson [15], Ottosen and Ristinmaa [16] and Krenk [17].

The finite element method is a numerical method to solve differential equations which are used to describe physical problems in mechanics engineering. For instance, a physical problem is described over a region by a differential equation. To solve the differential equation, the region is divided into several finite elements. For each element, approximations are made that holds for that specific element. With this approach, a simple approximation for how a variable varies within an element can be used to describe a more complex variation over the whole region.

In the finite element method, so-called shape functions are used for approximating the variation of the unknown variable within the elements. In solid mechanics, the displacements in x -, y -, and z -direction are the unknown variables.

4.1 Linear static problems

In a static problem, the purpose is to find force equilibrium according to Newton's first law. Figure 4.1 illustrates a simple problem containing a spring. The spring stiffness, k [N/m], describes how the spring deforms if a force is applied to it.

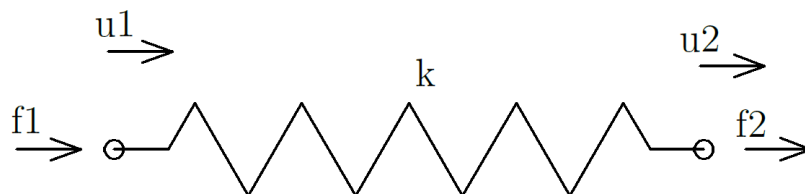


Figure 4.1: Spring with stiffness k .

The equation system which describes the spring in Figure 4.1, is written

$$\begin{bmatrix} k & -k \\ -k & k \end{bmatrix} \begin{bmatrix} u_1 \\ u_2 \end{bmatrix} = \begin{bmatrix} f_1 \\ f_2 \end{bmatrix} \quad (4.1)$$

$$\mathbf{k}_e \quad \mathbf{u} = \mathbf{f} \quad (4.2)$$

where \mathbf{k}_e is referred to as the element stiffness matrix. \mathbf{u} is the displacement vector containing the unknown displacement in node 1 and 2. \mathbf{f} is the external force vector containing the external force in node 1 and 2.

This system contains one degree of freedom in each node, namely the displacement in the horizontal direction. To solve the system of equations, either the force or displacement in each equation must be known. In addition, the displacement u_1 or u_2 must be known, otherwise, the system represents a rigid body motion. For instance, $u_2=0$ can resemble the spring attach to a wall in node two and if a known force, f_1 , is applied to the system the displacement u_1 and the reaction force at node 2, f_2 , can be solved.

The simple spring problem described by Figure 4.1 contains only one spring element. A finite element problem usually contains several elements, each with an element stiffness matrix assembled to a global stiffness matrix describing the stiffness for the entire region containing multiple elements.

All static linear problems using the finite element method implies solving the equation

$$\mathbf{K}\mathbf{u} = \mathbf{f}. \quad (4.3)$$

In solid mechanics, the global stiffness matrix, \mathbf{K} , describes how the region deforms when external forces are applied to it. \mathbf{u} is the displacement vector containing the unknown displacement of every node in the region. \mathbf{f} is the external force vector.

Figure 4.2 illustrates an 8-node solid element. Each node contains three degrees of freedom, namely the displacement in x -, y - and z -direction. Every degree of freedom gives rise to an equation, for an 8-node solid element it implies an equation system with a 24×24 stiffness matrix, a 1×24 displacement vector and a 1×24 external force vector.

The main difficulty is to establish the stiffness matrix \mathbf{K} . For a solid 3D body it is derived from differential equations which describe an equilibrium condition for the body, where stresses within the body give rise to internal forces, to establish equilibrium, the internal forces must be equal to the external forces. By approximating the displacement field in the element, the differential equation can be solved.

Beam and shell elements

An issue with solid elements is that it usually results in a very large number of equations with a large computational cost as a result of it. Another difficulty is to understand the result from the finite-element model because the output only contains stresses and strains.

To reduce the computational cost, some approximations can be done for structural components with certain characteristics. For instance, beams have one dimension that is significantly larger than the other two and can with a good approximation be modelled with beam elements due to that its behaviour is dominated by the stress in the longitudinal

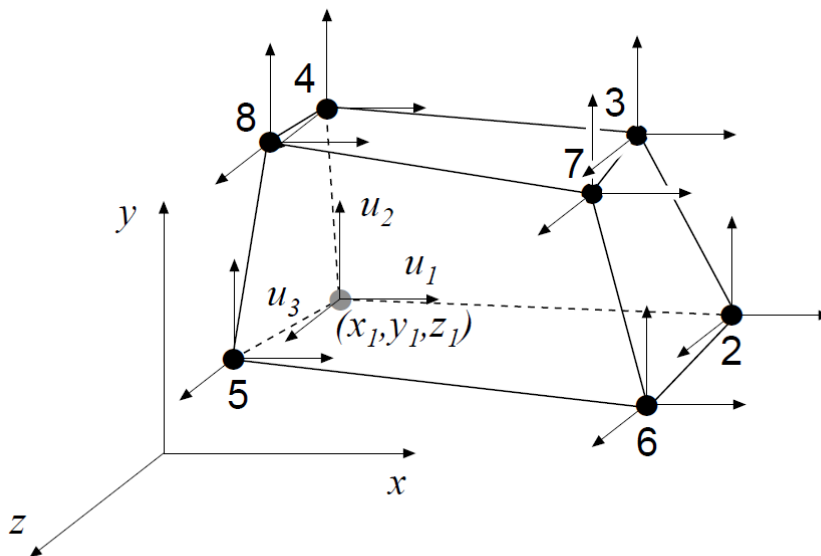


Figure 4.2: 8-node solid element, retrieved from [18].

direction. With the use of beam elements equilibrium is achieved through shear forces, bending moments and normal forces, which also makes the result much easier to interpret for a structural engineer.

Structural components with two dimensions which are significantly larger than the third (thickness), for example slabs, can with a good approximation be modelled with shell elements. In shell elements, stresses in the thickness direction are neglected.

4.2 Non-linear material

If the material of the region is described by a linear-elastic material model, it is straightforward to solve Equation 4.3. If instead a non-linear material model is used, due to the non-linearity of the material, the global stiffness matrix \mathbf{K} changes as the strain of the material changes. It requires a step-wise incremental solution procedure for solving Equation 4.3. This is usually done by an iteration scheme, for example the Newton-Raphson algorithm, which implies solving the equation system [16]

$$(\mathbf{K}_t)(\mathbf{a}^i - \mathbf{a}^{i-1}) = \mathbf{f}_{n+1} - \mathbf{f}_{int} \quad (4.4)$$

where \mathbf{a}^i is the current displacement for iteration, i , which is to be solved, \mathbf{a}^{i-1} is the displacement in the previous iteration. \mathbf{f}_{n+1} is the new known load and \mathbf{f}_{int} is the internal forces in the previous iteration. \mathbf{K}_t is the tangent stiffness matrix describing the stiffness of the region with the current strain of the material.

Using the Newton-Raphson algorithm and solving the equation implies controlling the equilibrium of forces while the load is applied. It is achieved in the Newton-Raphson algorithm by controlling that the internal and external forces are equal. If not, a systematic iteration procedure is performed where the displacements are adjusted until the external

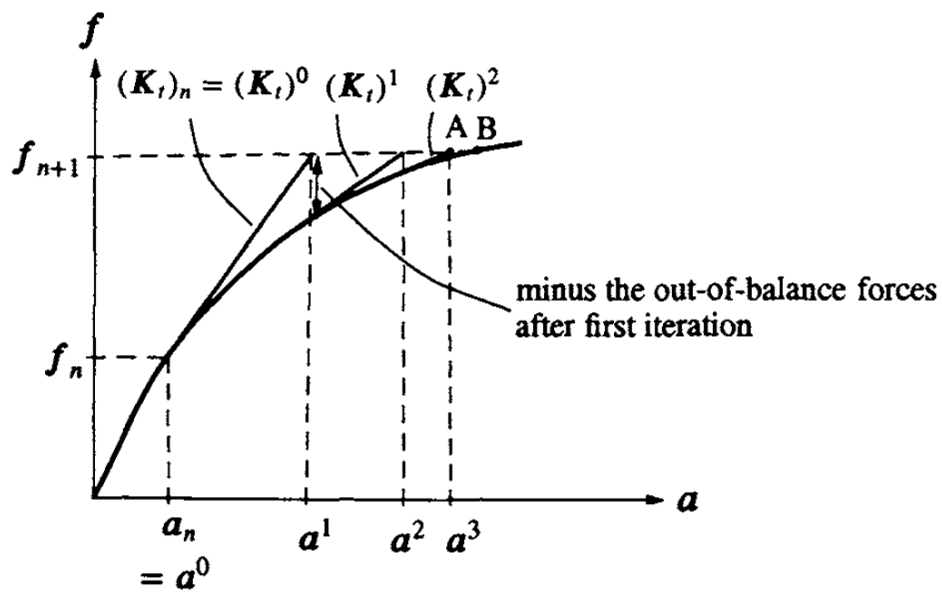


Figure 4.3: The Newton-Raphson algorithm, retrieved from [16].

and internal forces are equal enough. The principle is illustrated in Figure 4.3 and by the iteration scheme in Algorithm 1.

For a more detailed description of non-linear material solution procedure, the reader is referred to Ristinmaa and Ottosen [16].

For load step $n=0,1,2,3,\dots,n_{max}$.

- Apply the new load.
- Iterate $i=1,2,3,\dots$ until: $\mathbf{f}_{n+1} \approx \mathbf{f}_{int}$
 - Compute the stiffness matrix, \mathbf{K}_t .
 - Determine the new displacements, \mathbf{a}^i by solving Equation 4.4.
 - Determine the strains for iteration i .
 - The stress, σ^i , is determined from the strains.
 - Compute the internal forces, \mathbf{f}_{int} .

End iteration loop.

- Accept new displacements, stresses, strains and internal forces.

End load step.

Algorithm 1: Newton-Raphson iteration scheme.

Plasticity

A plastic material is a typical non-linear material. To model plasticity a yield criterion is used to determine when the material yields. Plasticity is a material specific property and different yield criteria are used for different materials. For more detailed information about plasticity theory, the reader is referred to Ristinmaa and Ottosen [16].

The von Mises yield criterion is often used to model the plasticity of steel and is written

$$\sqrt{3J_2} - \sigma_{y0} = 0 \quad (4.5)$$

where

$$\begin{aligned} \sqrt{3J_2} = \sigma_{eff} = & \left[\frac{1}{2} [(\sigma_{11} - \sigma_{22})^2 + (\sigma_{22} - \sigma_{33})^2 + (\sigma_{33} - \sigma_{11})^2] \right. \\ & \left. + 3(\sigma_{12}^2 + \sigma_{23}^2 + \sigma_{31}^2) \right]^{1/2} \end{aligned} \quad (4.6)$$

σ_{y0} = Initial yield stress in pure tension.

Figure 4.4 illustrates the von Mises yield surface in a principal stress space. If the surface is reached due to the stresses within the material, the material will yield. The figure shows an interesting characteristic of this material model, namely that an infinite hydrostatic stress, where $\sigma_{11} = \sigma_{22} = \sigma_{33}$, can be applied without yielding of the material.

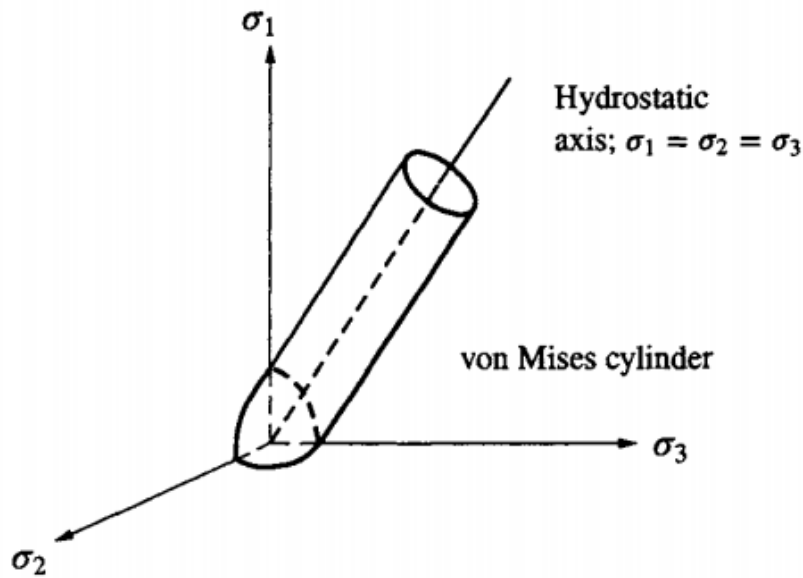


Figure 4.4: von Mises in a principal stress space, retrieved from [16].

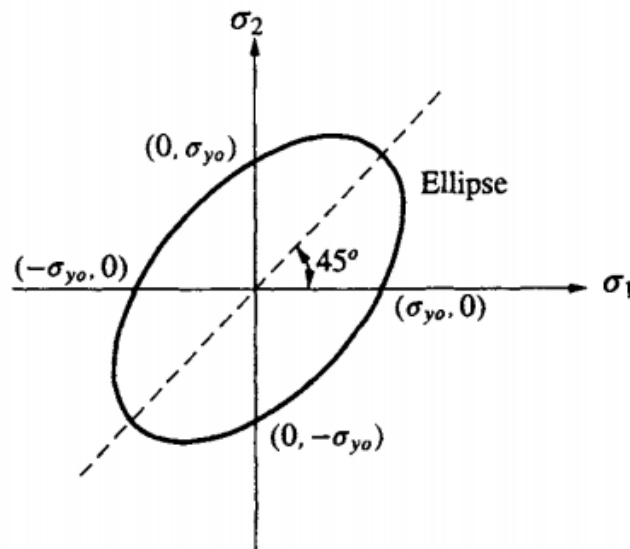


Figure 4.5: von Mises yield criterion in the σ_1 - σ_2 -plane, retrieved from [16].

Consider the cylinder representing the von Mises yield surface in Figure 4.4. In a plane stress problem, where $\sigma_3 = 0$ the yield surface is represented by an ellipse in the σ_1 - σ_2 -plane which is shown in Figure 4.5. An interesting characteristic is that in pure compression or tension in two perpendicular directions, the yield starts at a higher value than in one-dimensional tension or compression. Although, if for instance loading is applied as compression in the 1-direction and tension in 2-direction, the material starts to yield at a lower stress compared to the one-dimensional situation.

If the yield surface is constant and the material behaves linear elastic within the yield surface, it is called an ideal-elastic-plastic material. In one-dimensional loading an ideal-elastic-plastic material is represented by the stress-strain curve shown in Figure 4.6.

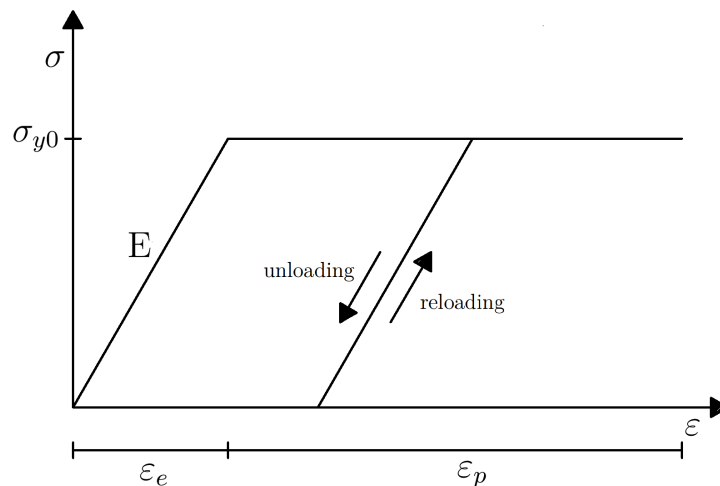


Figure 4.6: Stress-strain curve for an ideal-elastic-plastic material with one-dimensional loading-unloading-reloading. ε_e is the elastic strain and ε_p is the plastic strain.

Steel is not ideal plastic and usually hardens as it undergoes a plastic deformation. A hardening model commonly used is the isotropic hardening plasticity model. For the von Mises yield surface shown in Figure 4.4, isotropic hardening means that

$$\sigma_y = \sigma_y(\varepsilon_p) \quad (4.7)$$

where σ_y is the yield stress and ε_p is the plastic strain. An increased yield stress implies that the diameter of the yield surface has increased. If the material is unloaded and loaded again, it will yield at a higher stress.

Effective plastic strain

A plastic strain measure often used is the effective plastic strain which includes the strain in all directions and can be interpreted in the same way the von Mises effective stress. The effective plastic strain is written

$$\varepsilon_{eff}^p = \left(\frac{2}{3} \varepsilon_{ij}^p \varepsilon_{ij}^p \right)^{\frac{1}{2}} = \frac{2}{3} [(\varepsilon_{11}^2 + \varepsilon_{22}^2 + \varepsilon_{33}^2) + 2(\varepsilon_{12} + \varepsilon_{23} + \varepsilon_{13})] \quad (4.8)$$

4.3 Non-linear geometry

In chapter 4.2, the change of material elasticity, as it underwent deformation, gave rise to a non-linear problem. Non-linearity could also occur due to a change of geometry in the structure being analysed. If the displacements are small enough the effect of the changed geometry could be neglected. It is usually the case in structural engineering where linear finite element method is most often used.

In the present section a short introduction to the principle of non-linear-geometrical behaviour is presented. For a more detailed description and derivation of the non-linear finite element method the reader is referred to Krenk [17].

To solve non-linear geometrical finite element problems, the same concept as for non-linear material is used where the load or displacement is applied in increments. For every load increment, the geometry of the structure changes and therefore also its stiffness. The new stiffness, referred to as the tangential stiffness of the system, \mathbf{K}_t , could be determined after every load increment, by for instance using the Total Lagrangian formulation, where

$$\mathbf{K}_t = \mathbf{K}_0 + \mathbf{K}_\sigma + \mathbf{K}_u. \quad (4.9)$$

\mathbf{K}_0 is the initial linear stiffness matrix used in the linear finite element method, \mathbf{K}_σ is the contribution due to internal forces and \mathbf{K}_u is contribution due to displacements and the changed geometry.

Strain measures

Another difference compared to the linear static method is how strain is measured. In linear static analyses, a strain measure, referred to as engineering strain is used. For a one-dimensional bar engineering strain is given by.

$$\varepsilon = \frac{l - l_0}{l_0} \quad (4.10)$$

Where l is the current length and l_0 is the initial length of the one-dimensional bar.

An example of another strain measure is the logarithmic strain which for the one-dimensional bar is given by [19].

$$\varepsilon = \ln\left(\frac{l}{l_0}\right). \quad (4.11)$$

The logarithmic strain is often used in non-linear finite element programs. A comparison between engineering and logarithmic strain is shown in Figure 4.7. The strain has been plotted as a function of the stretch given by

$$\Lambda = \frac{l}{l_0} \quad (4.12)$$

and as the diagram shows, for a minor stretch, the strain measure does not differ but the difference increases with an increase of the stretch.

4.4 Dynamic problems

Consider the spring in Section 4.1 attached to a wall in node 2 and a mass in node 1, see Figure 4.8. If a force is applied to the mass in node 1, the displacement u_1 can be solved where the system is in static equilibrium. The solution will not depend on how the load vary with time just the magnitude and direction.

In a dynamic situation, the solution is dependent on how the force varies with time. For instance, if a force, $f(t)$, is applied instantly with a maximum value, it will cause acceleration of the mass, m . The moving mass will result in a larger maximum spring force and deformation than in the static problem because an additional force is needed to stop the mass according to Newton's second law of motion. Finally, the spring would reach a steady state with a sinusoidal variation of the displacement with respect to time.

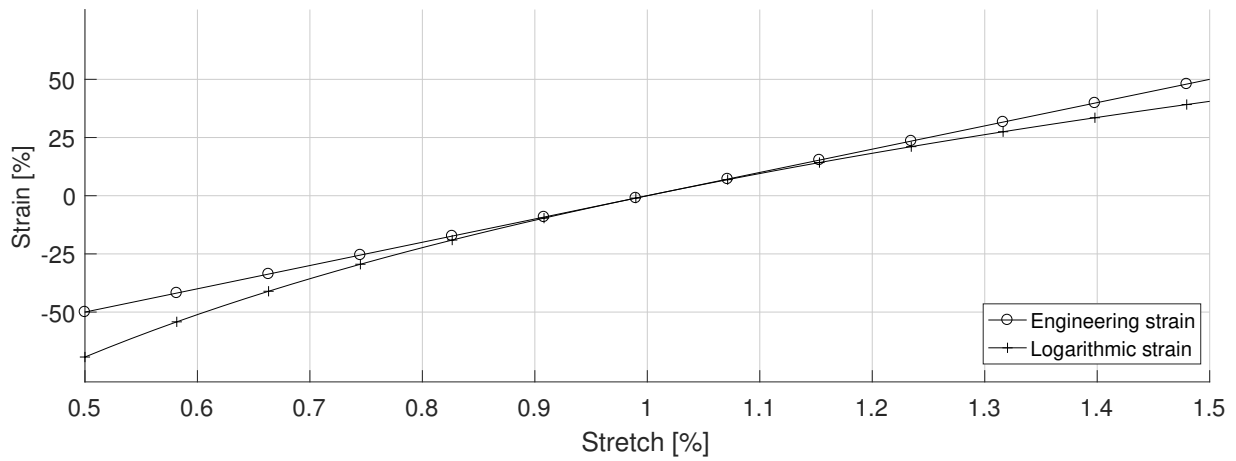


Figure 4.7: Comparison of strain measures. The figure shows logarithmic and engineering strain as a function of the stretch in a one-dimensional bar.

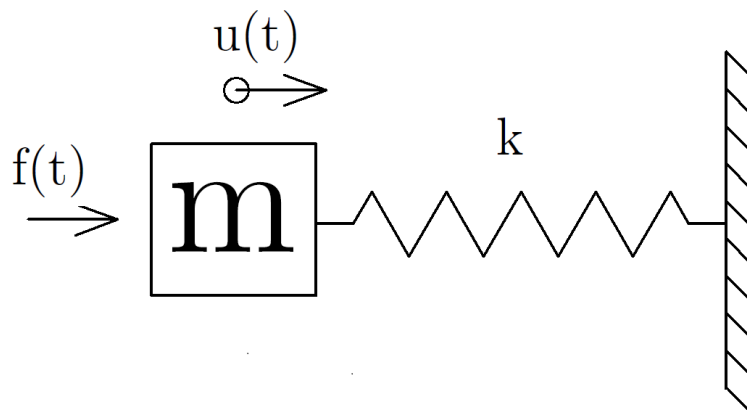


Figure 4.8: Dynamic single degree of freedom system containing a spring with stiffness k , attached to a mass, m

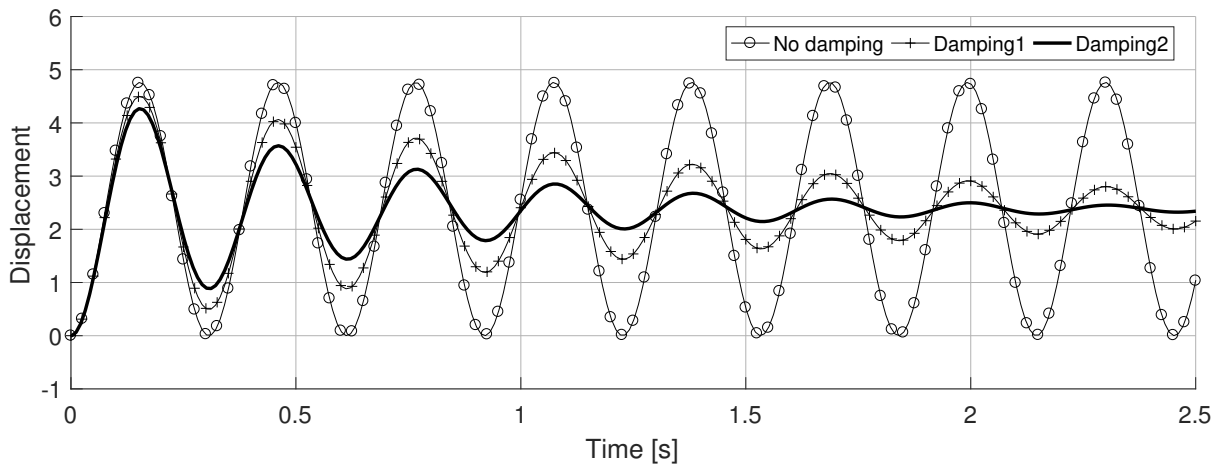


Figure 4.9: The effect of damping when an instant load is applied to the mass in Figure 4.8.

The dynamic system illustrated in Figure 4.8 is described by the equation of motion, which compared to the static equation also includes mass and acceleration. For a multi-degree of freedom system, the equation of motion is written

$$\mathbf{M}\ddot{\mathbf{u}} + \mathbf{K}\mathbf{u} = \mathbf{f}(t) \quad (4.13)$$

where

$$\begin{aligned} \mathbf{M} &= \text{Mass matrix} \\ \mathbf{K} &= \text{Stiffness matrix} \\ \ddot{\mathbf{u}} &= \text{Acceleration vector} \\ \mathbf{u} &= \text{Displacement vector} \\ \mathbf{f} &= \text{External load vector.} \end{aligned} \quad (4.14)$$

Solving the dynamic equation system usually involves a time stepping iteration scheme. In structural dynamics, the dynamic implicit method is often used which is suitable for problems with long duration in time [19].

Damping

The spring in the example above is a very idealised model, in a more realistic model, it would finally reach a static state. This is because the energy in the system is dissipated due to damping. Damping in structures is difficult to estimate by mathematical models because the energy dissipating mechanisms, such as friction in connections and cracking of concrete are complicated events [20].

Figure 4.9 illustrates how damping affects the displacement over time when an instant constant load is applied to the mass in Figure 4.8.

In the equation of motion, damping is represented by the damping matrix \mathbf{C} and results in damping forces which vary with the velocity. The equation of motion including damping is written

$$\mathbf{M}\ddot{\mathbf{u}} + \mathbf{C}\dot{\mathbf{u}} + \mathbf{K}\mathbf{u} = \mathbf{f}(t) \quad (4.15)$$

where

\mathbf{M} = Mass matrix

\mathbf{C} = Damping matrix

\mathbf{K} = Stiffness matrix

$\ddot{\mathbf{u}}$ = Acceleration vector

$\dot{\mathbf{u}}$ = Velocity vector

\mathbf{u} = Displacement vector

\mathbf{f} = External load vector.

A damping model often used is Rayleigh damping. It consists of mass-proportional damping and stiffness proportional damping which together forms the C-matrix [20].

$$\mathbf{C}_M = a_0\mathbf{M} \quad \mathbf{C}_K = a_1\mathbf{K}_T \quad (4.16)$$

Where \mathbf{M} is the constant mass matrix and \mathbf{K}_T is the tangent stiffness matrix.

a_0 and a_1 are chosen by solving the equation system.

$$\begin{bmatrix} 1/\omega_i & \omega_i \\ 1/\omega_j & \omega_j \end{bmatrix} \begin{bmatrix} a_0 \\ a_1 \end{bmatrix} = \begin{bmatrix} \zeta_i \\ \zeta_j \end{bmatrix} \quad (4.17)$$

Where ζ_i is the damping ratio for the angular frequency w_i . Damping ratios in structures usually vary between 1-20% [20]. With the Raleigh damping model, the damping ratio is dependent on the frequency of the vibration in the structure. This is illustrated in Figure 4.10, where the total damping is a sum of the mass proportional and stiffness proportional damping and varies with the frequency.

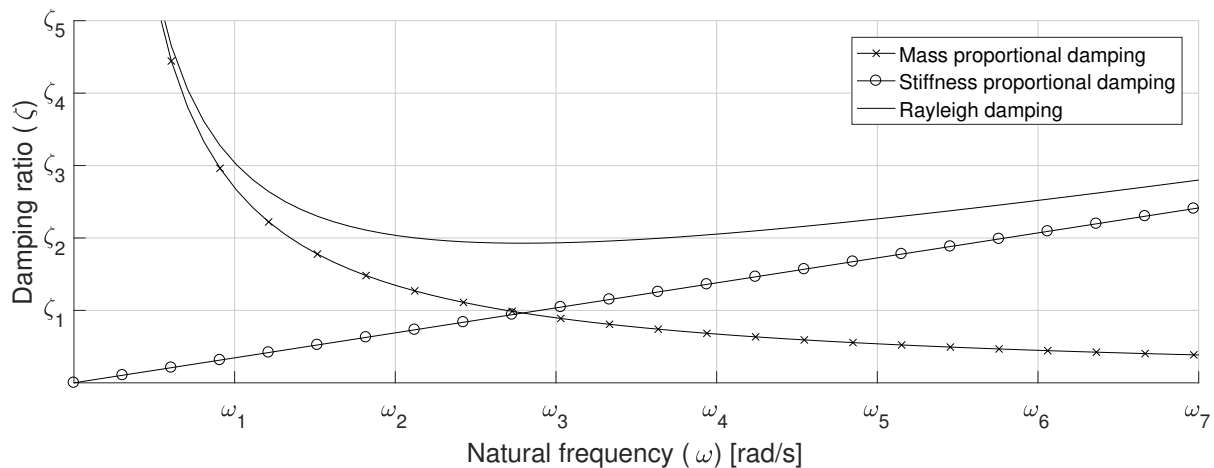


Figure 4.10: Raleigh damping.

5 Non-linear analysis of beams

Bridging over failed columns is, as discussed in the theory of progressive collapse design, essential to avoid a progressive collapse of a building. Bridging over failed columns is enabled by cable action of the ties, that is, the continuous beams in the studied building. It is only possible to achieve cable action of numerical beam models if non-linear effects are taken into account. It is usually not the case when designing structures, where linear analyses are often used. Therefore, it is not obvious what actually happens in a non-linear analysis of a beam that is loaded to failure.

In the following chapter, an investigation was performed to study the non-linear effects in beams. Various numerical models of single beams were created and loaded to failure using the finite element program Abaqus [21]. The purpose of this study was to enhance the understanding of the results from non-linear analyses of beams, it is important when the results from the progressive collapse analysis are to be interpreted.

Another purpose was to investigate how the results differ between beams modelled with solid elements as compared to beams modelled with beam elements. It is especially important in the beam-element model of the HSQ-profiles because some simplifications of the cross-section are needed. Therefore, it is important to ensure that the simplified cross-section in the beam-element model can represent a beam with the real cross-section.

5.1 Method

The finite element program, Abaqus, was used to create the numerical models.

In the facade of the studied building, the span length between supports is 5.4 m. In the event of a removed column, the span length is doubled to 10.8 m, which was the length chosen for all beam models.

The ends of the beams were fully restricted to displacement and rotation because the connections in the studied building, between columns and beams, are considered as moment stiff.

An evenly distributed load was applied on the beam, the magnitude of the load was greater than the capacity of the beam which resulted in a failure. Figure 5.1 illustrates how the beam was modelled.

The material was modelled as an ideal-elastic-plastic material, described in Section 4.2, with an elastic modulus E of 210 GPa and Poisson's ratio of 0.3. Steel S355 was used, it has a capacity of 355 MPa before it reaches its yield stress [22]. Plasticity was modelled with a von Mises yield criterion without hardening, see Section 4.2.

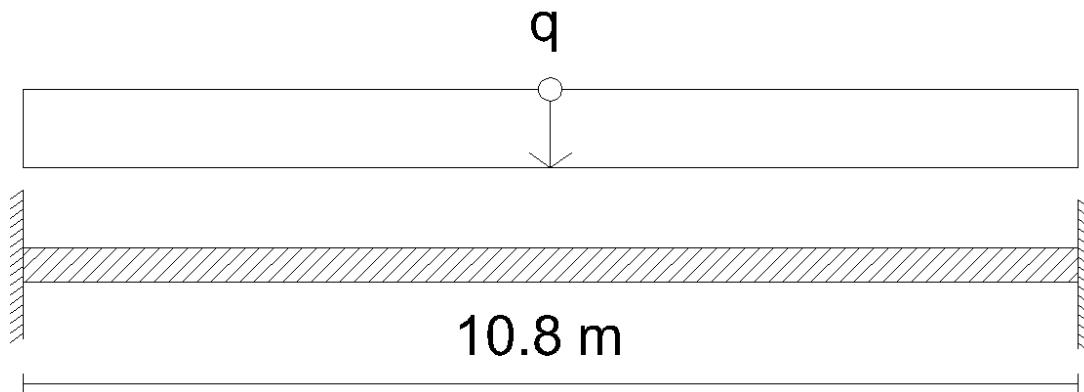


Figure 5.1: Support and loading conditions for the studied beam.

5.2 Modelling and results

5.2.1 Rectangular-/quadratic cross-sections

Modelling

HSQ-profiles are used in the building, but rectangular cross-sections were, for simplicity, studied at first. Beams with three type of cross-sections were modelled and their behaviour was studied, as they were loaded to failure. The studied cross-sections are shown in Figure 5.2.

The beam cross-section dimensions were chosen with an equal cross-section area so that the normal force capacity was equal, but not the moment capacity. When designing a typical building, cross-section C would most likely be used due to a larger moment capacity using the same amount of material as cross-section A and B.

The modelling of the quadratic cross-section (B) was done using both solid elements and beam elements and the results were compared. The purpose was to see how the use of beam elements would affect the results and beam behaviour because beam elements does not account for all effects.

For the solid-element models, boundary conditions were applied by restricting all displacements of the nodes at the red surface as illustrated in Figure 5.3. For the beam-element model, all displacement and rotational degrees of freedom were restricted at the ends.

The Load was applied as a surface traction load on the solid-element model and a line load on the beam-element model. The surface traction load was adjusted so that the total load was equal for all models, namely 1 MN/m.

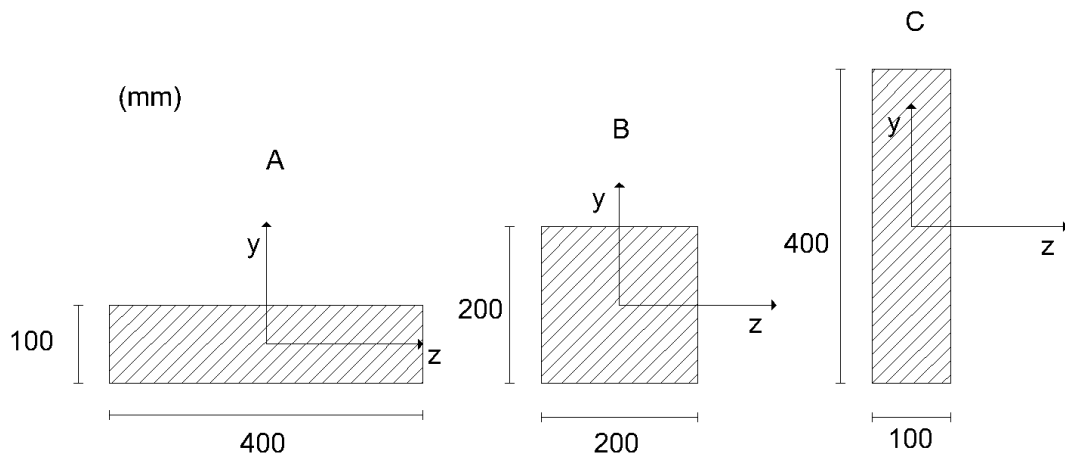


Figure 5.2: Cross-section dimensions used for the beam models.

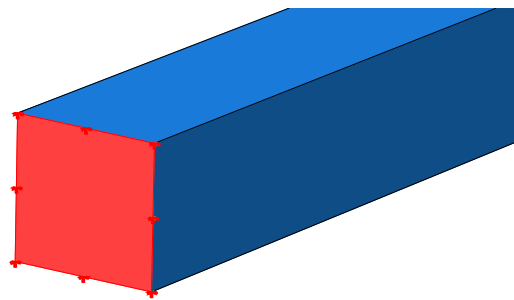


Figure 5.3: The principle of how boundary conditions were applied to the solid-element beam. The displacements in each node at the red surface were restricted.

Results

Quadratic cross-section – beam and solid elements

The results from analysing a beam with a quadratic cross-section, modelled with solid elements and beam elements were compared by extracting moment and normal force as a function of the applied load. This was done at two points in the beam, referred to as "Edge" and "Middle", see Figure 5.4.

In Figures 5.5–5.7 the results are presented from an analysis of a beam with a quadratic cross-section modelled with solid elements and beam elements. Figures 5.5–5.6 show the moment and normal force at point Edge and Middle. Figure 5.7 shows the displacement at point Middle.

The results show a typical behaviour for a beam when non-linear effects are included. At first, the moment at both point Edge and Middle increases quite dramatically while the normal force is limited. The moment at point Edge reaches a maximum first, at this load, the normal force starts to increase faster and contributes to the load capacity of the beam. In a linear analysis, the only way to increase the load, when the maximum

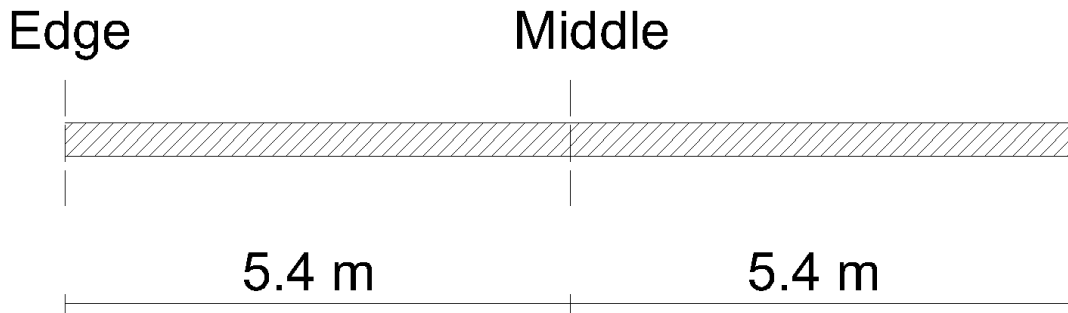


Figure 5.4: Beam cuts at point Edge and Middle where internal forces were extracted.

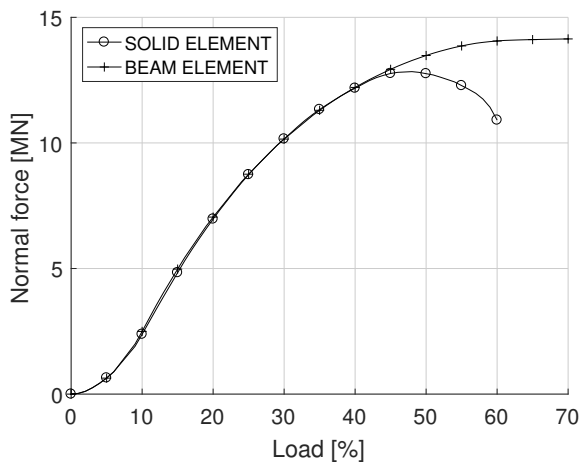
moment at point Edge is reached, would be to increase the moment at point Middle.

It is shown in Figure 5.7 that the beam stiffness is greater in the beginning when equilibrium is achieved through the increase of bending moment. When the moment reaches a maximum, at about 10% of the load, the beam starts to act similar to a cable and carries the load through normal force. At 10% load, the displacement is too small for the beam to effectively act as a cable, which is why the deformation starts to accelerate.

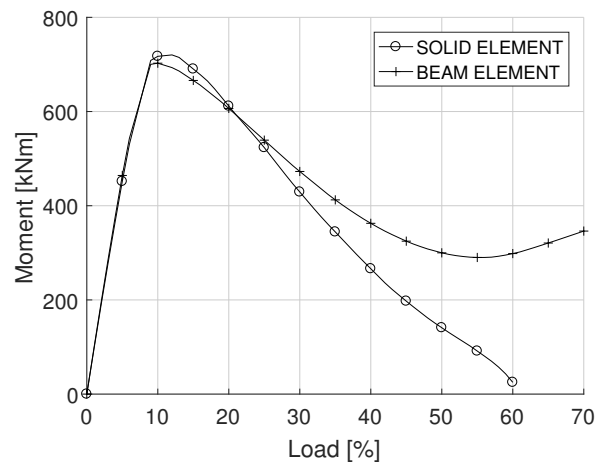
A difference using the beam-element model, compared to the solid-element model, was that the capacity was significantly larger with beam elements. This is due to that a change of the cross-section geometry is not accounted for using beam elements. It leads to an ability, in the beam-element model, to increase the external load even when the maximum normal force in the beam is reached. The beam keeps deforming which increases the external load capacity even if the normal force is constant in the beam. It is a problem if the beam elements overestimate the capacity because beam elements will often be used when progressive collapse analyses are performed.

The solid-element beam model was not capable of deforming with a constant normal force to achieve equilibrium, it was probably due to the large strain at the supports, see Figure 5.8. The cross-section area drastically decreases in size, which also decreases the normal force capacity in the beam. Figures 5.5a and 5.6a show that the normal force decreases but the external load is still increasing. The large deformation that can be seen in Figure 5.7, enables an increase of the external load even if the normal force in the beam is decreasing.

Figure 5.9 shows the stress distribution in the beam cross-section of the quadratic solid-element beam while it was loaded to failure. At first, the load carrying mechanism is dominated by bending moment in the beam, the stress distribution is similar to a linear analysis. As the deformation and load increases, the yield stress is reached and the neutral axis is moving downwards due to the increased normal force in the beam.

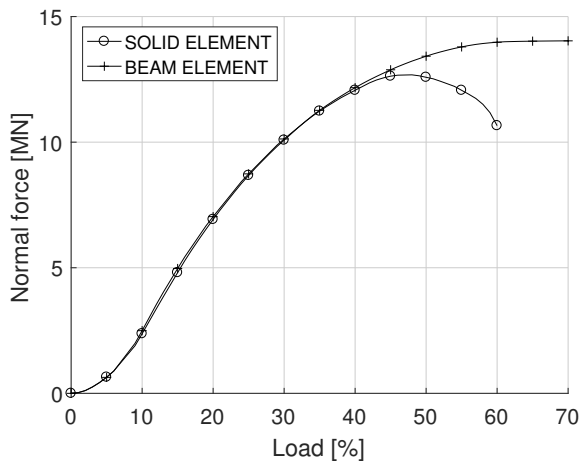


(a) Normal force.

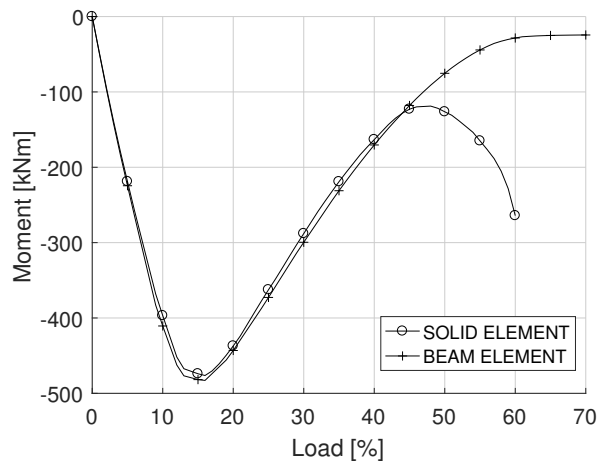


(b) Moment.

Figure 5.5: Moment and normal force at point Edge.



(a) Normal force.



(b) Moment.

Figure 5.6: Moment and normal force at point Middle.

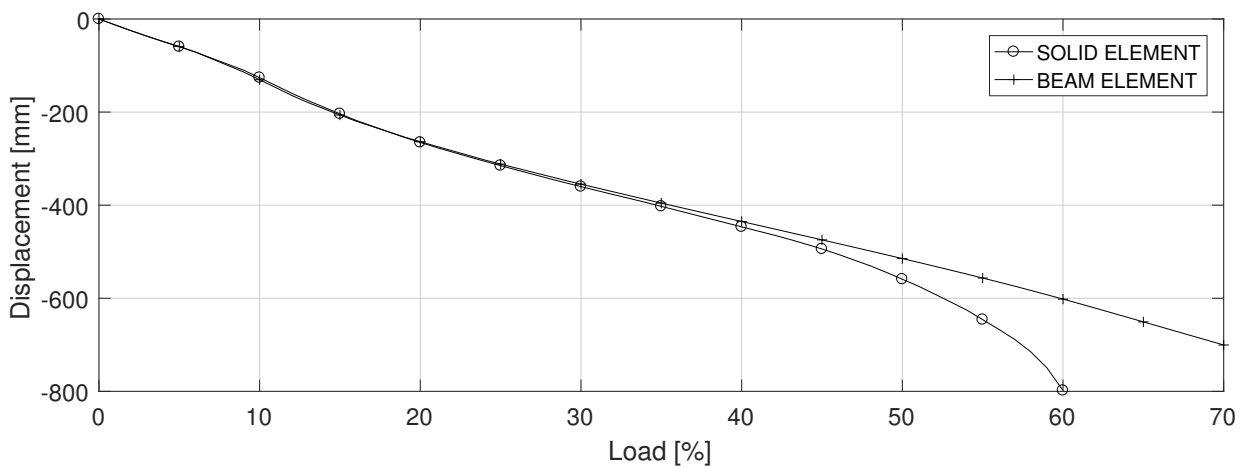


Figure 5.7: Vertical displacement at point Middle.

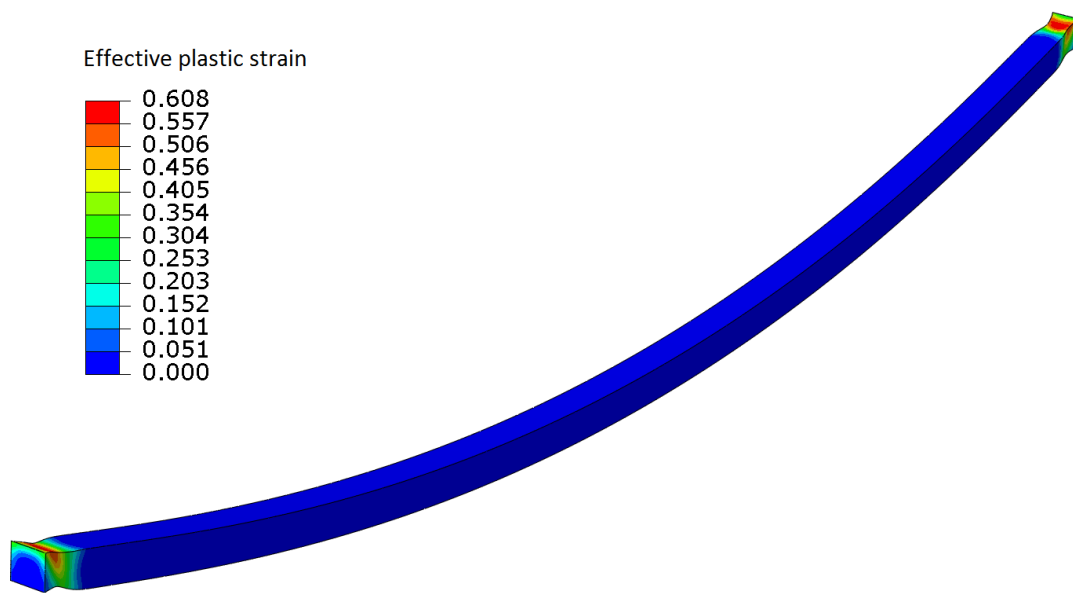
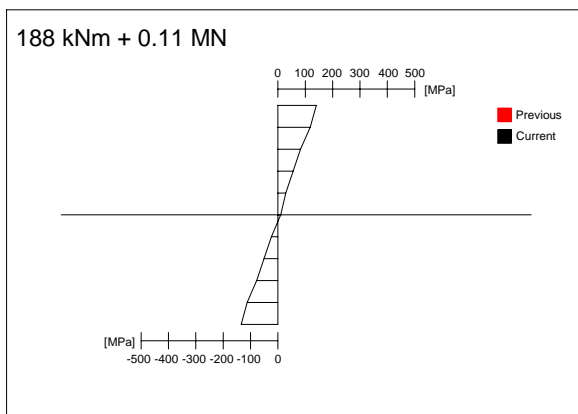
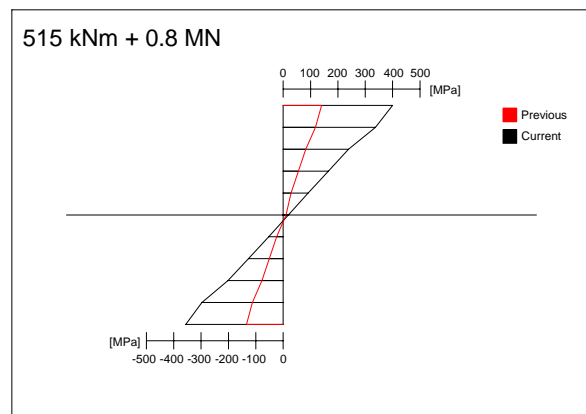


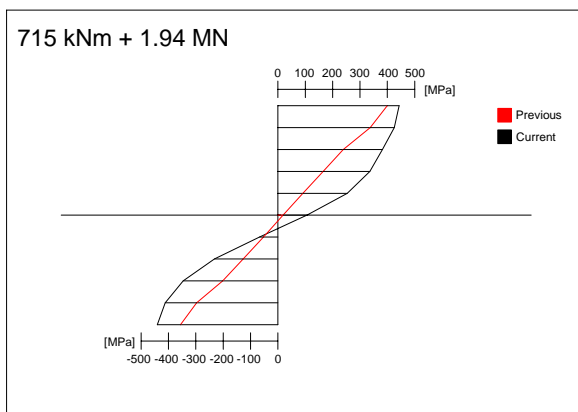
Figure 5.8: Large effective plastic strain in the solid-element beam, at the supports, when the maximum load was applied.



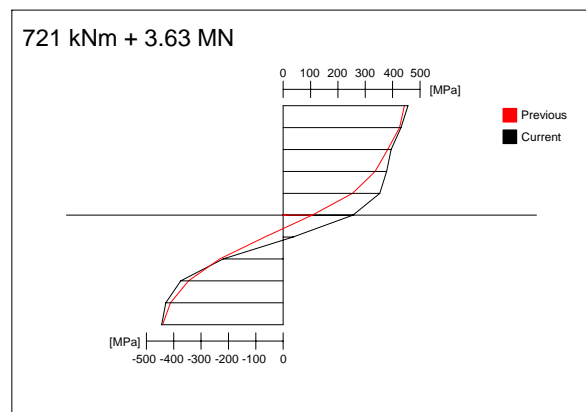
(a) 2% of the external load applied.



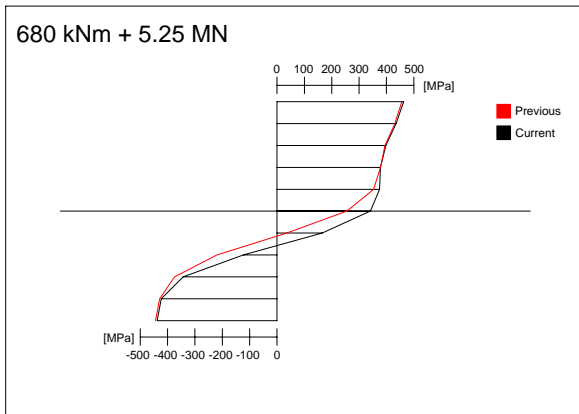
(b) 5.75% of the external load applied.



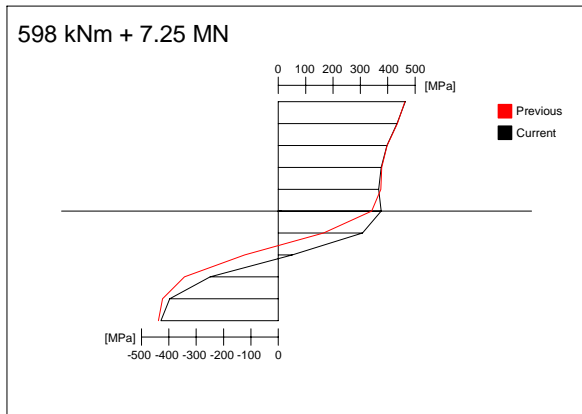
(c) 9.13% of the external load applied.



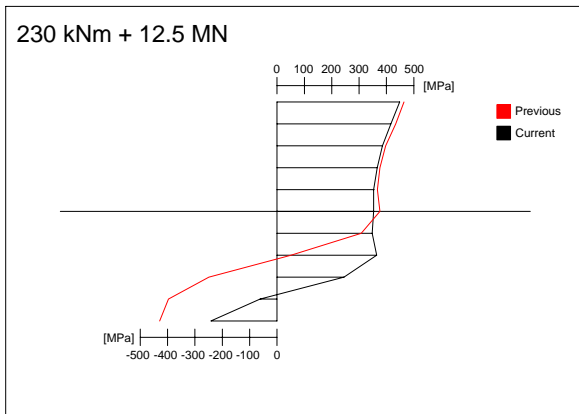
(d) 12.5% of the external load applied.



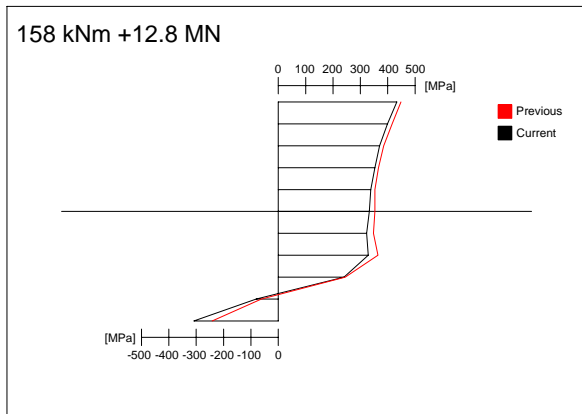
(e) 15.9% of the external load applied.



(f) 20.7% of the external load applied.



(g) 42.4% of the external load applied.



(h) 48.3% of the external load applied.

Figure 5.9: Moment, normal force and stress distribution at point Edge in the quadratic solid-element beam, when it was loaded to failure. Previous is the stress distribution with the moment and normal force from the previous figure and current is the stress distribution with the moment and normal force in the current figure.

Effect of cross-section dimensions

The following section presents the results from analyses of beams that was modelled with solid elements using three different beam cross-sections. The different cross-sections are referred to as rectangular lying (A), quadratic (B) and rectangular standing (C) as shown in Figure 5.2.

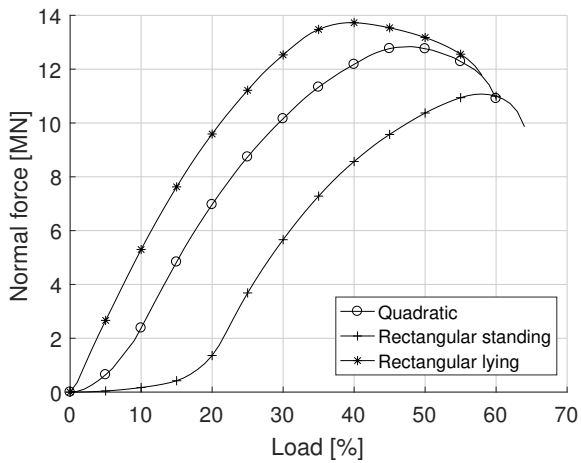
The moment and normal force at point Edge and Middle are shown in Figures 5.10 and 5.11. The displacement at point Middle is shown in Figure 5.12.

The developed moment differs due to the different moment capacity of the three cross-sections, as shown in Figures 5.10 and 5.11. The beam with a standing rectangular cross-section was much stiffer, which is shown in Figure 5.12. The less bending stiff beams had the highest increase of normal force. It is not surprising because the limited moment capacity must be compensated by a higher normal force in the beam to achieve static equilibrium. The maximum load of the beams with the three cross-sections did not differ much. For the capacity of the beam, it is mainly the cross-section area that is important rather than a large moment of inertia, if cable action can be utilised.

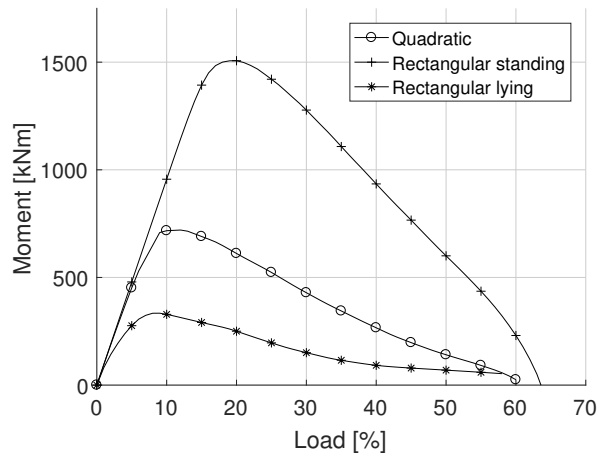
If the analyses had been done of real beams in a lab, a failure in the material would probably make the beam fail before the maximum load was reached. The effective plastic strain was, as shown in Figure 5.13, much higher for the standing rectangular cross-section. In Eurocode [22], steel class S355 should at least be capable of an elongation not less than 15%. Although it is a conservative limit for steel class S355, a more reasonable limit would be 20–25%. For class S235 an even higher strain of about 30% is possible [23]. In Appendix D the stress-strain relation for different steel classes is shown.

If for instance a 15% effective plastic strain would be allowed in the material, the least moment stiff cross-section is a better choice because it has a higher load capacity. It is because it can deform and make use of effective cable action without high strain in the material. However, the difference in strain, differ between the cross-sections, with the applied load. At a load less than 20%, the rectangular standing cross-section was a better choice, although, with a load at 30% the maximum strain (15%) was reached in the beam with the rectangular standing cross-section, but not in the two other beams. Figure 5.14 shows the effective plastic strain when 30% of the load was applied on the beams with the three different cross-sections.

It should be noted that the strain output from Abaqus is the logarithmic strain. For the strain limit of 15%, which is specified as a minimum for steel S355 in Eurocode [22], Eurocode does not mention which strain measure that should be used. However, for strains within 0–30%, the difference between logarithmic and engineering strain is considered as negligible, cf. Figure 4.7.

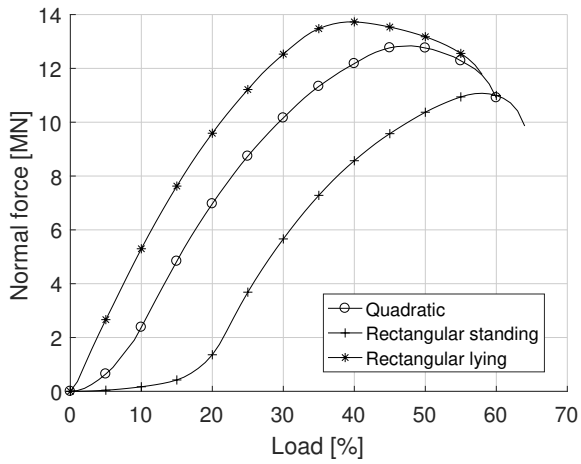


(a) Normal force.

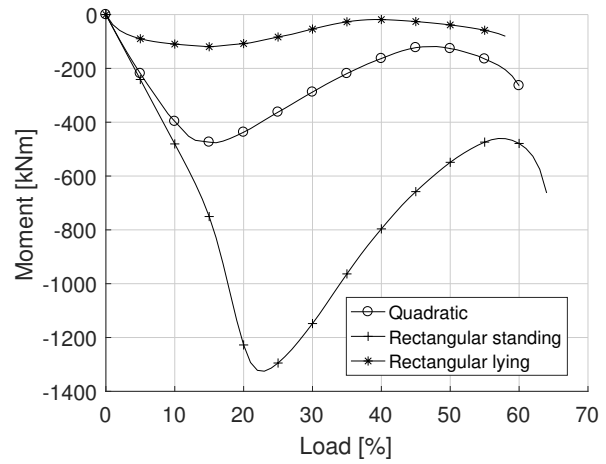


(b) Moment.

Figure 5.10: Moment and normal force at point Edge.



(a) Normal force.



(b) Moment.

Figure 5.11: Moment and normal force at point Middle.

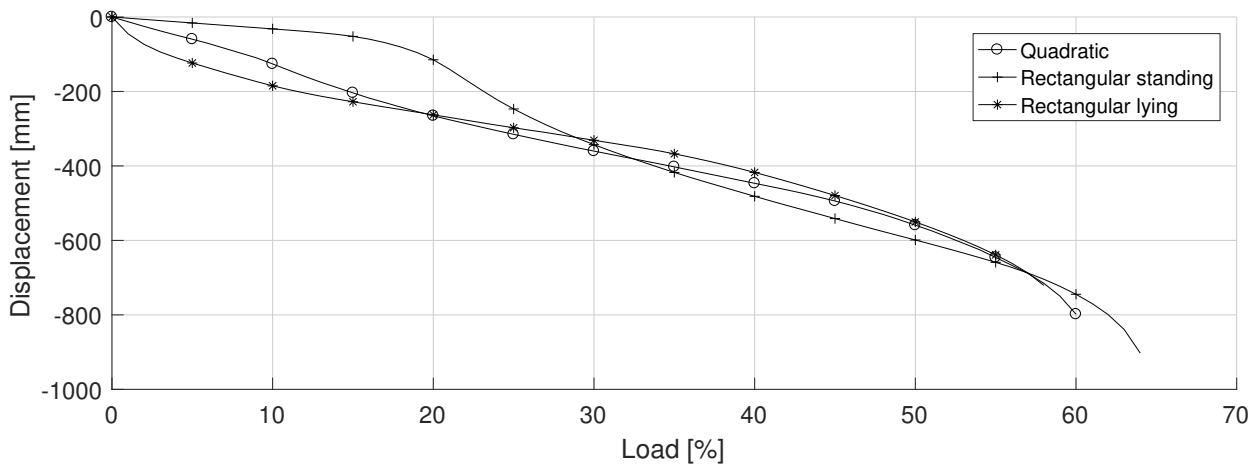


Figure 5.12: Vertical displacement at point Middle.

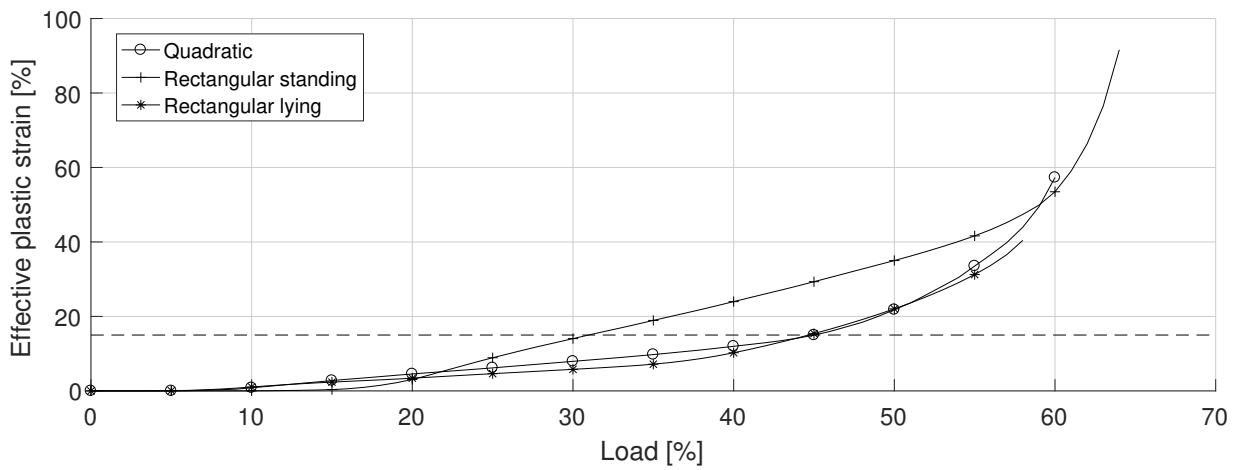


Figure 5.13: Maximum effective plastic strain in the beam using different cross-sections.

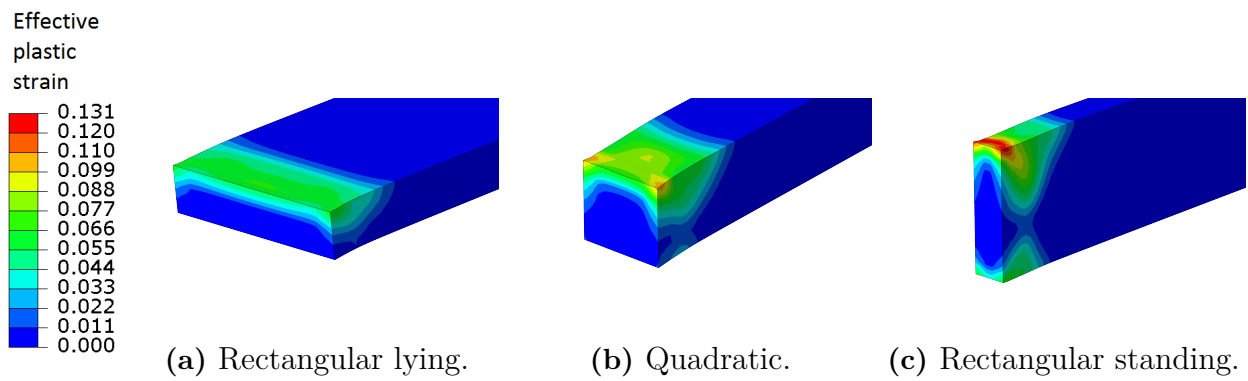


Figure 5.14: Maximum effective plastic strain using different cross-sections. 30% of the load was applied on the beams.

5.2.2 HSQ-profiles

Modelling

Two types of HSQ-profiles are used in the example building studied in the thesis. Both of these profiles were studied in the present chapter. The study was performed because the HSQ cross-section had to be simplified when beam elements were used. It was necessary to investigate how the simplification would affect the results and if the simplification was accurate enough, so that a beam modelled with the simplified cross-section would resemble a beam with the real cross-section.

The reason that the cross-section had to be simplified was due to some limitations in the beam-element theory. It is not recommended to model closed sections with branches using beam elements [21]. Bending stiffness around the z -axis in Figures 5.15 and 5.16, and cross-section area was considered the most important properties that needed to match between the real cross-section and the simplified one. Figures 5.15 and 5.16 shows the chosen simplified cross-sections that were used for the beam-element models.

A study was performed at first to determine the difference in torsional stiffness and bending stiffness of the simplified cross-section, compared to the real cross-section. It was done to investigate which effect a simplification of the cross-section had on the stiffness of the beam, which could affect the result of a progressive collapse analysis. The HSQ-profiles were modelled with solid elements with a correct cross-section and the simplified cross-section with beam elements. Both models were subjected to a force in the y -direction, a force in the z -direction and a torsional moment.

In the next step of the study, the beam was loaded to failure and the results between the beam-element model and the solid-element model were compared. This was done by applying an evenly distributed load of 200 kN/m on the beam models, with the conditions as shown in Figure 5.1. The beam model consisted of solid elements with the real cross-section, and beam elements with the simplified cross-section. The load was applied as a line load on the beam-element model and as a surface-traction load on the solid-element model. The boundary conditions were added by restricting all displacements of the nodes belonging to the surface at the ends, as for the quadratic cross-section, cf. Figure 5.3. In the beam-element model, the boundary conditions were applied by restricting the displacement and rotational degrees of freedom at the ends.

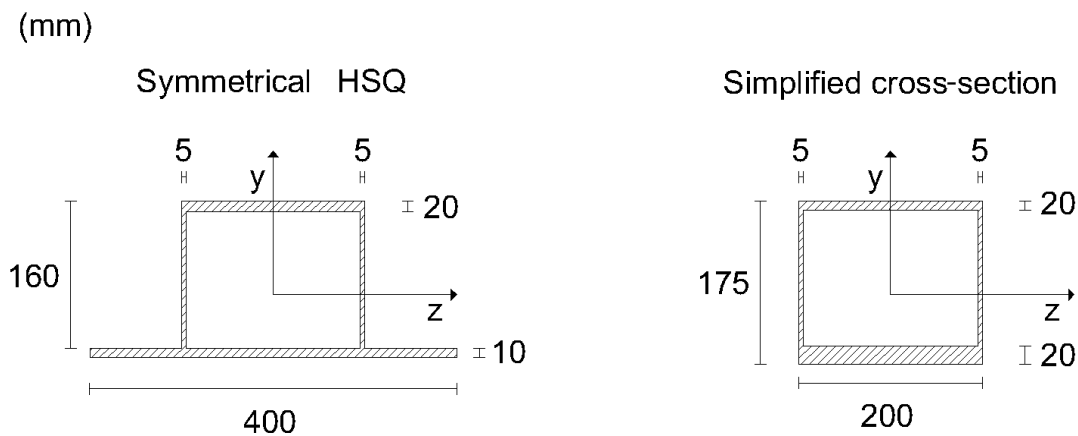


Figure 5.15: Simplified cross-section used in the beam-element model for the symmetrical HSQ-profiles.

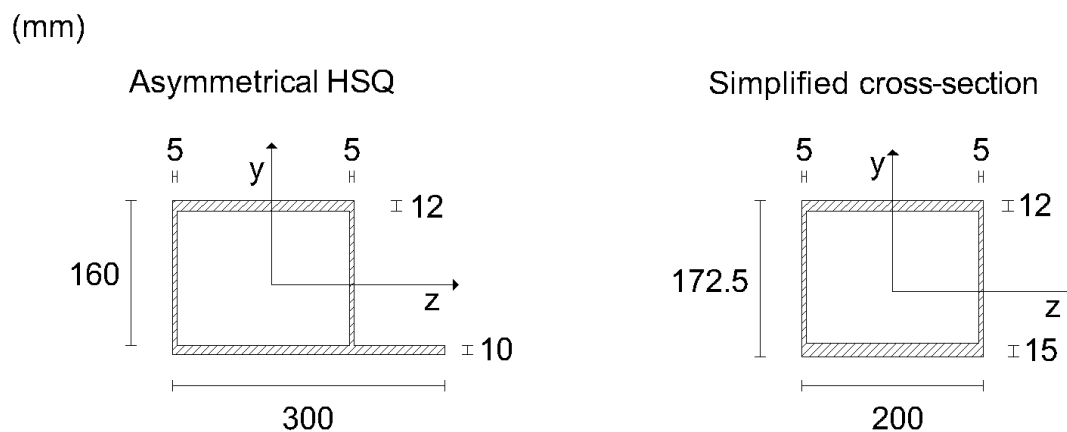


Figure 5.16: Simplified cross-section used in the beam-element model for the asymmetrical HSQ-profiles.

Results

Comparison of stiffness – simplified and real cross-section

Tables 5.1 and 5.2 show the differences in bending stiffness, torsional stiffness and cross-section area of the simplified and the real cross-section.

The stiffness in the vertical direction is almost equal for the simplified cross-section. The bending stiffness in the horizontal direction has decreased significantly while the torsional stiffness has increased. The cross section area is almost equal which will make the axial stiffness equal.

Table 5.1: Difference in stiffness between the solid-element model and beam-element model for the asymmetrical HSQ-profile.

Compared property		Solid-element	Beam-element	Stiffness difference [%]	
Vertical displacement	[mm]	58.8	55.1	Bending z	-6.3
Horizontal displacement	[mm]	44.1	62.9	Bending y	28.8
Rotation	[rad]	0.0034	0.0026	Torsional	-22.6
Cross section area	[mm ²]	6855	6855	Axial	0

Table 5.2: Difference in stiffness between solid-element model and beam-element model for the symmetrical HSQ-profile.

Compared property		Solid-element	Beam-element	Stiffness difference [%]	
Vertical displacement	[mm]	39.7	40.1	Bending z	0.9
Horizontal displacement	[mm]	25.0	50.7	Bending y	102.6
Rotation	[rad]	0.0032	0.0021	Torsional	-34.0
Cross section area	[mm ²]	9400	9350	Axial	0.5

Results from analysing the symmetrical HSQ-profile

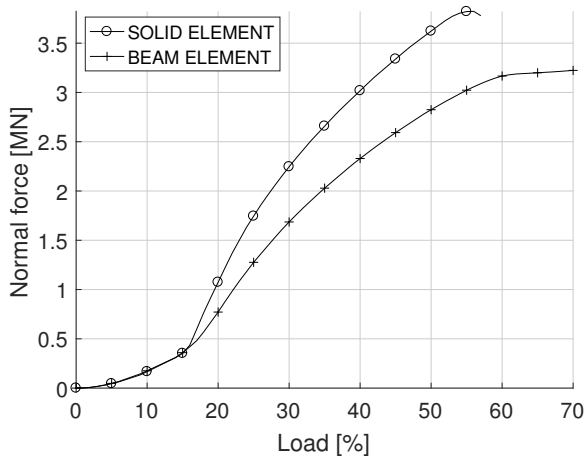
In Figures 5.17–5.19 the normal force, moment and displacement at point Edge and Middle are shown. There were some differences between the models in the developed normal force and moment in the beam. However, the overall behaviour was quite similar with a maximum of the moment and normal force at almost the same load. The displacement at point Middle was also quite similar.

The capacity was, as for the beam with the quadratic cross-section, overestimated in the beam-element model. However, it is unlikely that the full capacity, shown in the figures, could be utilised due to the large strain in the material, which would cause a fracture.

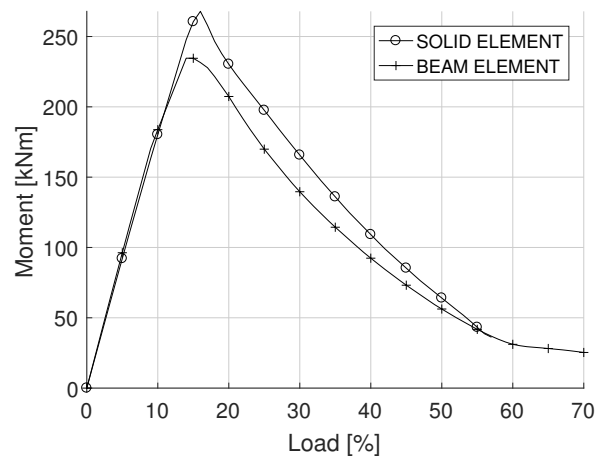
One way to say that the capacity of the beam is reached could be by limiting the strain to a certain value. There are, however, some difficulties in predicting the strain with finite element models. The element size have quite a large impact on the maximum strain developed in the beam. It is illustrated by Figure 5.20, where the maximum effective plastic strain as a function of the applied load is shown. The figure shows results using varying mesh size for the beam-element models and the solid-element models.

With a finer element mesh, there is a localisation of the maximum strain and the maximum value becomes very high in single material points. This is illustrated in Figure 5.21 which shows the effective plastic strain in the beam when 50% of the total load was applied. Another effect neglected in these models is the hardening of the material. It would probably have limited the maximum effective plastic strain developed in single material points. The hardening in these points would cause the effective plastic strain to spread more.

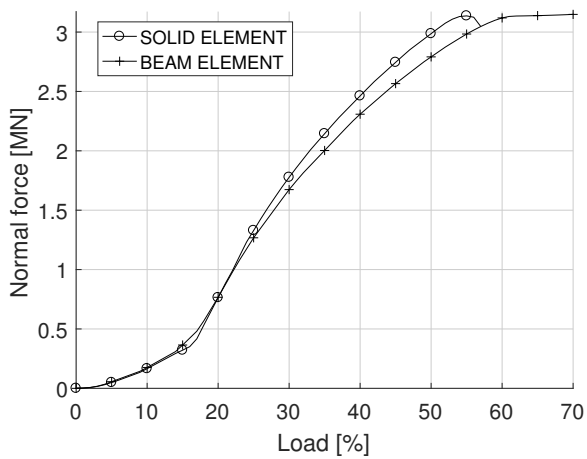
There were also some difficulties with local buckling of the flanges, see Figure 5.22. That occurred for quite a low load with a fine element mesh due to the large moment, which at the supports results in a large compression stress at the lower part of the cross-section. Some strengthening of the flanges could be needed there.



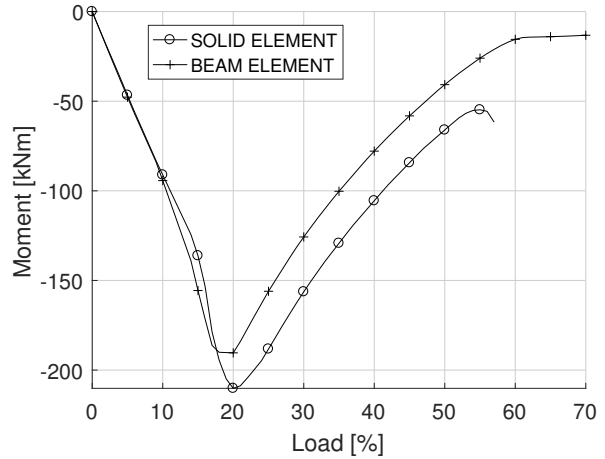
(a) Normal force.



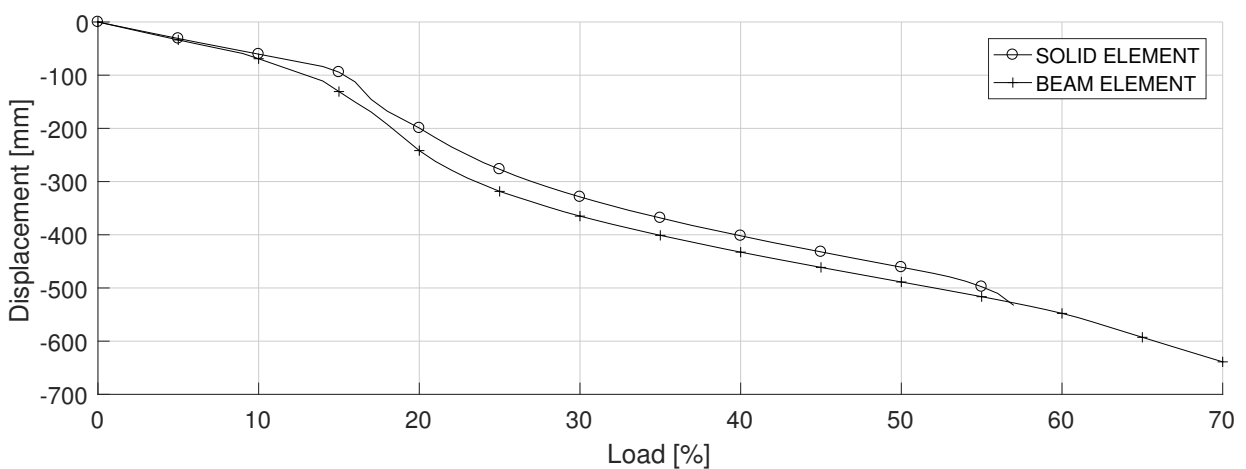
(b) Moment.

Figure 5.17: Moment and normal force at point Edge.

(a) Normal force.



(b) Moment.

Figure 5.18: Moment and normal force at point Middle.**Figure 5.19:** Vertical displacement at point Middle.

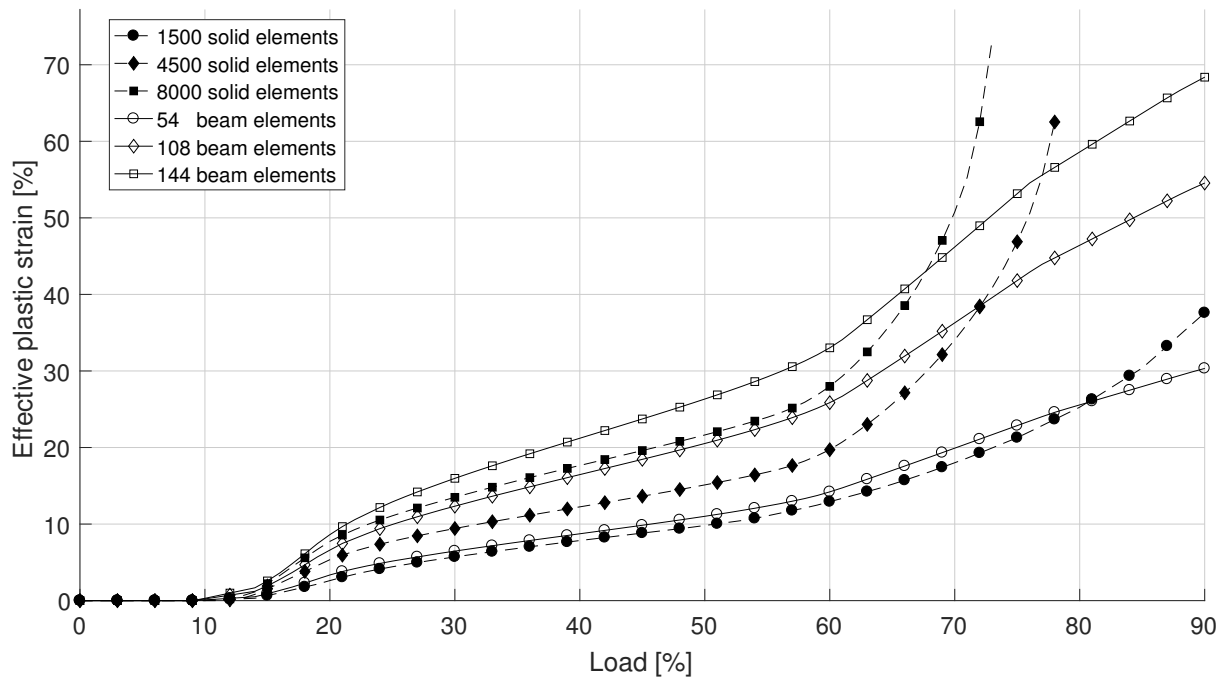


Figure 5.20: Maximum effective plastic strain as a function of the applied load using different mesh sizes.

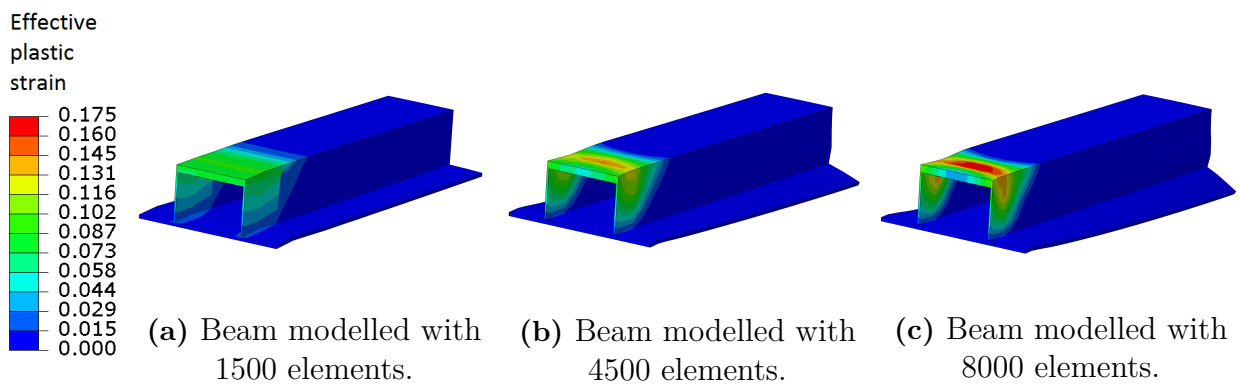


Figure 5.21: The effect that the mesh size had on the maximum effective plastic strain in the beam. The figure shows solid-element beams when 50% of the total load was applied.

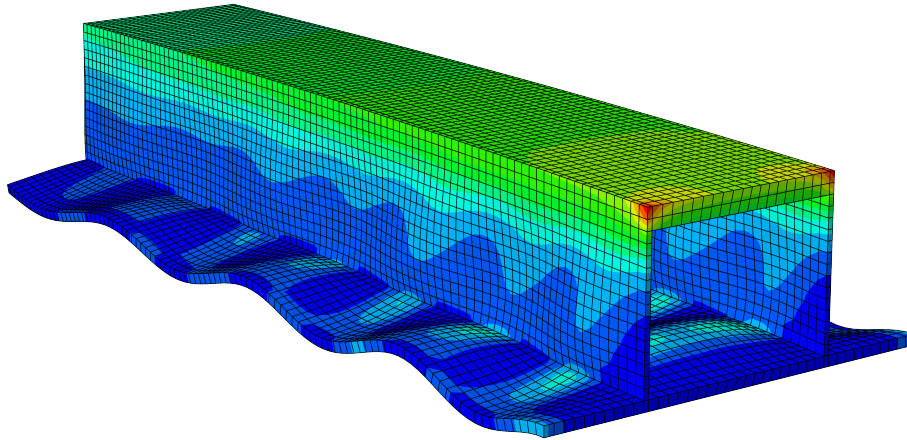


Figure 5.22: Local buckling of the symmetrical HSQ-profile.

Results from analysing the asymmetrical HSQ-profile

In Figures 5.23–5.25, the normal force, moment and displacement at point Edge and Middle are shown for the asymmetrical HSQ-profile. There were some differences between the normal force and moment in the beam but the overall behaviour of the beam was quite similar, especially the displacement at point Middle.

As for the symmetrical HSQ-profile, the beam-element model had a larger capacity. Although, it is unlikely that the full capacity, shown in the figures, could be utilised due to the large strain in the material which would cause a fracture.

Results from the analysis of the symmetrical HSQ-profile showed that the element size had quite a large impact on the maximum strain developed in the beam. It was, not surprising, also the result when using asymmetrical profiles. Figure 5.26 shows the maximum effective plastic strain in beams modelled with solid and beam elements, with different mesh sizes.

The effect of different mesh sizes is illustrated in Figure 5.27, it shows the effective plastic strain in the beam when 50% of the total load was applied.

As for the symmetrical HSQ-profile, local buckling of the flanges occurred at a quite low load with a fine mesh, see Figure 5.28. Some strengthening of the flanges could be needed there for the asymmetrical HSQ-profile as well.

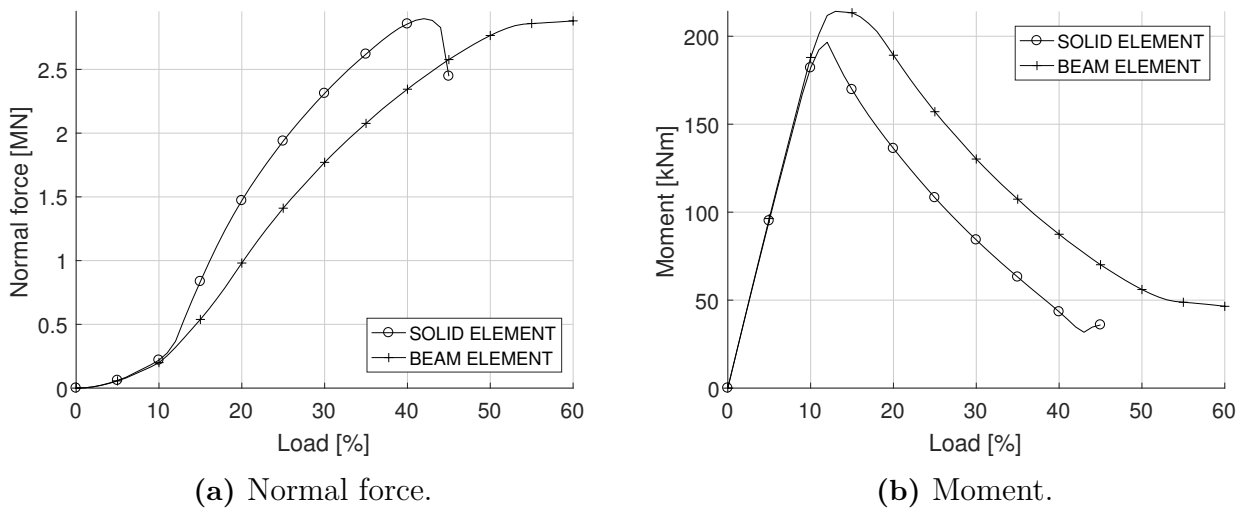


Figure 5.23: Moment and normal force at point Edge.

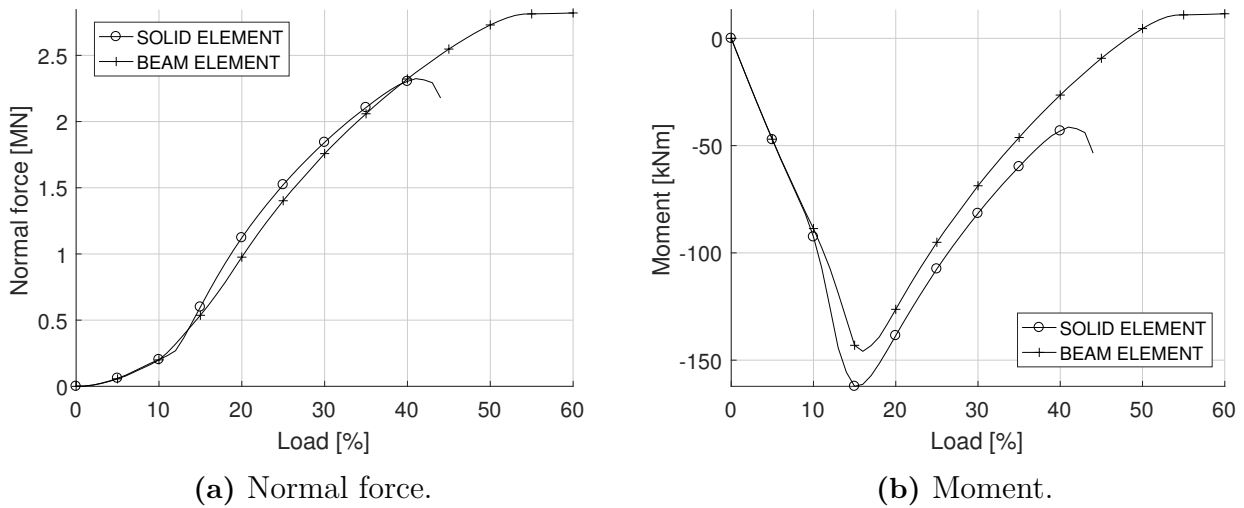


Figure 5.24: Moment and normal force at point Middle.

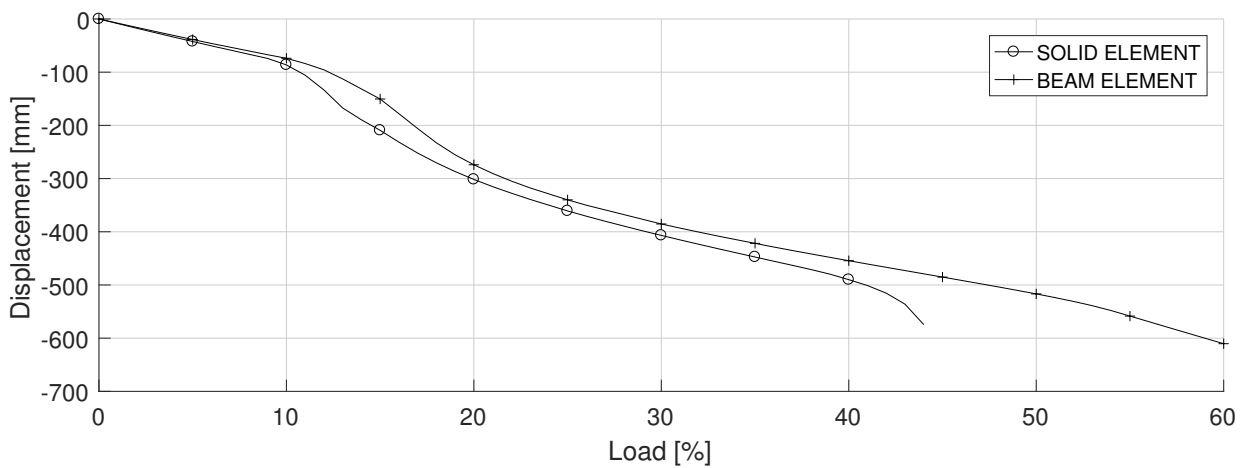


Figure 5.25: Vertical displacement at point Middle.

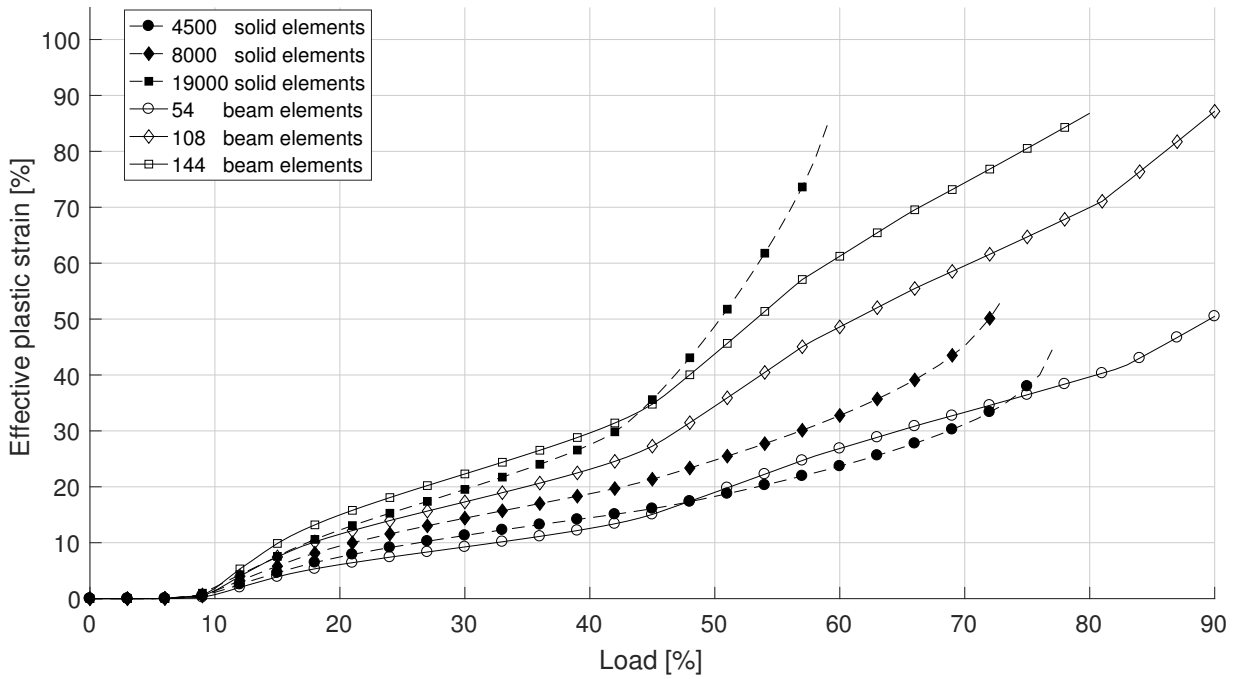


Figure 5.26: Maximum effective plastic strain as a function of the applied load using different mesh sizes.

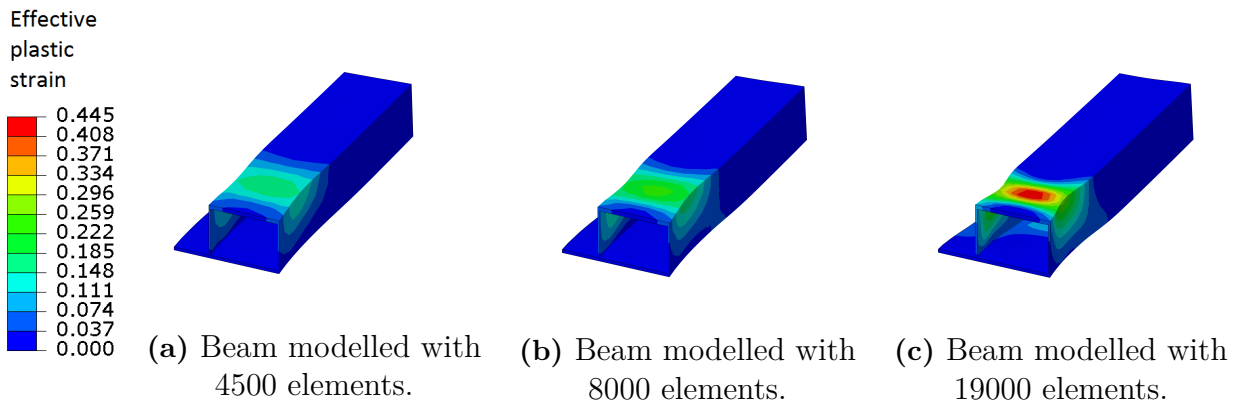


Figure 5.27: The effect that the mesh size had on the maximum effective plastic strain in the beam. The figure shows solid-element beams when 50% of the total load was applied.

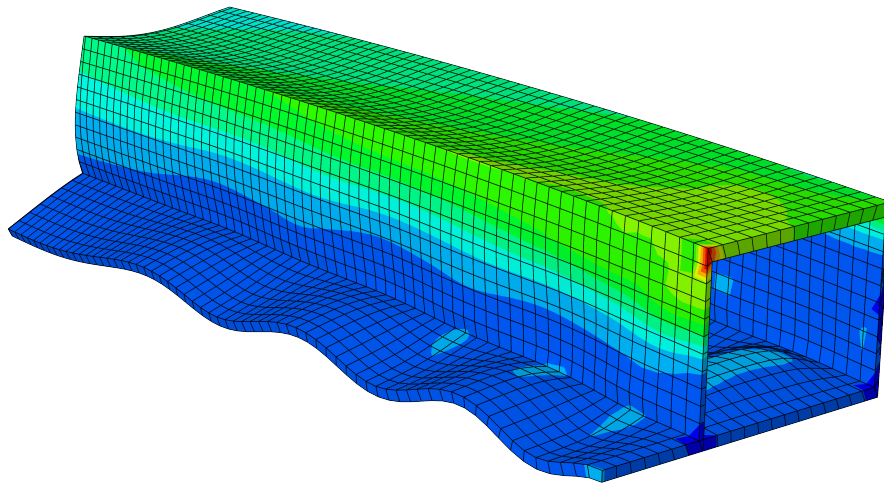


Figure 5.28: Local buckling of the asymmetrical HSQ-profile.

5.3 Summary and discussion

Analyses of a beam modelled with beam elements and solid elements using a simple quadratic cross-section showed that the beam-element model tend to overestimate the capacity in comparison to a model with solid elements. It is likely due to the simplifications in the numerical model using beam elements which underestimate the strain developed at the supports and that the change of the cross-section geometry is not accounted for.

The cross-section area tends to, with non-linear effects included, be more important for the capacity than the bending stiffness. Less bending stiff beams could be a better choice due to its capability to deform without developing large strains in the material, cf. Figure 5.13 and 5.14.

Due to limitations in the beam-element theory, a simplified cross-section was used to model the HSQ-beams with beam elements. It resulted in a difference in bending, torsional and axial stiffness which Tables 5.1 and 5.2 show. However, the simplified cross-sections shown in Figure 5.15 and 5.16 did not differ much in bending around the y-axis and its axial stiffness, which was considered the most important properties of the cross-section when used in the modelling of a real building.

HSQ-beams modelled with beam elements using the simplified cross-sections showed similar behaviour as the beam modelled with solid elements. Although, it should be noted that the beam-element models overestimate the capacity. The use of a strain limit would avoid an overestimation of the capacity but the maximum strain is difficult to estimate because it depends on the size of the mesh, both for the solid-element and the beam-element models. It seems as the beam-elements, at reasonable effective plastic strain values (0–30%), gives similar results as the solid elements. This is positive because it implies that the effective plastic strain can be estimated well in the progressive collapse analysis, where beam elements will be used. It should, however, be noted that a proper element size has not been determined and it remains an uncertainty.

6 2D progressive collapse analysis

In the following chapter the modelling and results from a progressive collapse analysis of the building described in chapter 1.4 are presented. A 2D model of the facade, see Figure 1.4, was created with the purpose to investigate the ability of the building to develop alternate load paths if a facade column fails. The difference of the results from LS, NLS and NLD analyses, was investigated to evaluate the possibility to use different analysing methods.

6.1 Method

The finite element program Abaqus was used in the analyses.

Beams and columns were chosen with reasonable dimensions so that they could resist an ultimate limit state load according to Eurocode [24]. The ultimate limit state load is determined by

$$q = \gamma(1.2G + 1.5Q_{k1} + 1.5\psi_{0,i}Q_{k,i}) \quad (6.1)$$

where

G = Permanent load

Q = Varying load

ψ = load factor

γ = Safety factor.

LS, NLS and NLD analyses were performed and followed the procedure described in Chapter 3.2.

Two different column removal locations were chosen in the facade, namely a corner column (column 1) and a column in the middle (column 5). The removal was performed in Abaqus with the "Model change" procedure, which enables a removal of an element in the model, in this case, a column. In the static analysis, the column was not modelled at all. In the dynamic analysis, an initial static step was first performed to determine the initial stress state. After the static initial step, the column was removed with "Model change" and a dynamic implicit step was started.

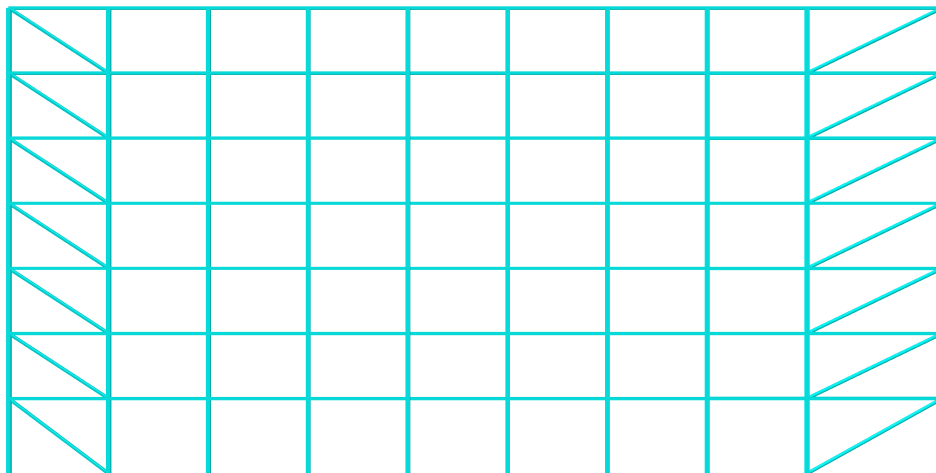


Figure 6.1: The geometry of the modelled facade, with added diagonals. Dimensions were chosen according to Figure 1.4.

6.2 FE-model of the 2D structure

6.2.1 Geometry

Beams and columns in the facade of the studied building were modelled as shown in Figure 6.1. Diagonals were added to represent the horizontal stiffness of the hollow-core slab. Without these diagonals, cable action of the beams would be limited due to an incapacity of the model to support horizontal forces.

Reasonable dimensions of beams and columns were chosen by performing a linear static analysis and extracting internal forces in beams and columns. The external load was determined according to equation 6.1 with the assumption that the slab is simply supported and the load is distributed equally between the facade and inner supports. The permanent load consists of the self-weight of the hollow-core units, a 55 mm top layer of concrete and a load representing unknown loads. The live load was chosen to 2.5 kN/m² which applies to office areas according to Eurocode. The line load was determined with a span length $L=10.516$ m and loads, $Q=2.5$ kN/m², $G=5.3$ kN/m² and a safety factor, $\gamma=1$.

$$q = (1.2 \cdot 5.3 + 1.5 \cdot 2.5) \frac{10.516}{2} \approx 54 \quad [\text{kN/m}] \quad (6.2)$$

For the facade beams, a cross-section was chosen with dimensions according to Figure 5.16. Columns were modelled with a box cross-section representing a VKR-profile, see Appendix A, with the dimension 250×250×10 mm. The compression force capacity for the columns is 2.73 MN according to Eurocode [22], with consideration of buckling and the buckling length equal to the height between the ground and the first storey.

Beams were modelled with beam elements with an element length of 0.1 m. It implies that 108 elements were used in a span length of 10.8 meters, as was done in the analysis of beams in Chapter 5.

6.2.2 Material model

The chosen material model was the same as used in Section 5.1, which was an ideal-elastic-plastic material model with a von Mises yield criterion with the yield stress 355 MPa, see Section 4.2.

The elastic modulus and Poisson's ratio were chosen in accordance with the strength of steel, which is $E=210$ GPa and $\nu=0.3$ [22].

6.2.3 Boundary conditions and loading

Beam-to-column and column-to-ground connections were modelled as moment stiff, which implies that all displacements and rotational degrees of freedom were restrained at these points.

The load was determined with the accidental action load combination according to Eurocode. The load factor ψ_1 was chosen, the factor is used for frequent load combinations in Eurocode [25] and is recommended by the authors of [11] for the accidental action load combination.

$$q = (g_k + \psi_1 q_k) \frac{L}{2} = (5.3 + 0.5 \cdot 2.5) \frac{10.516}{2} \approx 35 \text{ [kN/m]} \quad (6.3)$$

L is the width of the floor, g_k the permanent load and q_k the live load used in Equation 6.2. This load was applied on all beams in the 2D model.

For the static analysis, a dynamic load factor of 2 was applied by adding a line load of 35 kN/m at areas which were affected by the column removal in accordance with the procedure described in Section 3.2.2. The value 2 was chosen because it is the largest value for the dynamic load factor used for NLS analyses according to the UFC, see Section 3.2.2. The principle of how the dynamic load factor was applied is shown in Figure 6.2.

In the static analysis, results will be presented as a function of the dynamic load factor (DLF). A dynamic load factor between 0 and 1 is when only the accidental load combination has been applied. When the whole accidental load combination has been applied (DLF=1), the load seen in Figure 6.2 was applied on chosen surfaces, which equals to a dynamic load factor between 1 and 2.

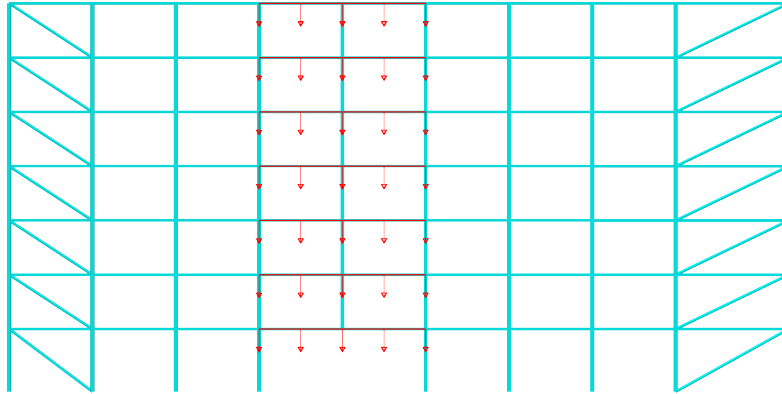


Figure 6.2: The red area is showing the principle of how the dynamic load factor was applied in the static analysis.

6.2.4 Mass and damping

In the dynamic analysis, mass was applied by increasing the density of the material of the beams. All loads on the structure come from masses, this implies that the mass could be determined by dividing the accidental load combination with the gravitational constant chosen to 10 m/s^2 . To get the same mass per meter the mass was divided by the cross-section area of the beam. It resulted in a density that was determined by

$$\rho = \rho_{steel} + \frac{Load/G}{A_{cross-section}}. \quad (6.4)$$

Rayleigh damping was used, see Section 4.4. A dynamic analysis was performed first to determine the dominating frequencies. The Rayleigh parameters a_0 and a_1 were chosen by solving the equation system in Equation 4.17 using two frequency values, one just below and one above the dominating frequencies. It resulted in an equation system solved using the frequencies 1 and 6 Hz, and a chosen damping ratio of $\zeta=5\%$.

$$\begin{bmatrix} \frac{1}{2 \cdot 1 \cdot 2\pi} & 1 \cdot 2\pi \\ \frac{1}{2 \cdot 6 \cdot 2\pi} & 6 \cdot 2\pi \end{bmatrix} \begin{bmatrix} a_0 \\ a_1 \end{bmatrix} = \begin{bmatrix} 0.05 \\ 0.05 \end{bmatrix} \rightarrow \begin{bmatrix} a_0 \\ a_1 \end{bmatrix} = \begin{bmatrix} 0.5386 \\ 0.0023 \end{bmatrix} \quad (6.5)$$

The used Rayleigh damping is shown in Figure 6.3. At 1 and 6 Hz, an exact damping ratio of 5% is obtained, between these frequencies, the damping varies from 3.5% to 5%. The curve also shows that vibrations at very low and high frequencies will have a higher damping.

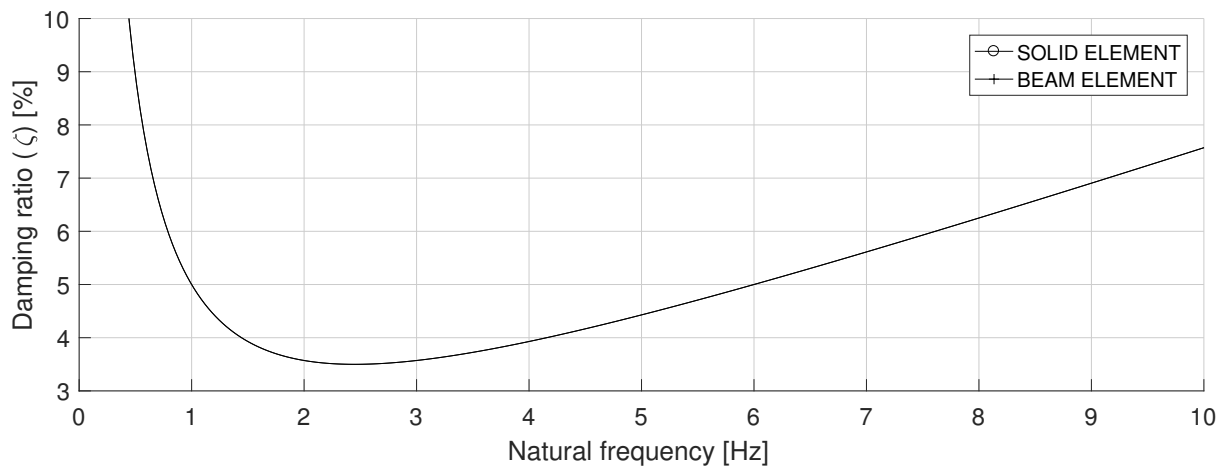


Figure 6.3: Damping of the structure using Rayleigh damping.

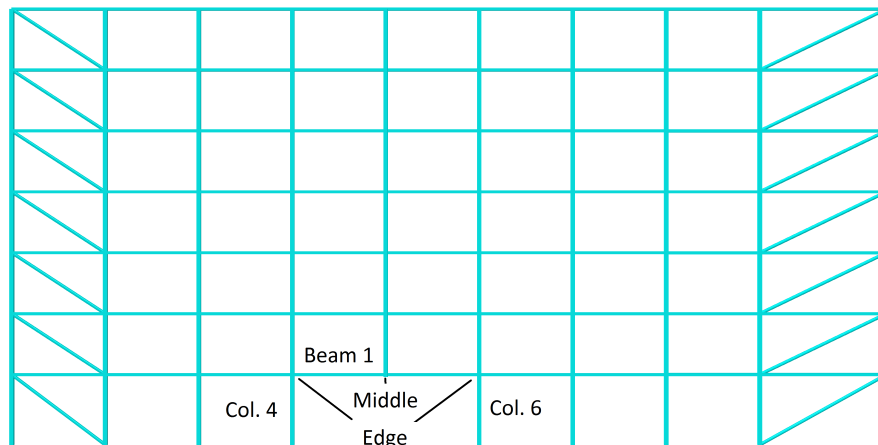


Figure 6.4: Locations in the model where internal forces were extracted.

6.3 Column 5 removal

The following section presents the results that were obtained when column 5 was removed and an LS, NLS and NLD analysis were performed.

Beams connected to columns 4 and 6 are referred to as Beam 1–7. Both points in Beam 1–7 located at the connection to columns 4 and 6 are referred to as point Edge. The point in Beam 1 located at the location of the removed column is referred to as point Middle, see Figure 6.4.

The overall ability of the model to develop alternate load paths was studied. It was done by extracting internal forces developed in Beam 1–7, which has to transfer parts of the load carried by the removed column to adjacent elements. The developed normal force in adjacent columns was also extracted. In the NLD analysis the dynamic effects were studied and the result of the NLS analysis was compared to estimate the dynamic load factors and if they could represent the overall dynamic effects.

6.3.1 LS analysis

The deformation of the model, just before failure is shown in Figure 6.5. It is not surprising that the deformation was quite limited in the LS analysis. Figure 6.6 shows the moment in Beam 1, which was extracted at point Edge, at the connection to adjacent columns 4 and 6, and at point Middle. The beam failed with a fully developed plastic joint at about 70% of the applied accidental load combination. It was an expected result because the span length is doubled. The span length has a larger impact on the maximum moment than the load. Even if the load was decreased compared to the ultimate limit state load, which the model was designed for, it did not compensate for the increased span length.

No normal force was developed in the beam because it was a geometric linear static analysis, hence cable action was not possible. Static equilibrium is achieved only by the development of moment in the beam. The moment increases the most at point Edge, but as it reaches the yield stress, the moment is redistributed to point Middle. When the moment capacity was reached at point Middle the beam failed.

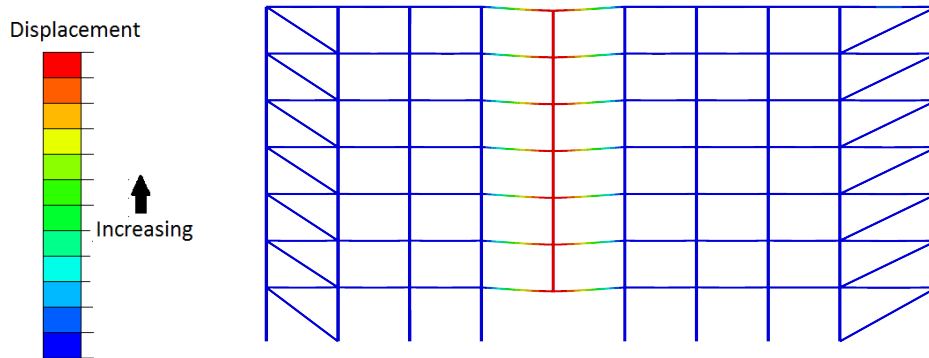


Figure 6.5: Deformation of the model just before failure.

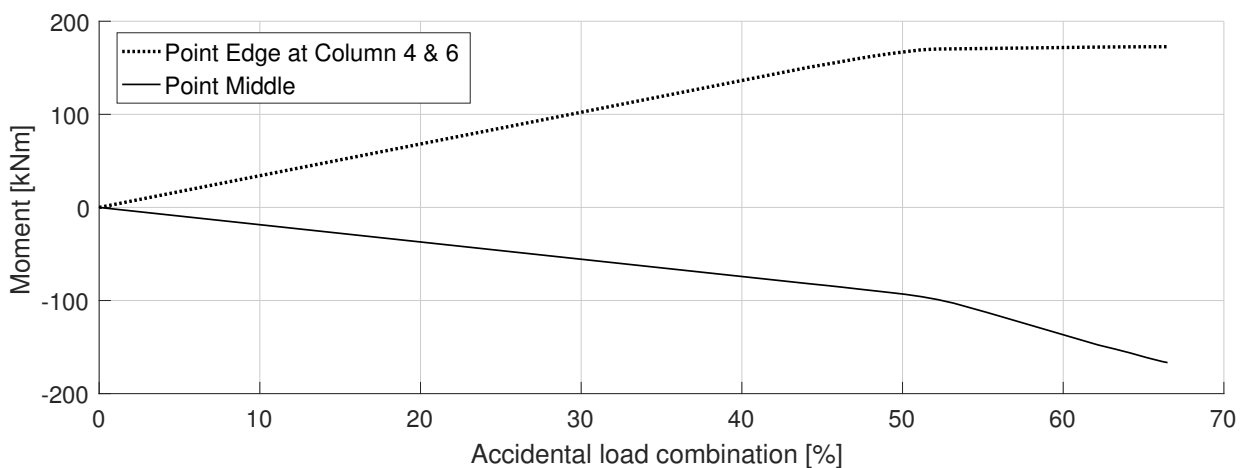


Figure 6.6: Moment in Beam 1 at point Middle and at point Edge, at the connection to columns 4 and 6.

6.3.2 NLS analysis

Without the diagonals at the building edges, the NLS analysis resulted in such a large horizontal force in the beams which led to a failure of the whole structure. The diagonals stiffened the structure and the results are illustrated in Figure 6.7, which shows the deformation just before failure at a dynamic load factor close to 1.6.

In Figures 6.8–6.10 the displacement at point Middle, moments and normal forces at point Edge and Middle are shown as a function of the dynamic load factor.

Studying the first-floor beam, up to 0.6 of the load the behaviour was almost identical to the LS analysis, which means a relatively small deformation and normal force in the beam. At this load, the LS analysis failed, but with non-linear effects included, cable action of the beams increased the load capacity.

The results show a behaviour with an increasing cable action, which was consistent with the analysis performed in Chapter 5. One difference was that with a dynamic load factor at about 1.2 the normal force in the beam decreases and moments increases. This was probably due to a limited ability of the model to support the large normal forces in the beams.

It is clear that cable action in beams located higher up in the building was very limited. It is probably because the horizontal stiffness of the building is lower higher up, and the ability to support the horizontal forces at the upper floors is limited compared to the first floor where the normal force effectively was transferred to the ground by the diagonals. The effect of this was also that no suspension mechanism to the upper intact floors was obtained by the remaining parts of column 5. Instead, column 5 was compressed which implies that Beam 1 was supporting the upper floors.

Failure occurred at a dynamic load factor at about 1.6 and as Figure 6.5 shows, the horizontal force deforms the columns and creates plastic joints at their connection to the ground.

A dynamic load factor at about 1.6 resulted in failure. Although high strain would probably have caused the failure at a lower load. In Figure 6.11 the maximum effective plastic strain in Beam 1 is shown. With a minimum limit strain of 15%, as given in Eurocode [22], the beam would fail without the dynamic effects included (dynamic load factor equal to 1). If a higher effective plastic strain, 20-25%, is tolerated, which is not unreasonable [23], the capacity increases dramatically to a dynamic load factor of 1.3–1.4.

The normal forces in adjacent columns 4 and 6 are shown in Figure 6.12. An almost equal load was transferred to the columns and their capacity was nearly reached.

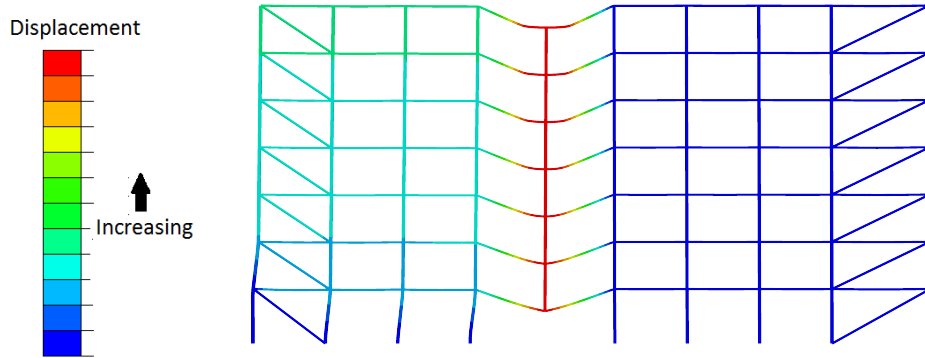


Figure 6.7: Deformation of the model just before failure.

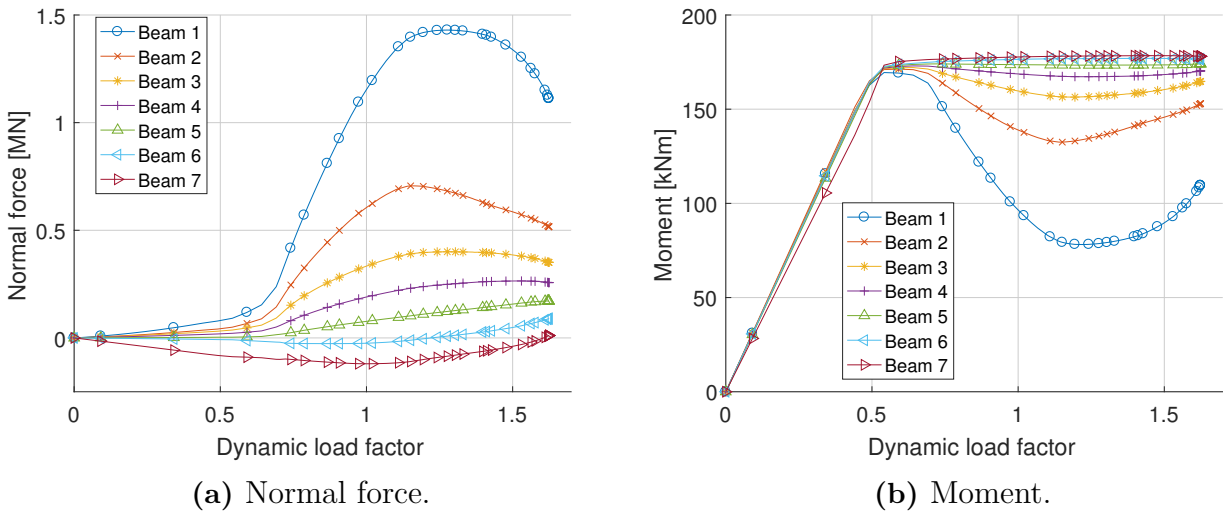


Figure 6.8: Moment and normal force in Beam 1-7 at point Edge.

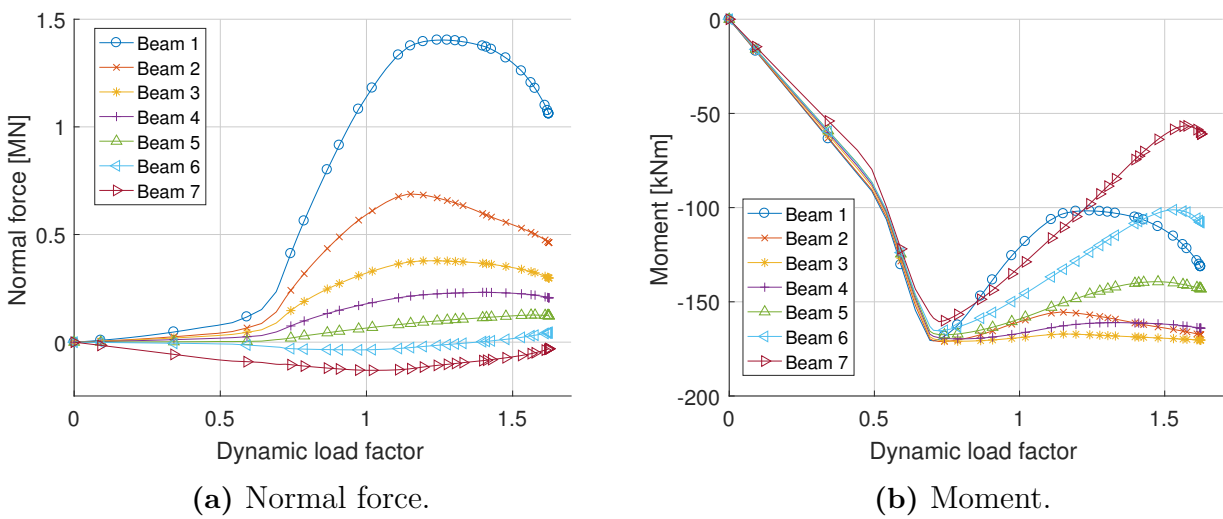


Figure 6.9: Moment and normal force in Beam 1-7 at point Middle.

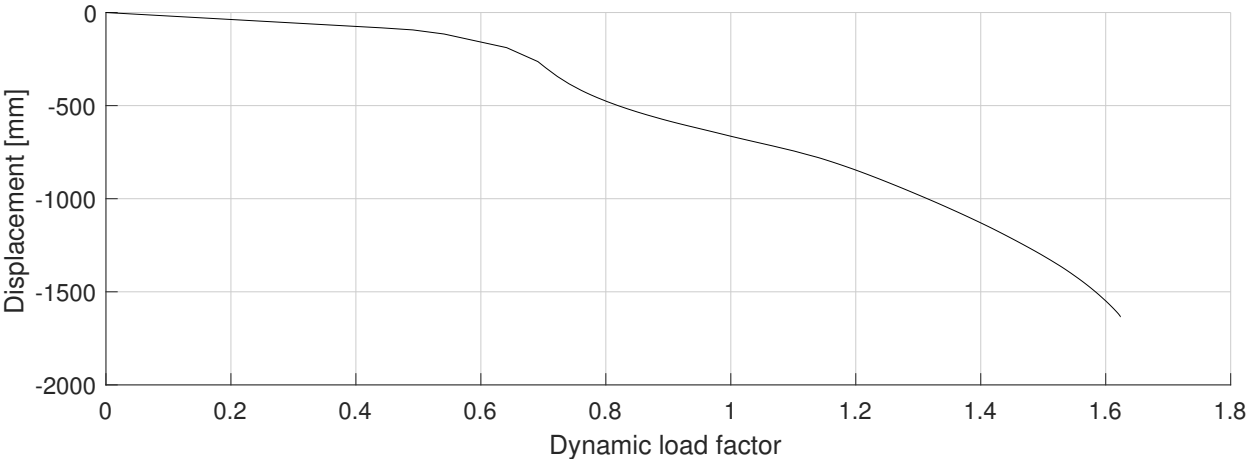


Figure 6.10: Vertical displacement of point Middle in Beam 1.

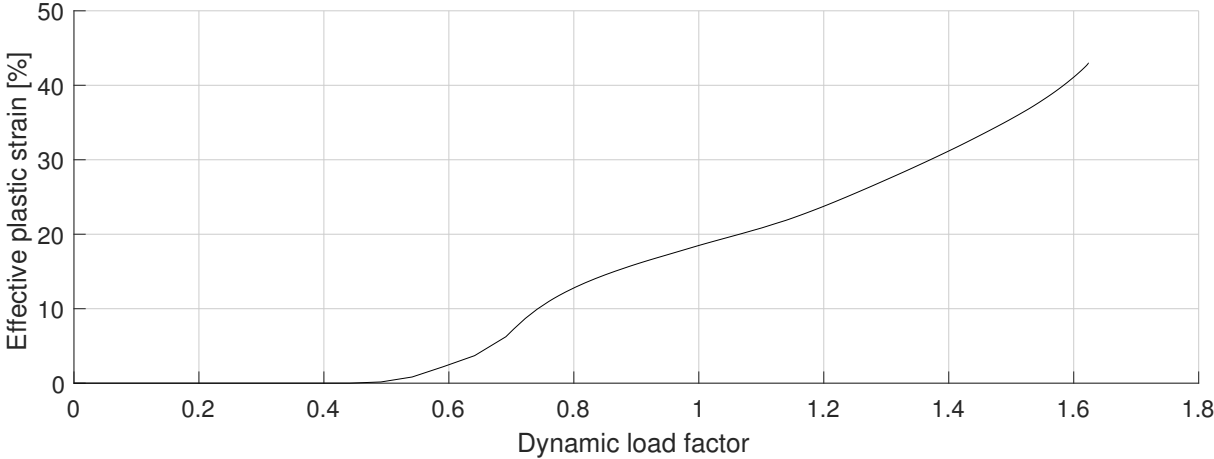


Figure 6.11: Maximum effective plastic strain in Beam 1.

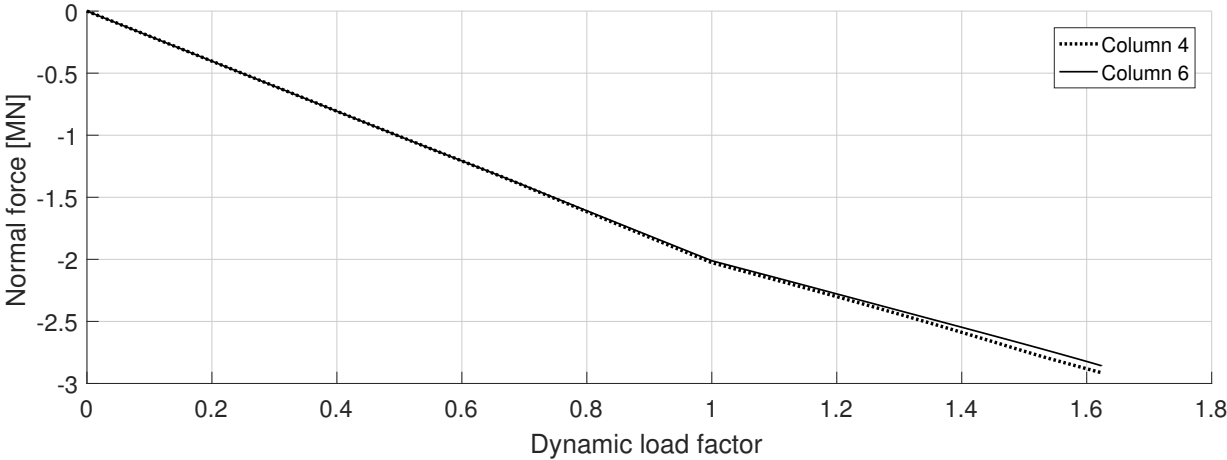


Figure 6.12: Normal force in adjacent columns 4 and 6.

6.3.3 NLD analysis

Effect of damping and plasticity

When performing dynamic analyses, properties such as damping and plasticity has a large impact on the results. In Figures 6.13 and 6.14, the effect of these properties is shown. It was investigated by removal of column 5 and extracting the displacement of point Middle in Beam 1 and the normal force in adjacent column 4 as a function of time.

Figure 6.13 shows that damping has a small impact on the displacement and normal force when an elastic material model is used. With a plastic material, the damping has a much larger impact on the displacement. Figures 6.14a and 6.14b show that the plasticity has quite a large impact on the amplitude force in columns adjacent to the removed column 5.

If the purpose is to check how adjacent columns respond due to the column failure, a pure elastic model with no damping would give the most conservative results. In the UFC [9], a maximum dynamic load factor of 2 (in NLS analyses) should be chosen if the structure remains elastic, this is because if it remains elastic, the responding forces become higher. By adding damping and plasticity the responding forces in the structure will be reduced because the kinetic energy is dissipated due to plastic deformations and damping.

In the static analysis, internal forces arise only due to deformations which differ to a dynamic analysis with damping included, where the internal forces arise due to the deformations but also from velocity and damping [21]. This is an effect that is important to understand when the results from NLD analyses are to be interpreted.

Figure 6.15 shows the moments developed in Beam 1 at point Edge for models with and without damping. As in the static analysis, the moment reaches a maximum and then decreases when the normal force starts to increase. A difference is that in the static analysis, the moment capacity in the beam was about 170 kNm, but the moment in Beam 1 in the dynamic analysis including damping was more than 200 kNm. This is an effect that was not seen when damping was excluded from the dynamic model. Without damping the internal forces entirely consist of forces due to deformation of the structure and the moment developed in the beam cannot be larger than the capacity.

There was a large difference in the maximum effective plastic strain developed in the model with and without damping. In the model with damping, the damping forces increased the moment capacity of the beam at point Edge, see Figure 6.15. At that point, the strain is most severe and the increased capacity had a large positive effect on the developed effective plastic strain, see Figure 6.16. The effective plastic strain was more than twice as high without damping as compared to when damping was included.

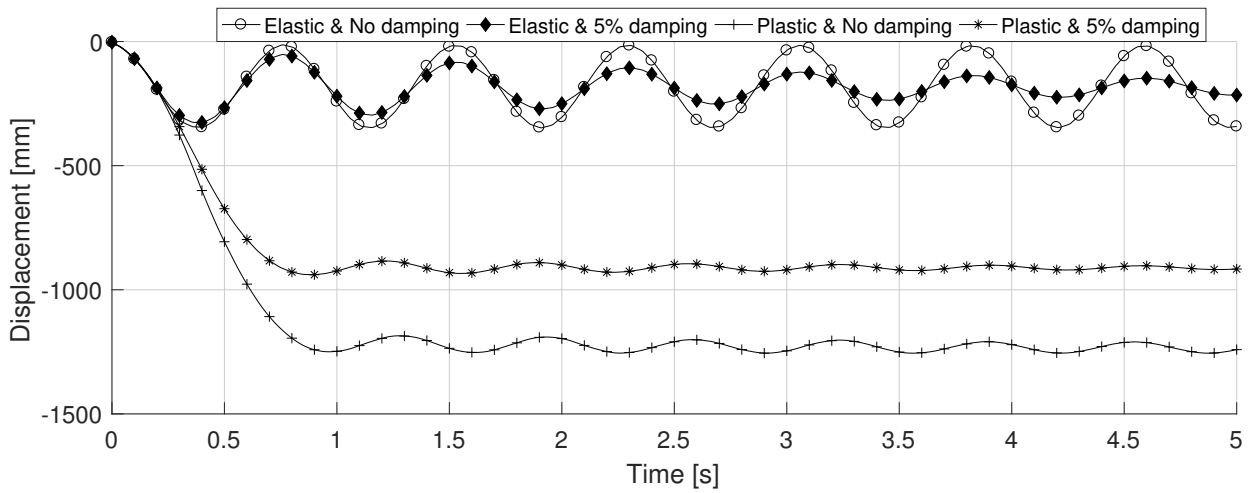


Figure 6.13: The effect that different material models and damping had on the displacement of point Middle in Beam 1.

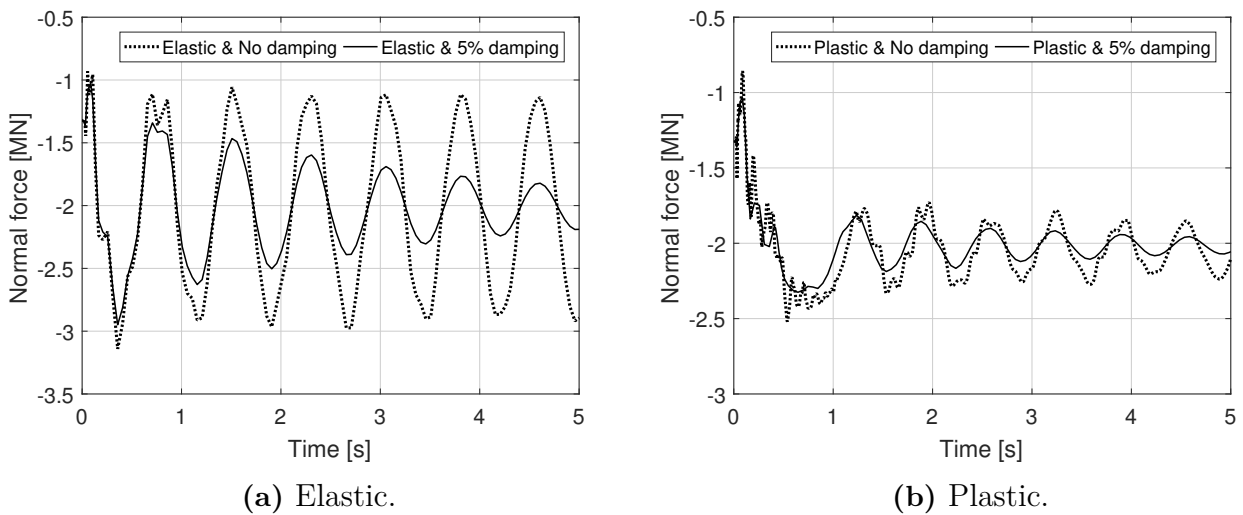


Figure 6.14: The effect that damping had on the developed normal force in adjacent columns 4 and 6.

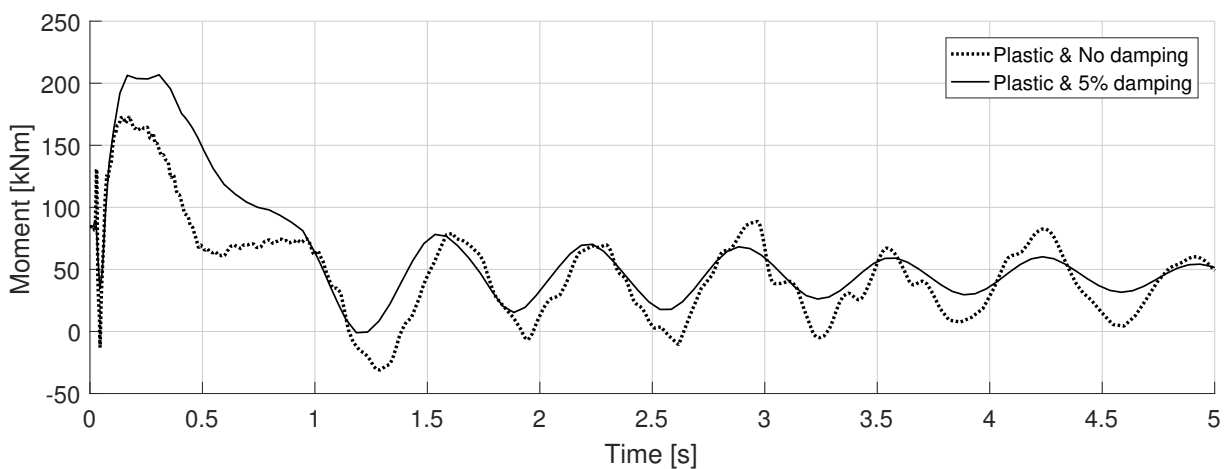


Figure 6.15: The effect that damping had on the developed moments in Beam 1 at point Edge.

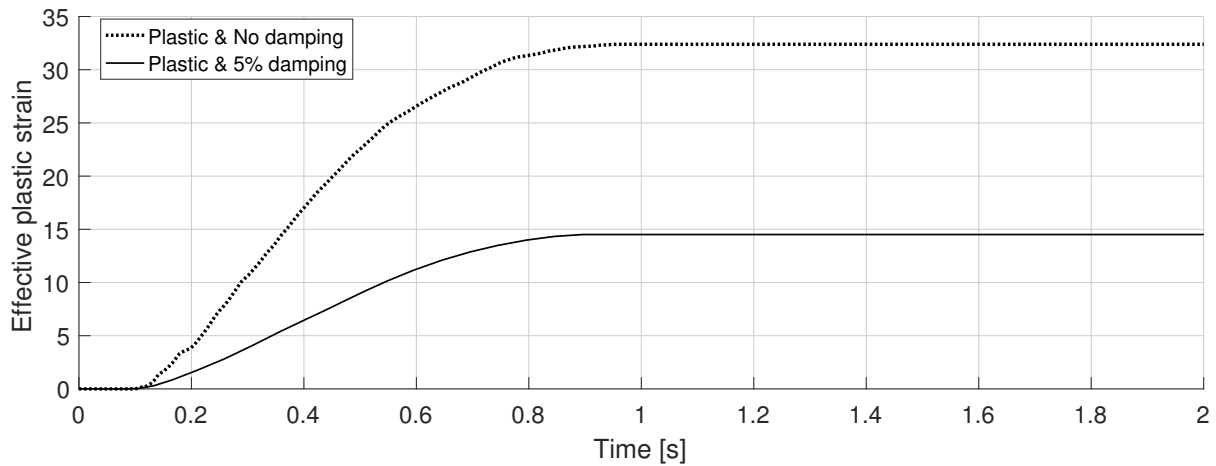


Figure 6.16: The effect that damping had on the developed maximum effective plastic strain in Beam 1.

Progressive collapse analysis

In Figure 6.17 the displacement of point Middle in Beam 1, as a function of time, is shown. A dynamic load factor of 1.27 lead to the same vertical displacement as in the NLS analysis.

Figures 6.18 and 6.19 show the moment and normal force in the Beam 1, at point Edge, at the connection to adjacent columns 4 and 6, and at point Middle. The result with a dynamic load factor of 1.27 from the NLS analysis is also shown in the figures for comparison. Note that the moment at point Edge was larger than the capacity of the beam due to damping.

The beam behaved in the same way as in the NLS analysis. The moment both at point Edge and Middle increased and reached a maximum at about 0.5 seconds, while the beam was still moving downwards, see Figure 6.17. The moment capacity was not enough in the beam to stop the load and moving mass, which required a development of cable action in the beam.

A dynamic load factor of 1.27 seemed to give a good approximation of the dynamic effects. The maximum normal force in the beam was almost equal between the NLD analysis and the NLS analysis with a dynamic load factor of 1.27.

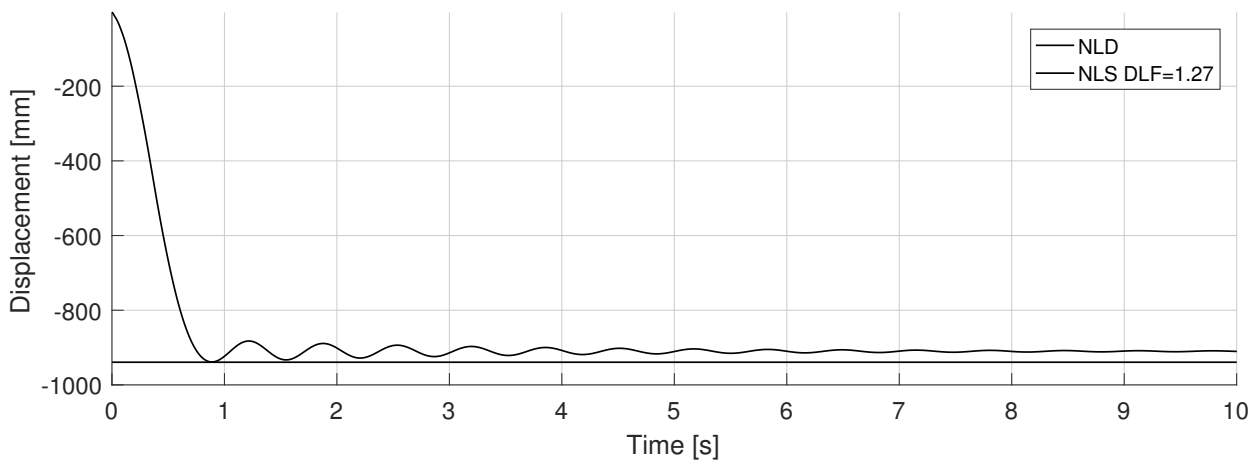
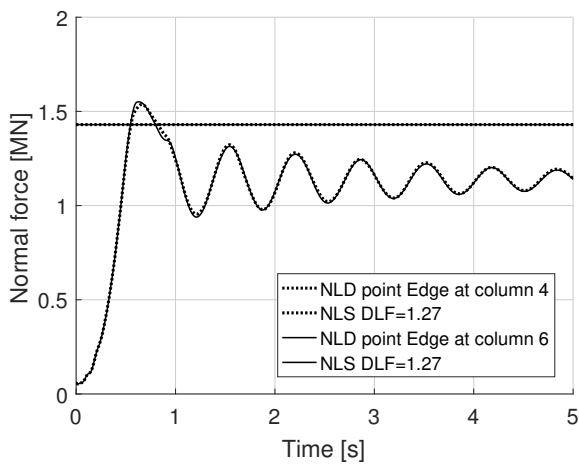
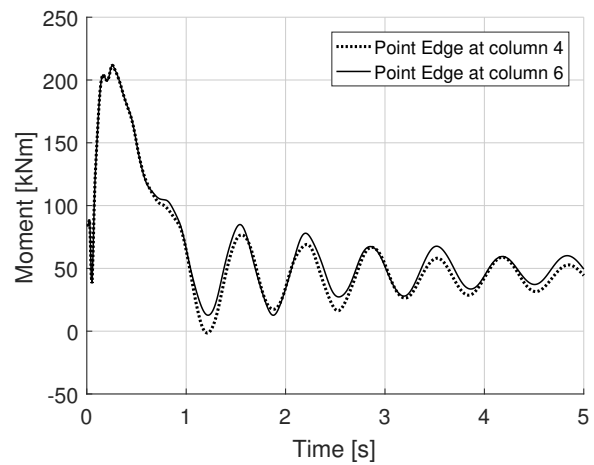


Figure 6.17: Vertical displacement of point Middle in Beam 1, comparison of the results of the NLS and NLD analysis.

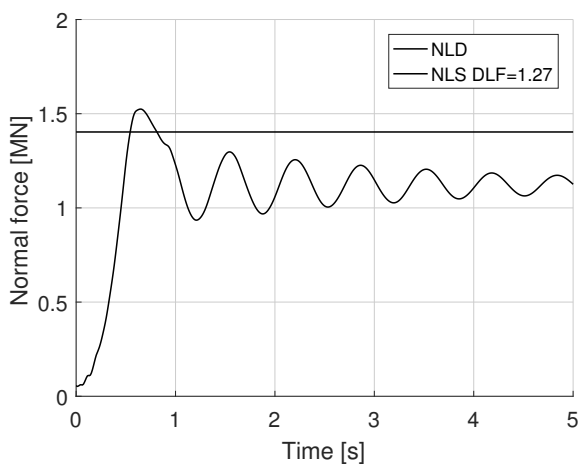


(a) Normal force, comparison of the results of the NLS and NLD analysis.

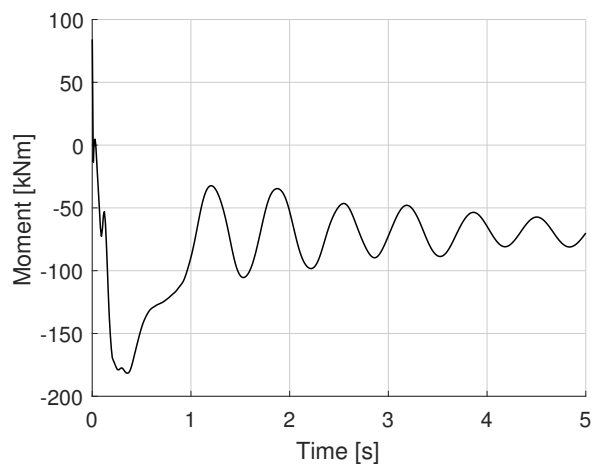


(b) Moment, result of the NLD analysis.

Figure 6.18: Moment and normal force in Beam 1 at point Edge, at the connection to adjacent columns 4 and 6.



(a) Normal force, comparison of the results of the NLS and NLD analysis.



(b) Moment, result of the NLD analysis.

Figure 6.19: Moment and normal force in Beam 1 at point Middle.

The Maximum effective plastic strain in Beam 1 is shown in Figure 6.20 together with the NLS result with a dynamic load factor of 1.27. The effective plastic strain was actually lower than in the static analysis due to the damping which, as mentioned, is very beneficial. By not including damping would give a strain of about 30%, cf. Figure 6.16, it is close to the value estimated in the NLS analysis with a dynamic load factor of 1.27. Based on these result there might be a risk of a fracture in the material if a strain limit of 20-25% is used.

In Figure 6.21 the normal force in adjacent columns 4 and 6 is shown. A dynamic load factor of 1.27 gave a good estimation of the dynamic effects.

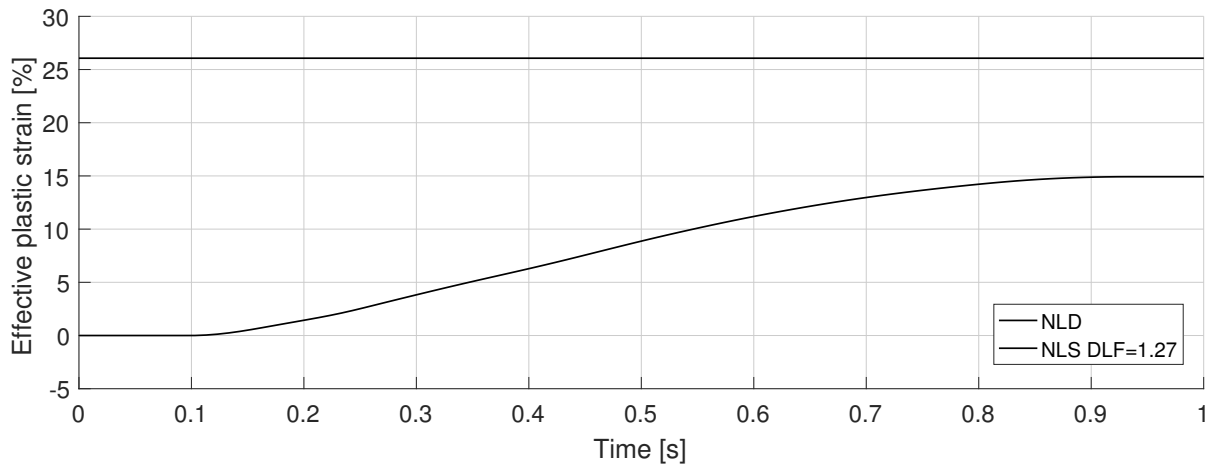


Figure 6.20: Maximum effective plastic strain in Beam 1, comparison of the results of the NLS and NLD analysis.

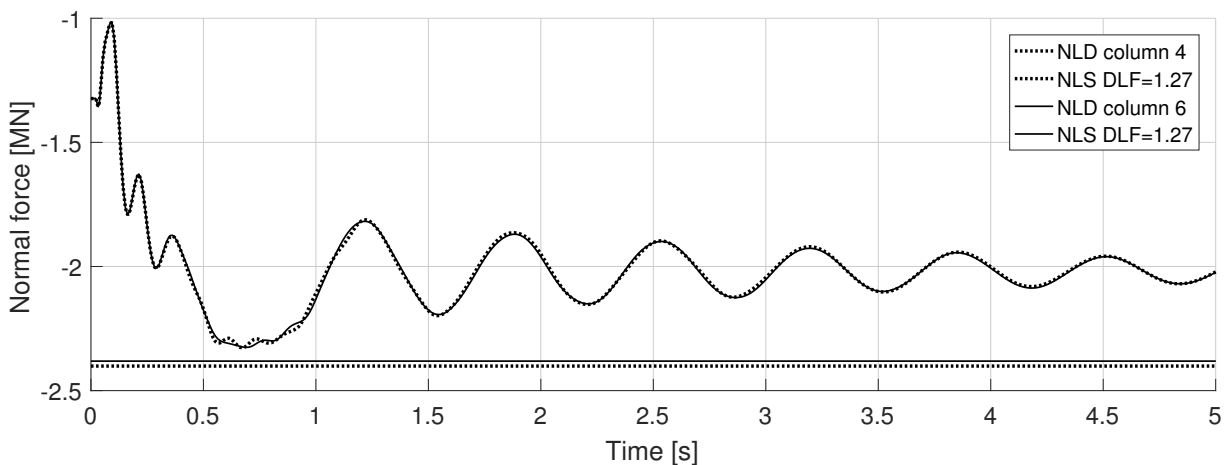


Figure 6.21: Normal force in adjacent columns 4 and 6, comparison of the results of the NLS and NLD analysis.

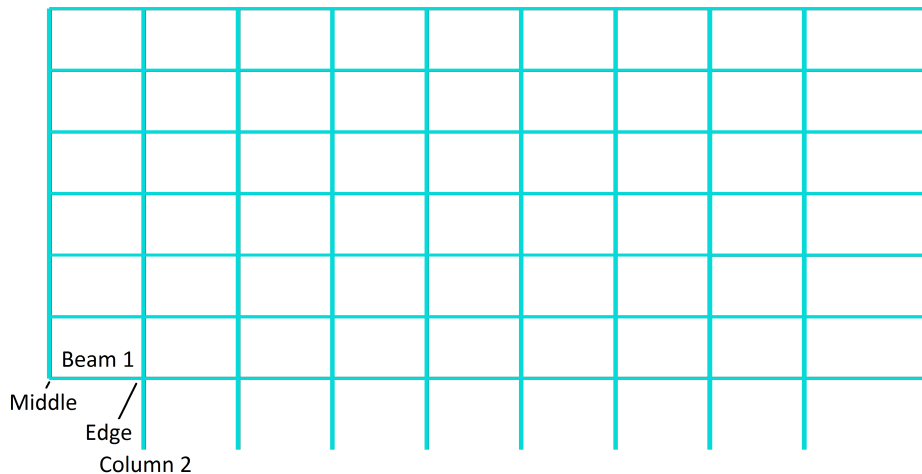


Figure 6.22: Locations in the model where results were extracted.

6.4 Column 1 removal

The following section presents the results that were obtained when column 1 was removed and an LS, NLS and NLD analysis were performed. The diagonals were not included in the model when column 1 was removed.

The first-floor beam connected to columns 1 and 2 is referred to as Beam 1. The point in Beam 1 located at the connection to column 2 is referred to as point Edge. The point in Beam 1 located at the location of the removed column is referred to as point Middle, cf. Figure 6.22.

The overall ability of the model to develop alternate load paths was studied. It was done by extracting internal forces developed in Beam 1, which has to transfer parts of the load carried by the removed column to adjacent elements.

6.4.1 LS analysis

The deformation of the model, just before failure is shown in Figure 6.23. Figure 6.25 shows the developed moment in Beam 1 at point Edge and Middle. The maximum moment was reached at point Edge first, the stiff connection between columns and beams allowed a redistribution of the moment to point Middle. As for the column 5 removal, the beam failed when less than 70% of the applied accidental load combination was applied.

6.4.2 NLS analysis

Figure 6.24 shows the deformation just before failure when column 1 was removed. In Figure 6.26 is the moment at point Edge and Middle shown. There was a small increase of the capacity compared to the LS analysis. This was most likely due to the decrease of lever arm for the load while the beam was deforming. Cable action in the beam for a corner column removal is not possible in a 2D model, a 3D model is needed to capture the effect illustrated in Figure 2.11.

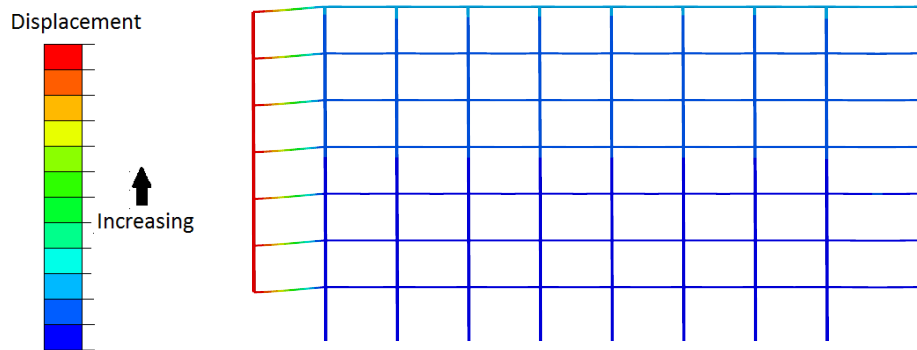


Figure 6.23: Deformation of the model in the LS analysis just before failure.

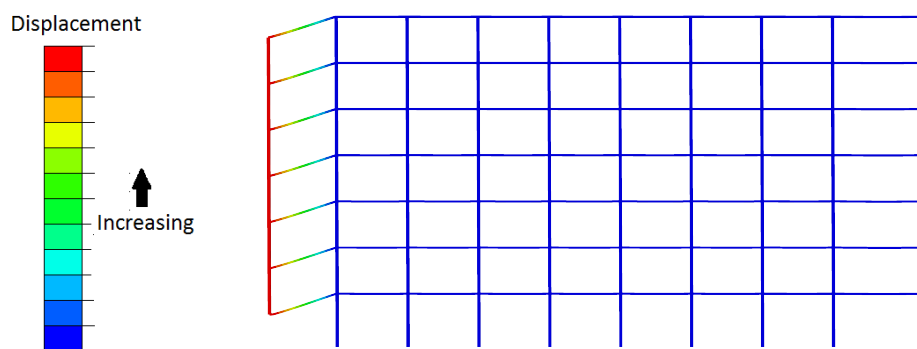


Figure 6.24: Deformation of the model in the NLS analysis just before failure.

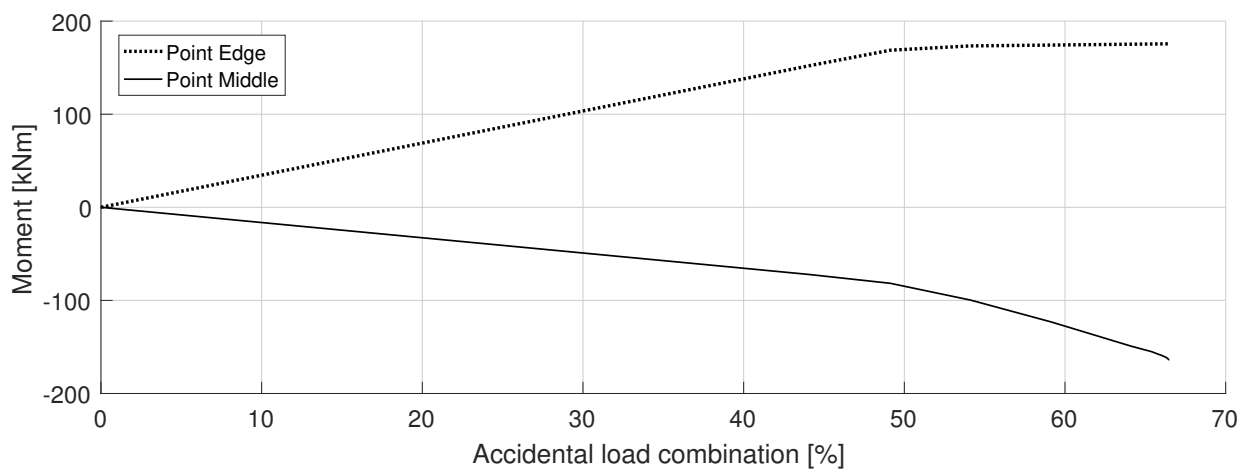


Figure 6.25: Moment in Beam 1 at point Edge and Middle, result of the LS analysis.

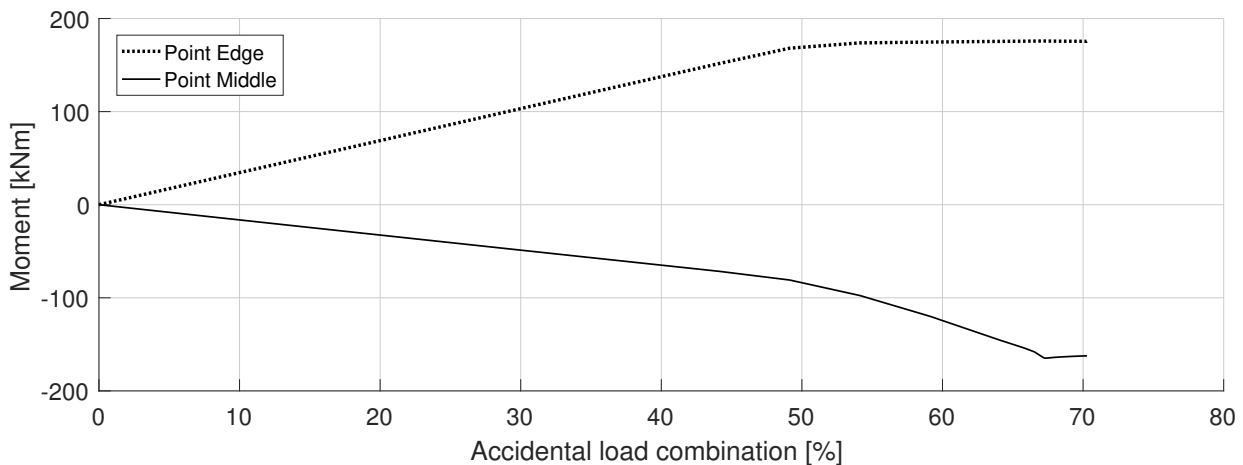


Figure 6.26: Moment in Beam 1 at point Edge and Middle, result of the NLS analysis.

6.4.3 NLD analysis

An NLD analysis with a removal of column 1 was not performed. The result from the NLS analysis showed that if column 1 was removed, Beam 1 would fail without consideration of the dynamic effects (dynamic load factor less than 1).

6.5 Summary and discussion

Column 5 removal

Using LS analysis is rejected because it gives, as predicted, a too conservative estimation of the beam capacity. Even though the load was decreased compared to the ultimate limit state load, it was not enough to compensate for the increased span length. The linear elastic results can, however, be used in an analytic estimate of the robustness of a building.

With the geometric non-linear effects included, the beams were capable of redistributing the accidental load combination up to a dynamic load factor of about 1.6. The large horizontal force due to cable action of the beams was most likely the reason why the model failed. The normal force could not be increased anymore which was needed to find equilibrium.

The large horizontal forces due to cable action of the beams required that diagonals were added to the model. The diagonals could resemble a slab that transfers the horizontal load to inner walls and elevator shafts. Without the diagonals, a 2D-model would be too conservative because a very limited cable action of the beams would be possible, and the geometric non-linear effects would not increase the capacity that much.

The dynamic analysis showed the importance of plasticity and damping which had a large effect on, for instance, the developed normal force in the adjacent columns. The used damping model had a very positive effect on the maximum effective plastic strain in the beam, which was twice as high without damping as to when damping was included. It is because of an additional moment capacity in the beam due to damping forces at the connection to adjacent columns, where the development of strain is most severe. In the

analyses a damping ratio of 5% was chosen for the entire model. A lower damping ratio of the beam might be appropriate because damping arises mainly from mechanisms, such as friction in connections and cracking of concrete, mechanisms that are not present in a steel beam.

A dynamic load factor of 1.27 for the NLS model was estimated by comparing the displacement of point Middle in Beam 1, between the NLS and NLD analysis. It gave a good representation of the overall dynamic effects, except for the effective plastic strain, which was lower in the dynamic analysis due to the damping model. However, without damping, the dynamic load factor estimated the effective plastic strain well.

Column 1 removal

All analyses using the 2D model failed when a load less than the accidental load combination was applied and column 1 was removed.

For a corner column removal, the 2D model is not detailed enough because cable action is not possible. To simulate the effect shown in Figure 2.11 a 3D model is required.

7 3D progressive collapse analysis

The present chapter describes the modelling and results from a progressive collapse analysis of the building described in Section 1.4. A 3D model of the building was created with the purpose of investigating the ability of the building to develop alternate load paths when different columns were removed.

The effect of using a 3D model compared to a 2D model was investigated by comparing the results obtained from the two models. The difference in results, from LS, NLS and NLD analyses were investigated to evaluate the possibility to use different analysing methods.

7.1 Method

The finite element program Abaqus was used in the analyses.

Columns and beams were chosen with reasonable dimensions by doing a linear static analysis with the ultimate limit state load applied in the 3D model. The ultimate limit state load is determined by Equation 6.1.

NLS and NLD analyses were performed and followed the procedure described in Section 3.2. The LS analysis was not performed using the 3D model, it was rejected based on the results from the 2D analysis, see Section 6.5.

Three different column removal locations were chosen in the building. A corner column (column 1), a facade column (column 5) and an inner column (column 11). The removal was performed in Abaqus with the "Model change" procedure, which enables a removal of an element in the model, in this case, a column. In the static analysis, the column was not modelled at all. In the dynamic analysis, an initial static step was first performed to determine the initial stress state. After the static initial step, the column was removed with "Model change" and a dynamic implicit step was started.

7.2 FE-model of the 3D structure

7.2.1 Geometry

The geometry of the 3D model is shown in Figures 7.1a–7.1c. Figure 7.1a shows all elements in the model including the slab, which consists of hollow-core units that are connected to the shear walls, to the simplified unsymmetrical HSQ-profiles in the facade and to the simplified symmetrical HSQ-profiles in the middle of the model. Figure 7.1b shows the vertical load bearing elements, that is, facade VKR-columns, inner VKR-columns

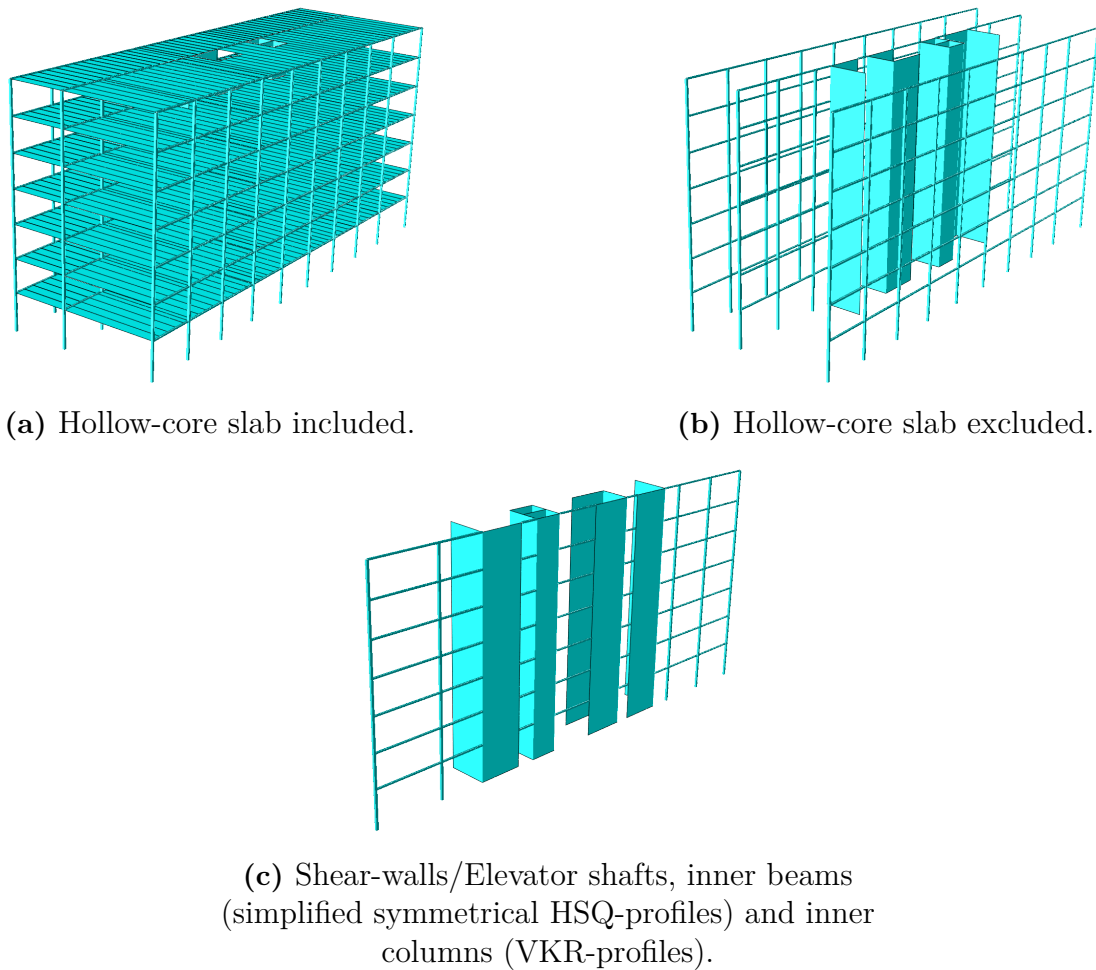


Figure 7.1: Isometric view of the modelled building.

and shear-walls/elevator shafts, which also act as horizontal stabilisation of the entire structure.

7.2.2 Walls/elevator shafts

Shear walls and elevator shafts were modelled with shell elements. Material was assumed to be concrete of quality C35 with the strength, according to Eurocode [10], of $E=34$ GPa, Poisson's ratio of 0.2 and a density of 2500 kg/m^3 . These were modelled assuming a linear elastic material model.

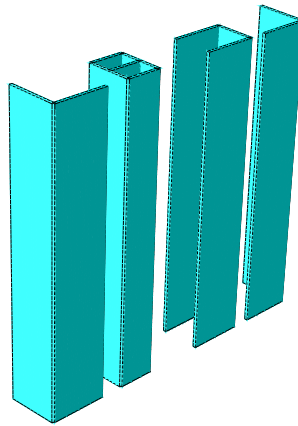


Figure 7.2: The horizontal stabilising shear walls and elevator shafts that were modelled with shell elements.

7.2.3 Facade

Beams were modelled with beam elements with an element length of 0.1 m. It implies that 108 elements were used in a span length of 10.8 meters, as was done in the analysis of beams in Chapter 5. A simplified cross-section shown in Figure 5.16 was used. The columns consisted of VKR-250×250×10 profiles modelled with beam elements using a box cross-section in Abaqus.

The material was modelled as steel S355 with strength properties according to Eurocode [22]. It implied an elastic modulus of 210 GPa, Poisson's ratio of 0.3 and density of 8000 kg/m³. Plasticity was modelled with a von Mises yield criterion with yield stress at 355 MPa, hardening was neglected.

7.2.4 Inner columns and beams

Inner beams consist of symmetrical HSQ-profiles. These were modelled with beam elements, with the same element size as the facade-beams, using a simplified cross-section shown in Figure 5.15.

Columns at the short-side facade (columns 11 and 15 in Figure 1.3) were modelled as VKR-250×250×10 profiles with a capacity of 2.73 MN according to Eurocode [22], with a buckling length equal to the height between the ground and the first floor. Inner columns 12–14 (cf. Figure 1.3) were modelled as VKR-250×250×10 profiles with a capacity of 3.35 MN. They were both modelled with beam elements using a box cross-section in Abaqus. Inner walls, columns and beams are shown in Figure 7.3.

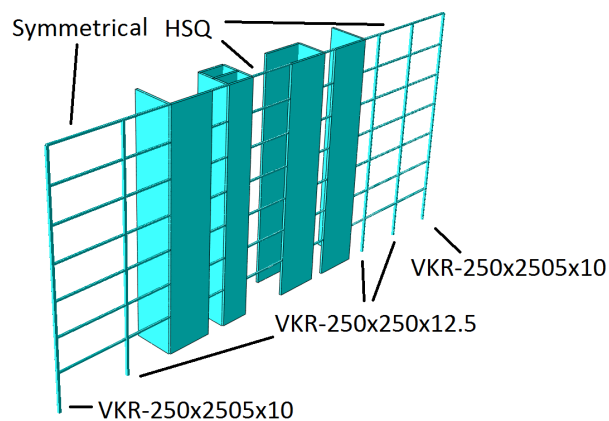


Figure 7.3: Inner columns that consist of VKR-profiles and beams that consist of symmetrical HSQ-profiles.

7.2.5 Slab

Modelling of the hollow-core slab was inspired by Johansson [26], who studied vibrations in hollow-core slabs by using shell elements with an orthotropic lamina material in Abaqus. The lamina material model requires two elastic modulus, three shear modulus and one Poisson's ratio.

Table 7.1 shows the material properties chosen for the model. The thickness was increased somewhat compared to Johansson to conform with the dimensions of the actual hollow-core units in the building.

Table 7.1: Material properties of the hollow-core units using an orthotropic lamina material in Abaqus.

t (m)	ρ (kg/m ³)	E_1 (GPa)	E_2 (GPa)	G_{12} (GPa)	G_{13} (GPa)	G_{23} (GPa)	ν_{12}
0.236	2775	44.4	8.7	3.92	0.2	0.1	0.39

Longitudinal joints between the hollow-core units were not included because the concrete is assumed to crack in these joints as described in the theory of progressive collapse design. By neglecting the concrete in the joints, load transferring was disabled in the transverse direction of the hollow-core slab and it behaved more as multiple beams, see Figure 7.4.

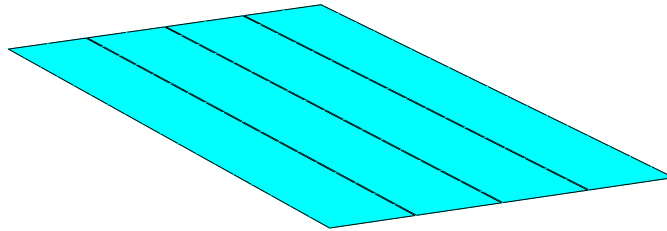


Figure 7.4: Part of the hollow-core slab modelled with shell elements. Note that the longitudinal joints were not modelled.

7.2.6 Mass and damping

As in the 2D model, the load in the dynamic analysis must be applied from the mass. The mass was applied to the model by adjusting the density of the slab by dividing the accidental load combination with the gravitational constant. With a permanent load of $G=5.3 \text{ kN/m}^2$, a live load of $q_k=2.5 \text{ kN/m}^2$, a gravitational constant of $g=10 \text{ m/s}^2$ and a thickness of 0.236 m , the density of the slab was determined by

$$(G + \psi_1 q_k) \frac{1}{gt} = (5.3 + 0.5 \cdot 2.5) \frac{1}{10 \cdot 0.236} \approx 2775 \quad [\text{kg/m}^3]. \quad (7.1)$$

7.2.7 Loading and boundary conditions

The load was applied as a surface traction on the entire slab. The accidental action load combination was used, as in the 2D model.

$$(G + \psi_1 q_k) = (5.3 + 0.5 \cdot 2.5) = 6550 \quad [\text{kN/m}^2]. \quad (7.2)$$

The dynamic load factor was applied in the same way as described in Figure 3.7. A dynamic load factor of 2 was used, which implies a surface traction of 6550 kN/m^2 , applied as illustrated in Figure 7.5.

In the static analysis results will be presented as a function of the dynamic load factor (DLF). A dynamic load factor between 0 and 1 is when only the accidental load combination has been applied. When the whole accidental load combination has been applied (DLF=1), the load seen in Figure 7.5 was applied on chosen surfaces, which equals to a dynamic load factor between 1 and 2.

Connections between the ground to columns and walls were modelled as moment stiff. All rotational and displacement degrees of freedoms were thus constrained at these points.

All beam to column and beam to wall connections were also modelled as moment stiff.

Two different connection types between the hollow-core units and its supporting beams and walls were investigated in the 3D model. One where the hollow-core units were constrained to walls and beams in both displacement and rotational degrees of freedom, referred to as restrained in the text.

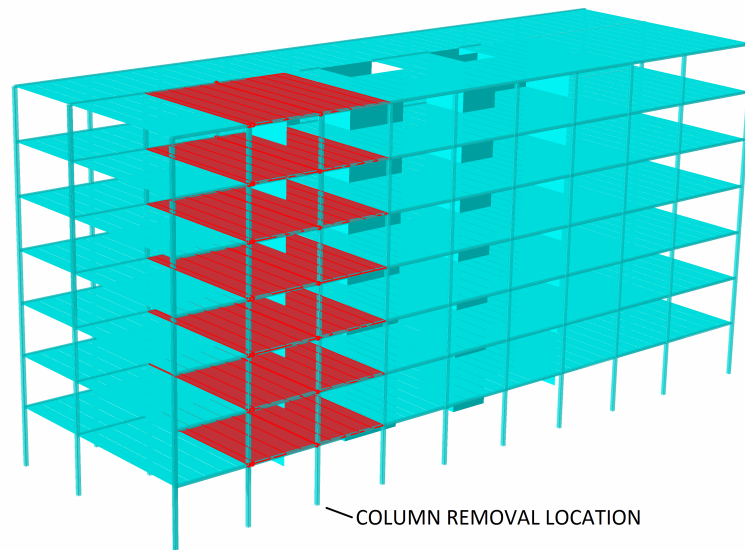


Figure 7.5: The principle of how the dynamic load factor was applied in the model. The red surface shows where a dynamic load factor was applied when column three was to be removed.

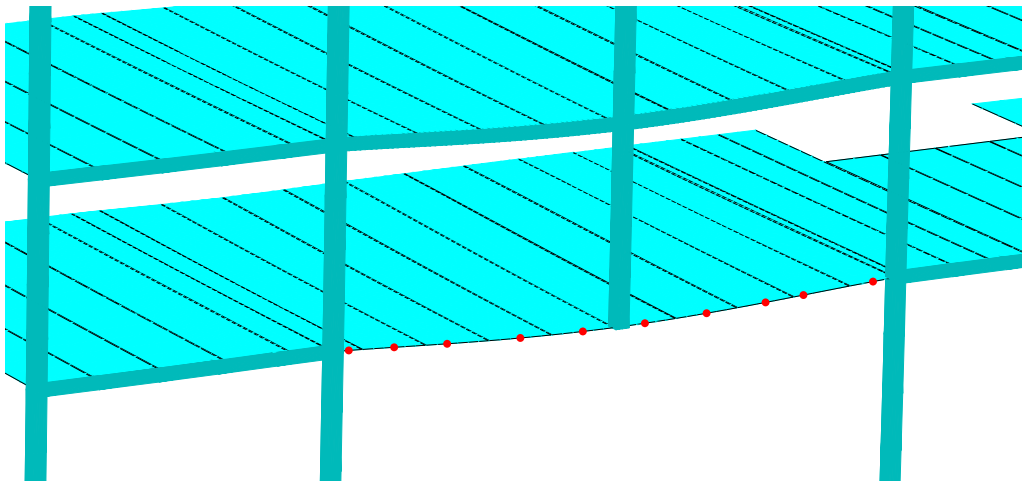


Figure 7.6: Connection type simply. Red dots show the principle of where the hollow-core units were constrained to the facade beam (in the displacement degrees of freedom).

For the other connection type, the hollow-core units were only constrained to beams/walls in the displacement degrees of freedom, which would represent a simply supported slab, referred to as simply in the text. The connection between the hollow-core units and the beams directly affected by the column failure were only tied at one point in the middle of the hollow-core units. It was done to represent a situation in which the surrounding concrete cracks, see Figure 2.9, and the hollow-core units are only connected by the reinforcement shown in Figure 2.10. Figure 7.6 illustrates how it was implemented in Abaqus.

7.3 Column 3 removal

In the following section, results are presented from a progressive collapse analysis when column 3 was removed. Both an NLS and NLD analysis were performed with the two different connection types of the hollow-core units, namely simply and restrained.

The beams connected to columns 2 and 4 are referred to as Beam 1–7. Points in Beam 1–7 located at the connection to columns 2 and 4 are referred to as point Edge. The point in Beam 1 located at the location of the removed column is referred to as point Middle, see Figure 7.7.

The overall ability of the model to develop alternate load paths was studied. It was done by extracting internal forces developed in Beam 1–7, which have to transfer parts of the load carried by the removed column to adjacent elements. The developed normal force in adjacent columns was also extracted.

The Load transferring from Beam 1 through the slab, and which affect the connection type had on it, was also studied.

In the NLD analysis the dynamic effects were studied and the result of the NLS analysis was compared to estimate the dynamic load factors and if they could represent the overall dynamic effects.

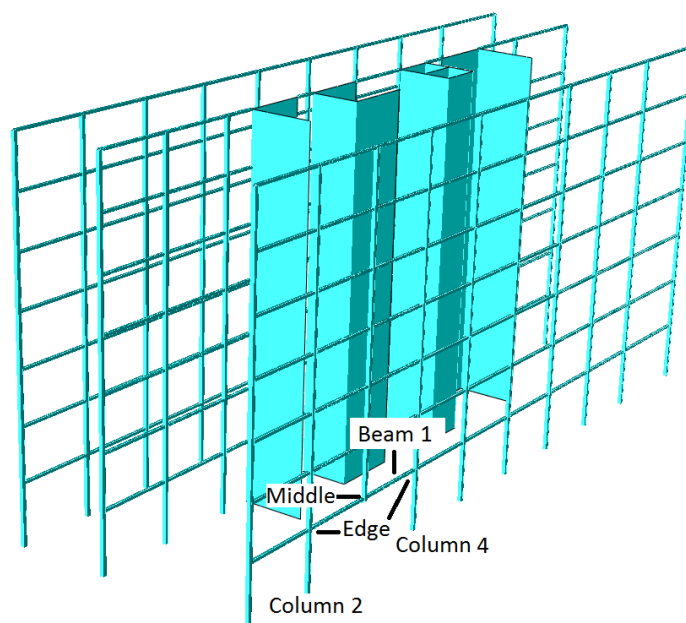


Figure 7.7: Locations in the model where results were extracted.

7.3.1 NLS analysis

For the column 3 removal, a parameter study was performed to determine the effect of the hollow-core unit stiffness. The stiffness properties of the slab in Table 7.1 were multiplied by a factor 1, 0.5 and 0.125, it was only implemented for the hollow-core units loaded with a dynamic load factor, remaining hollow-core units had the initial stiffness (factor 1). The less stiff hollow-core units were supposed to resemble a situation where there is some cracking of the concrete and that the in-cast rebar connection is a bit loose.

All analyses with a restrained connection type finished with a dynamic load factor of 2, meaning that the maximum capacity was not reached. The analysis with the connection type simply resulted in failure at a dynamic load factor about 1.8–1.9. Higher stiffness of the hollow-core units was beneficial, most likely due to a better ability to distribute forces, although the difference in the capacity was not that large.

The resulting deformation with connection type, simply, is shown in Figure 7.8 and the deformation with the restrained connection type is shown in Figure 7.9. As shown in the figures, the deformations were larger in the model with connection type simply. The reason to why the model with connection type simply failed, was most likely due to a limited capacity to support the horizontal forces in the structure, the large deformation observed of the corner column (column 1) strengthen this theory. Compare the deformation of column 1 in Figures 7.8 and 7.9.

Figures 7.10, 7.11 and 7.12 show the moments and normal forces that were extracted from Beam 1, at point Edge and at point Middle. Legends "Restrained 1" and "Simply 0.125" refers to the connection type of the hollow-core units and its stiffness factor. Legend "2D" is the result of the 2D analysis when column 5 was removed.

The normal forces and moments showed the same behaviour as seen in Chapters 5 and 6, which implies an increase of the moment at first, then an increase of the normal force. With the connection type, restrained, the hollow-core unit stiffness had a large impact

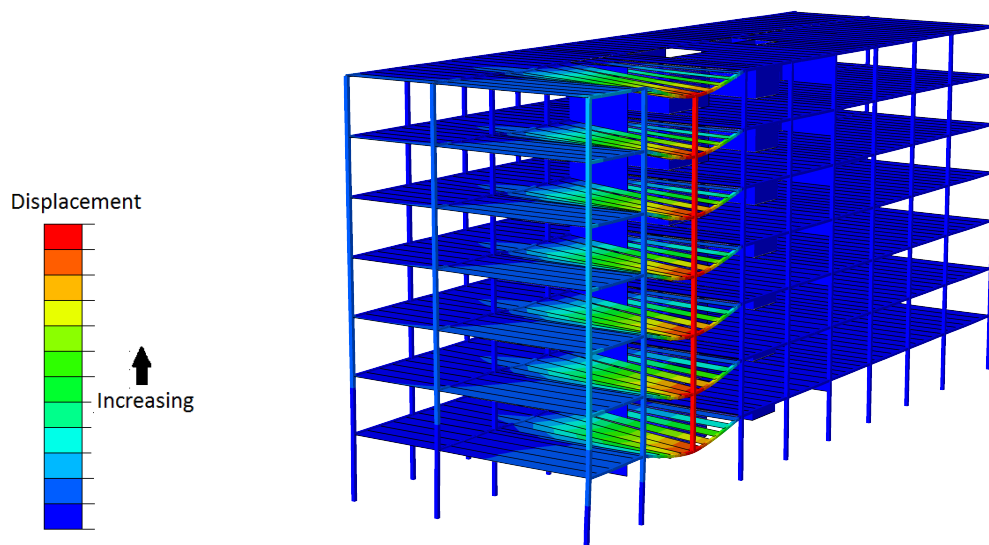


Figure 7.8: Deformation of the model just before failure when connection type simply was used.

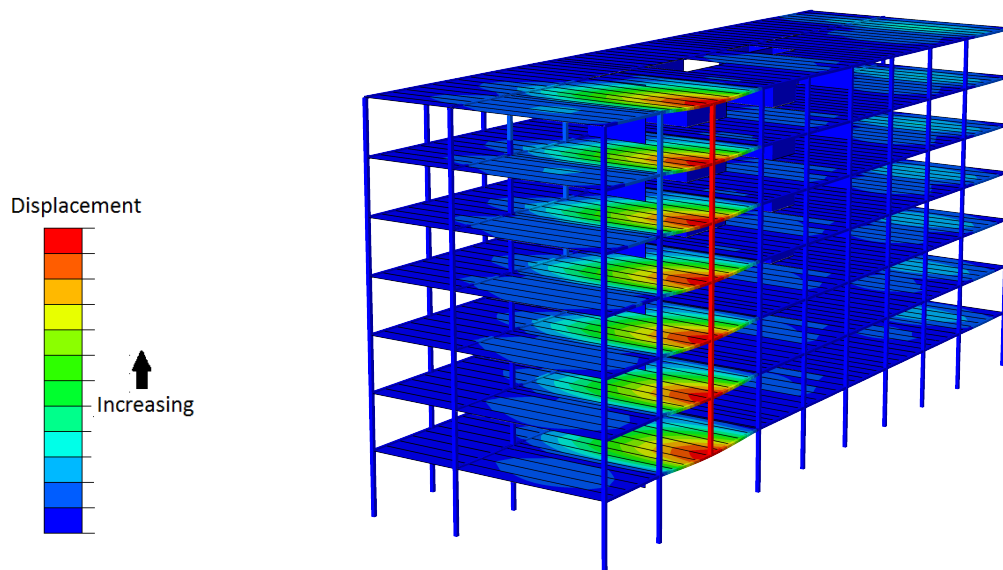


Figure 7.9: Deformation of the model just before failure when connection type restrained was used.

on the developed normal force in the beam. This is because the load was transferred, through cantilever action of the hollow-core units, from the beam to other parts of the building. With less stiff hollow-core units, this capacity was reduced and the load was taken up by Beam 1–7 instead.

There was a much higher normal force in the beam in the 2D analysis which is most likely due to a better capacity to support the normal force on the first floor in the 2D model due to the added diagonals. However, all 3D analysis, including the ones with connection type simply, reached a higher dynamic load factor than the 2D analysis. The reason for this can be that some load was transferred to the inner parts of the building. It can also be that the 3D model had a better ability to support the normal forces at floor 2–7, it is a theory that is strengthened by Figure 7.13, where the normal forces in the beams at all floors (Beams 1–7) are shown. It seems that all beams contributed by cable action, a result that was not seen in the 2D analysis, see Figure 6.8 and 6.9.

The theory that the ability of the model to support the horizontal forces determined the load capacity of the model, with connection type simply, is strengthened by looking at the normal force at the connection to column 2. After a dynamic load factor of about 1.7, the normal force seems to have reached a maximum, it is not seen at the connection to column 4 where the force still was increasing. The connection to column 4 can support a larger horizontal force because there is a larger part of the structure in that direction.

No suspension mechanism to upper intact floors was obtained by the remaining parts of the removed column. Instead, it was compressed and the upper beams were actually supported by beams at the lower floors.

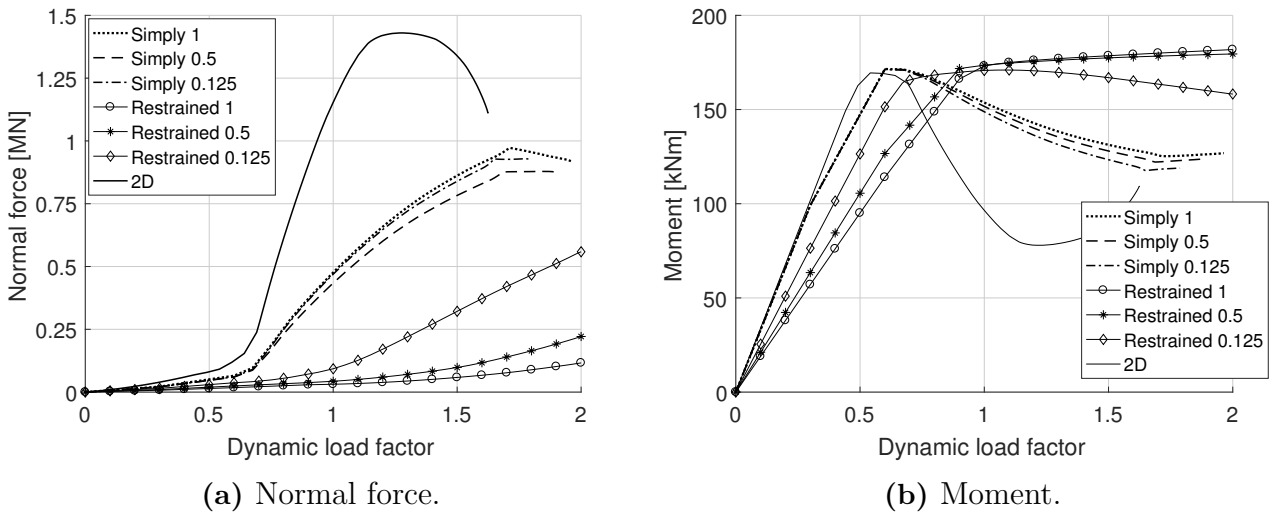


Figure 7.10: Moment and normal force in Beam 1, at point Edge, at the connection to column 2.

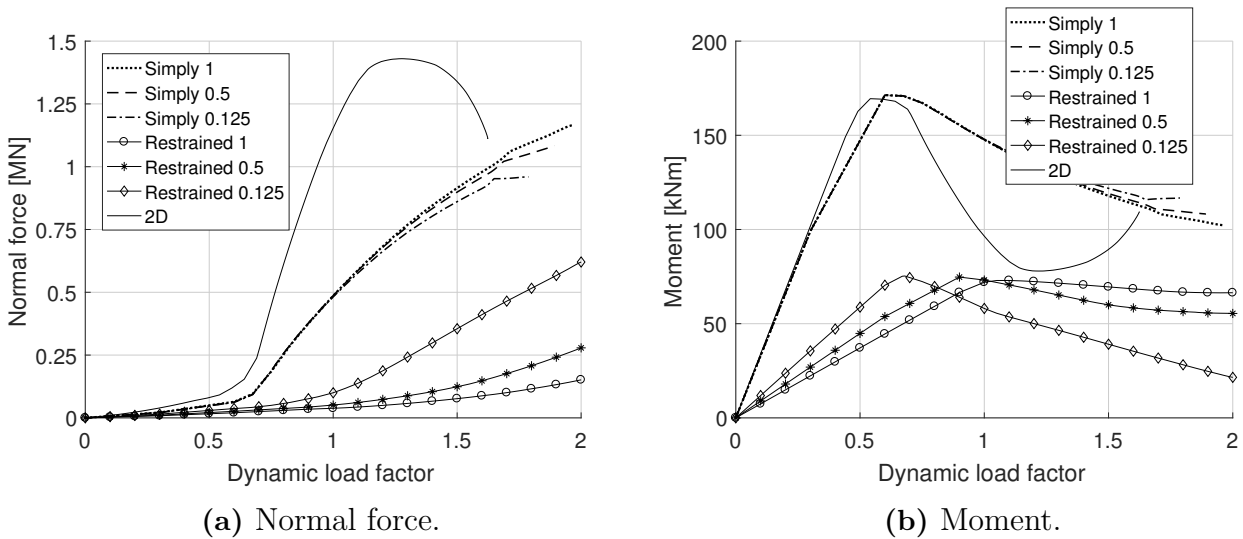


Figure 7.11: Moment and normal force in Beam 1, at point Edge, at the connection to column 4.

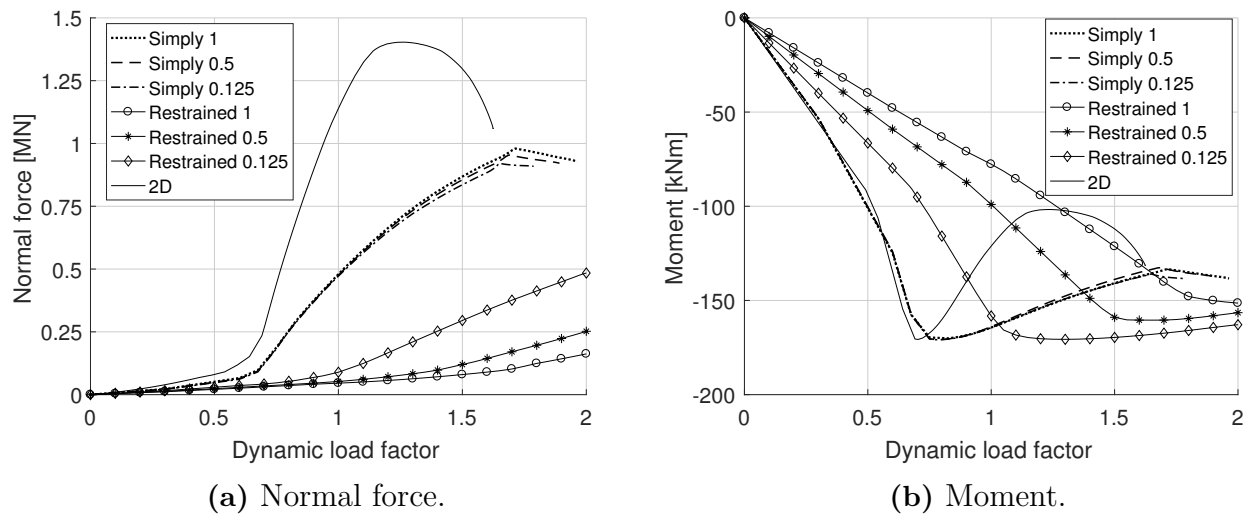


Figure 7.12: Moment and normal force in Beam 1, at point Middle.

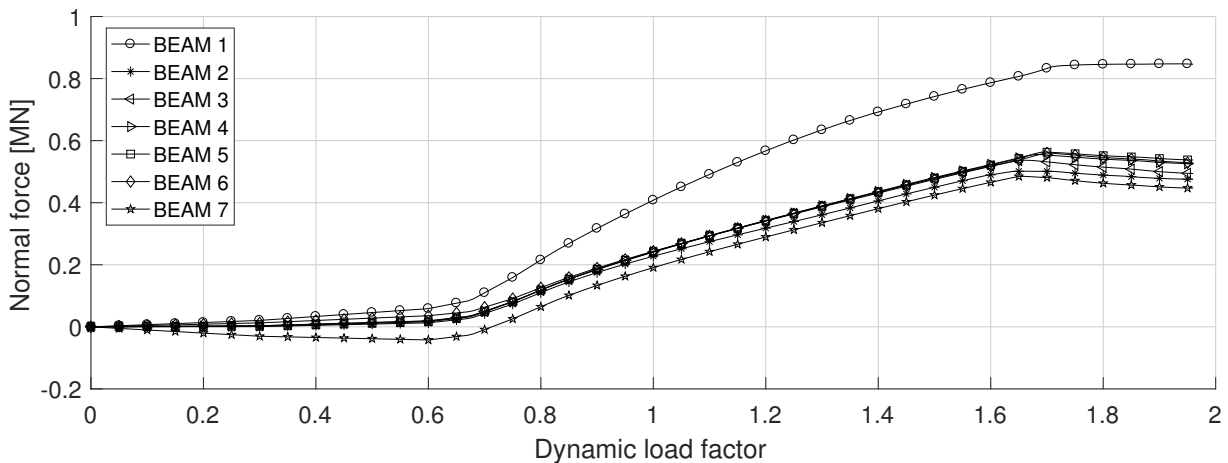


Figure 7.13: Normal force in Beam 1–7 at point Edge, at the connection to column 2.

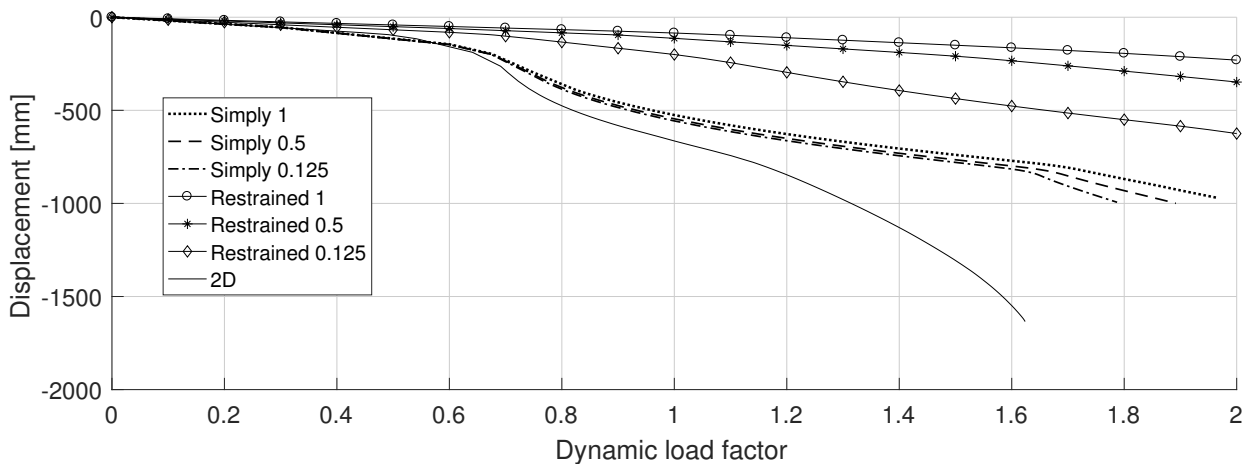


Figure 7.14: Vertical displacement of point Middle in Beam 1.

The displacement of point Middle in Beam 1 is shown in Figure 7.14. A higher stiffness of the hollow-core units was beneficial for the displacement, both in the analysis with connection type restrained and simply.

The maximum effective plastic strain in Beam 1 is shown in Figure 7.15. With connection type simply, a dynamic load factor of about 1.3–1.5 would give a risk of fracture in the material if the strain limit is assumed to be 15–25%, which is reasonable for steel S355, cf. Appendix D. If the minimum strain limit of 15% specified in Eurocode [22] is used, then Beam 1 would be considered to fail with a dynamic load factor of 1, which means that it fails without consideration of the dynamic effects. With the connection type restrained, there was only a risk of high (15%) effective plastic strain in Beam 1 with the low stiffness hollow-core units at a dynamic load factor about 1.9.

All analyses resulted in a higher capacity as compared to the 2D model. One reason for this could be due to a capability to transfer the load to inner parts of the building. This effect was investigated by first performing an analysis without a removal of the column and then comparing with the results when the column was removed. In both analyses

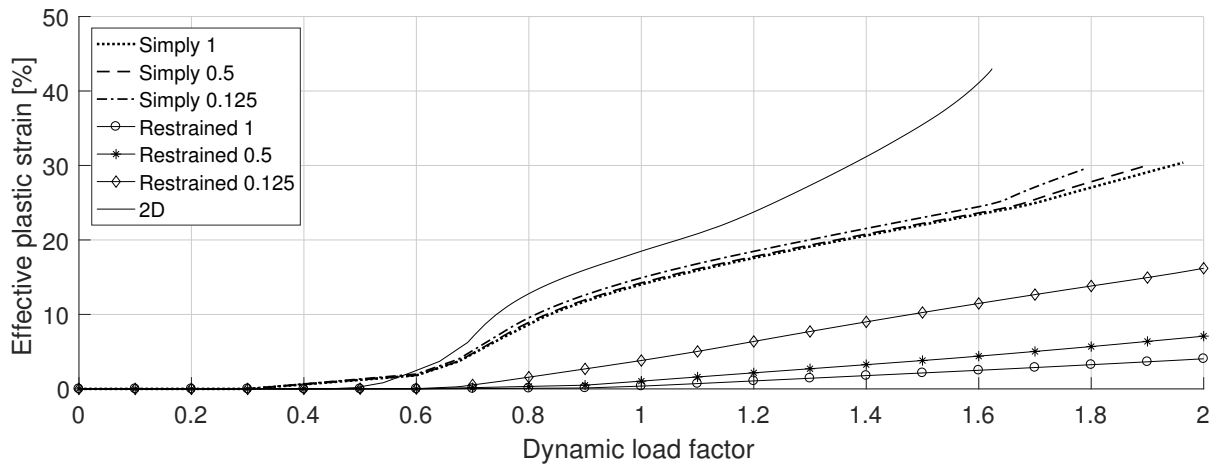
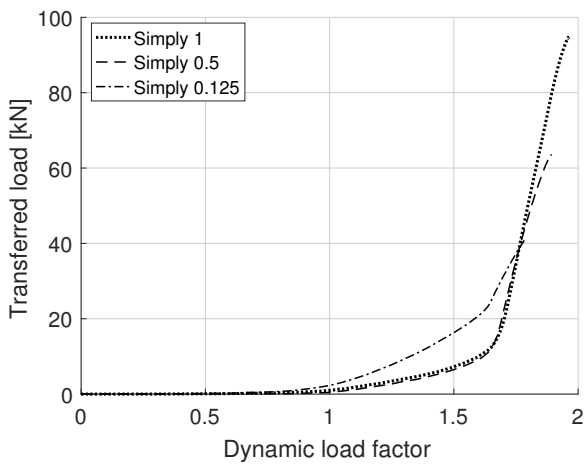


Figure 7.15: Maximum effective plastic strain in Beam 1.

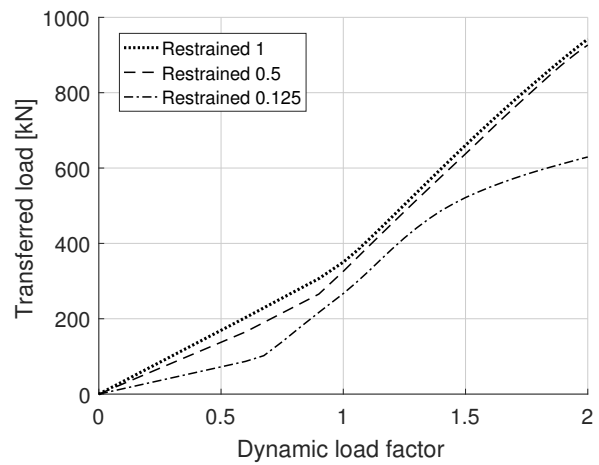
with the removed column and not removed column, the total applied load was equal. To investigate if the load were transferred to the inner parts of the building, a comparison was made, before and after the column removal, of the sum of all vertical reaction forces in every column to ground connection in the facade. If no load transferring to inner parts was present in the analysis where the column was removed, the load should just be transferred to adjacent columns in the facade. This would result in, that the sum of all vertical reaction forces in the facade are equal in the analysis where the column was removed, and the analysis where it was not removed.

In Figure 7.16, the difference between the total vertical reaction force in the facade, for the analysis without and with the column removal, is shown. As expected, the transfer was much higher with a restrained connection type. It also shows that there was a transfer with connection type simply, it is most likely due to a development of normal force and cable action in the hollow-core units.

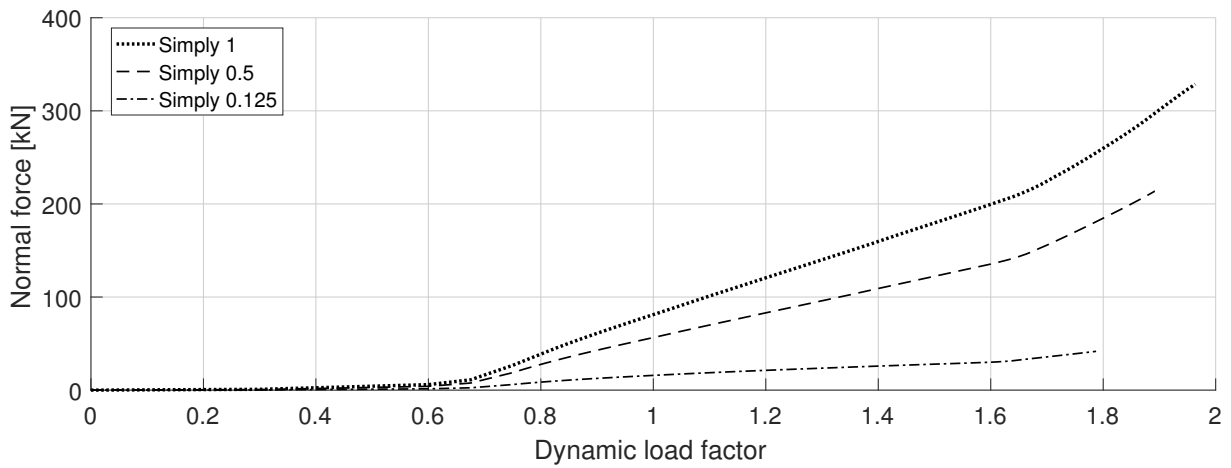
Figure 7.17 shows the sum of the normal forces in all hollow-core units where the dynamic load factor was applied. When the normal force increases, the transferred load also increases, this confirms the theory that cable action of the hollow-core units is beneficial. However, it is somewhat surprising that the transferred load was less, with a lower external load applied, using a higher stiffness of the slabs. The displacement was, on the other hand, larger, and it is difficult to determine all load transferring factors.



(a) Connection type simply.



(b) Connection type restrained.

Figure 7.16: Load that was transferred from the facade to other parts of the model.**Figure 7.17:** The sum of the normal forces in all hollow-core units where the dynamic load factor was applied. The results were obtained with connection type simply with different stiffness of the hollow-core units.

Figures 7.18–7.20 show the normal forces in adjacent columns 2, 4 and 13. The legend "Not removed" refers to an analysis in which the column was not removed. It was done to investigate how the adjacent columns were affected by the column removal.

For the facade columns (2 and 4), the load was increased dramatically due to the column removal with connection type simply. For the connection type, restrained, the load was distributed more effectively to inner columns.

Figure 7.20 shows that column 13 was not affected by the column removal if connection type simply was used and the dynamic load factor was less than 1.7. At a dynamic load factor of about 1.7, when the normal force in the hollow-core slab started to increase, the normal force in column 13 began to increase dramatically as well because of load transferring in the slab. The effectiveness of the load transferring is also dependent on the stiffness of the hollow-core units, which Figure 7.20 shows.

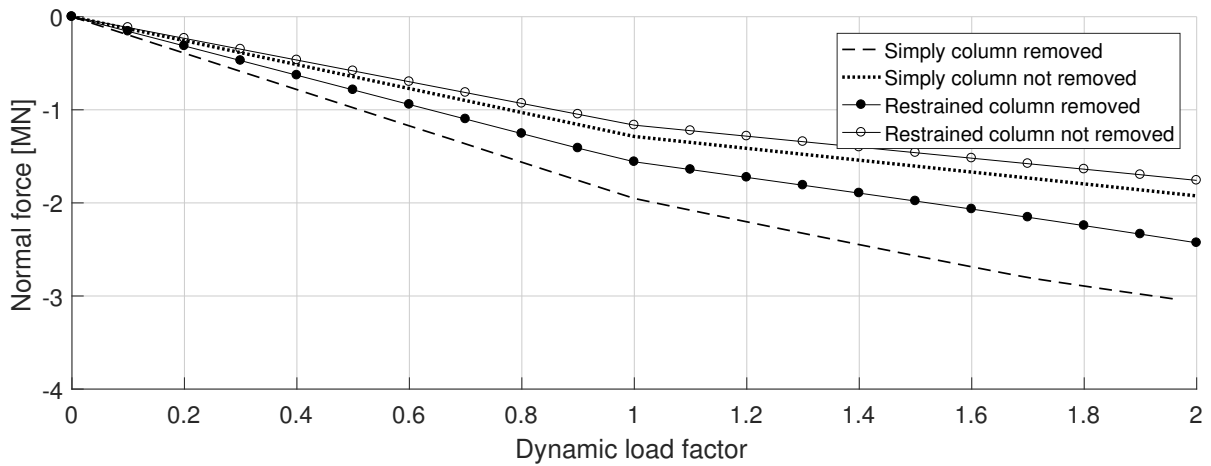


Figure 7.18: Normal force in adjacent column 2. Legend not removed refers to an analysis in which the column was not removed.

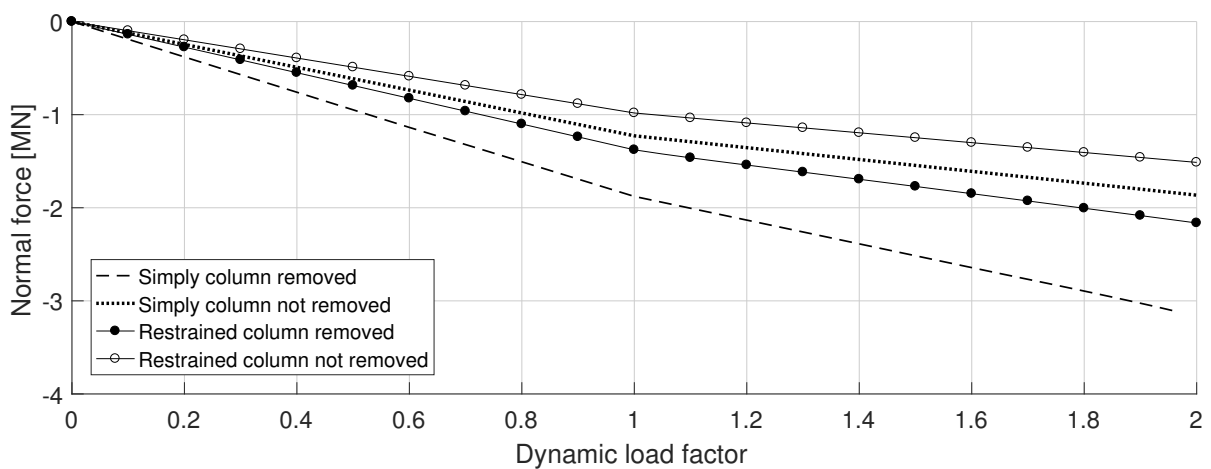


Figure 7.19: Normal force in adjacent column 4. Legend not removed refers to an analysis in which the column was not removed.

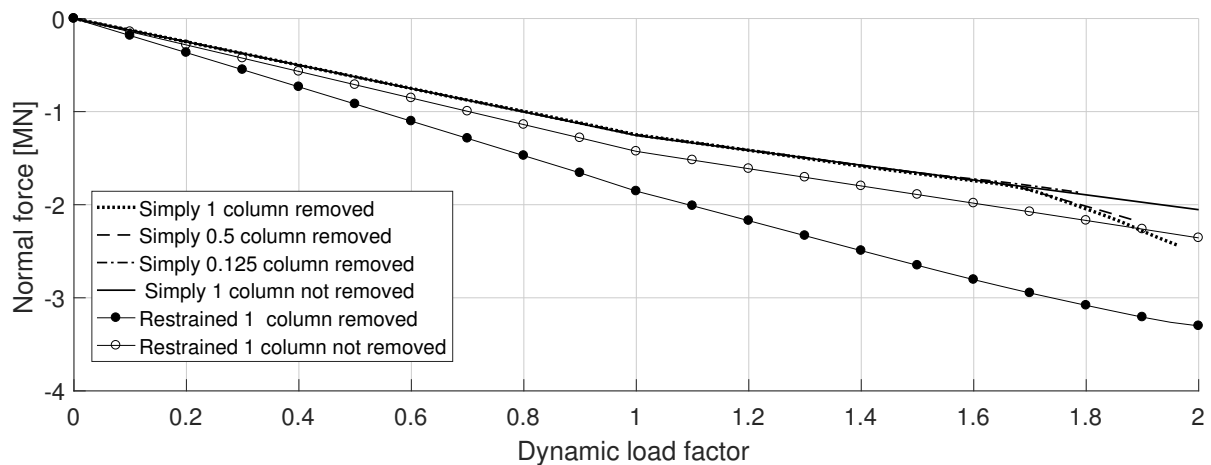


Figure 7.20: Normal force in adjacent column 13. Legend not removed refers to an analysis in which the column was not removed. The figure also shows the effect of the hollow-core unit stiffness when connection type simply was used.

7.3.2 NLD analysis

The following section presents the results from an NLD analysis when column 3 was removed. Results were extracted with the connection types simply and restrained. The stiffness of the hollow-core units was kept with full stiffness in all of the NLD analyses.

As in the 2D analysis, the displacement was used to estimate the dynamic load factor needed in the static analysis to account for the dynamic effects. Figure 7.21 shows the displacement of point Middle in Beam 1 for both slab connection types. A dynamic load factor of 1.45 gave a good estimation of the dynamic effects in the NLS analysis.

Figures 7.22 and 7.23 show the moment and the normal force in Beam 1 at point Edge, at the connection to adjacent column number 2 and 4, and at point Middle. For the normal force at point Middle, a dynamic load factor of 1.45 gave a good estimation of the dynamic effects in the NLS analysis.

At point Edge, at the connection to adjacent columns, the dynamic load factor of 1.45 overestimated the dynamic effects for both the analyses with connection type simply and restrained. The difference was most likely due to damping, which has a large impact on the internal forces developed at point Edge. Note that the moment, see Figure 7.22b, at about 0.3 s, is larger than the capacity of the beam.

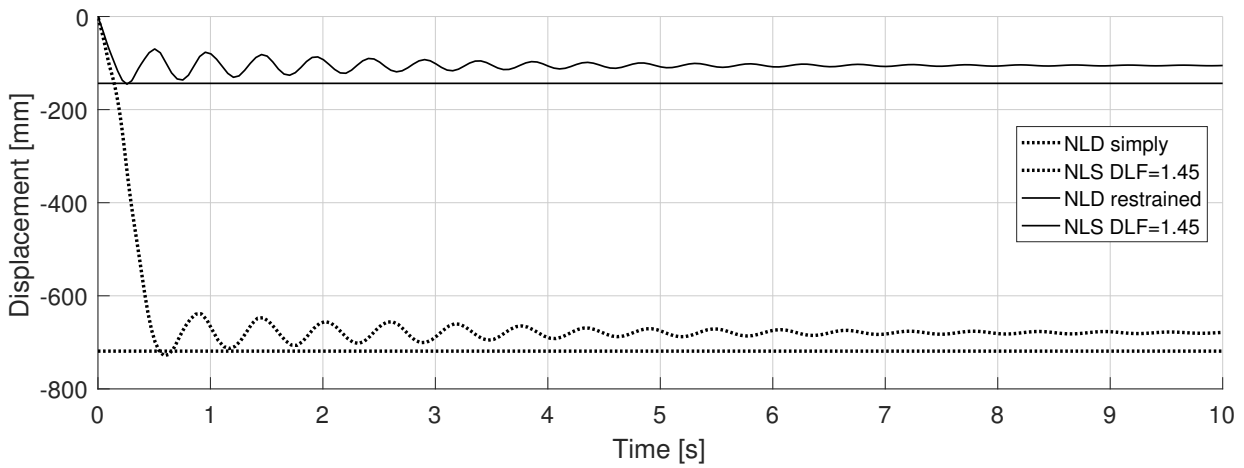
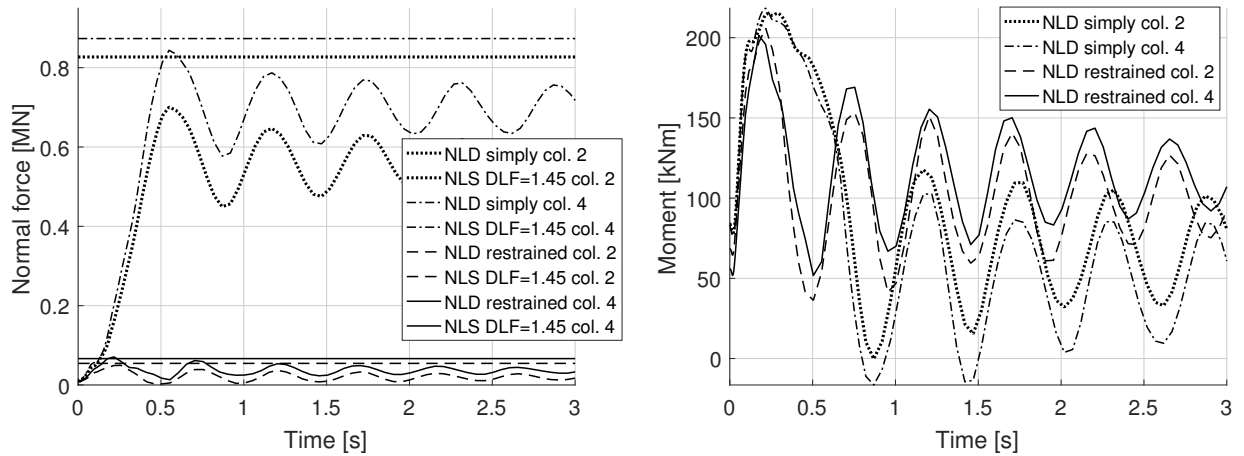


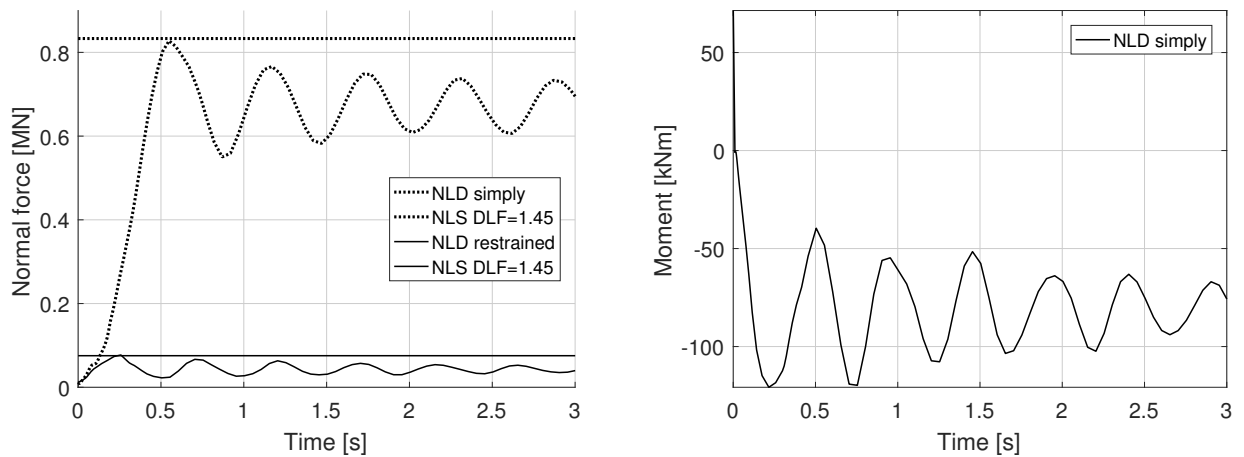
Figure 7.21: Displacement of point Middle in Beam 1, comparison of the results of the NLS and NLD analysis.



(a) Normal force, comparison of the results of the NLS and NLD analysis.

(b) Moment, result of the NLD analysis.

Figure 7.22: Moment and normal force in Beam 1 at point Edge, at the connection to adjacent columns 2 and 4.



(a) Normal force, comparison of the results of the NLS and NLD analysis.

(b) Moment, result of the NLD analysis.

Figure 7.23: Moment and normal force in Beam 1 at point Middle.

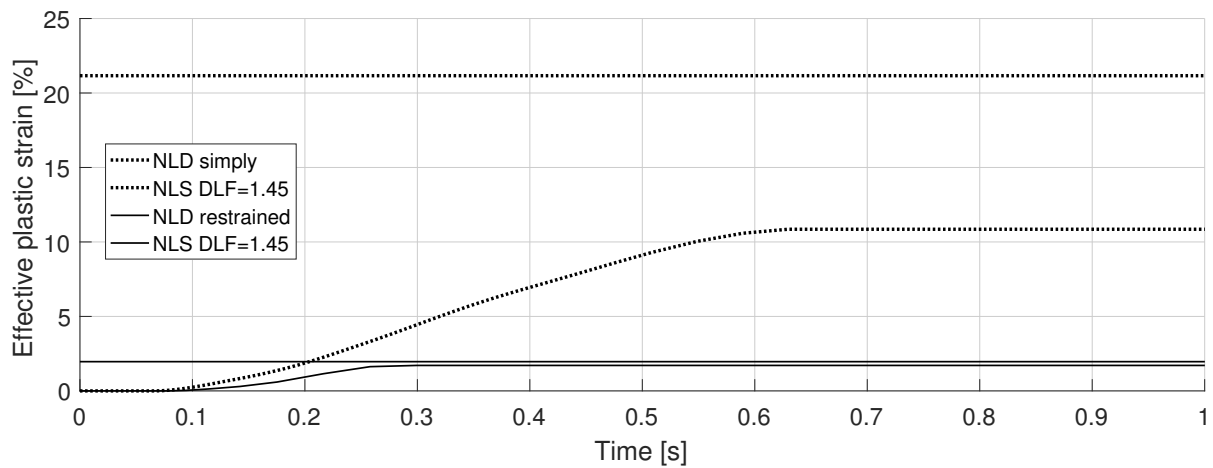


Figure 7.24: Maximum effective plastic strain in Beam 1, comparison of the results of the NLS and NLD analysis.

Because of the damping, the maximum effective plastic strain was also quite low compared to the effective plastic strain estimated with dynamic load factors in the NLS analysis, see Figure 7.24. At least with the connection type simply. In the NLD analysis, the effective plastic strain was lower than in the NLS analysis with a dynamic load factor of 1.

The normal forces in adjacent columns 4 and 13, shown in Figures 7.25–7.27, was well estimated with a dynamic load factor of 1.45. The force in column 2 was somewhat overestimated.

The capacity of 2.73 MN for columns 2 and 4, and the capacity of 3.35 MN for column 13, was not reached in the NLD analysis.

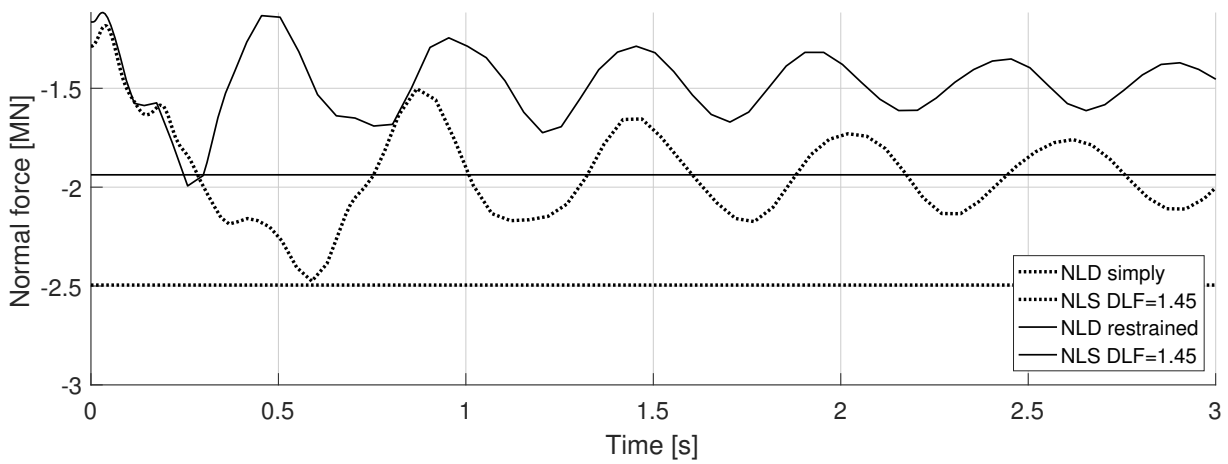


Figure 7.25: Normal force in adjacent column 2, comparison of the results of the NLS and NLD analysis.

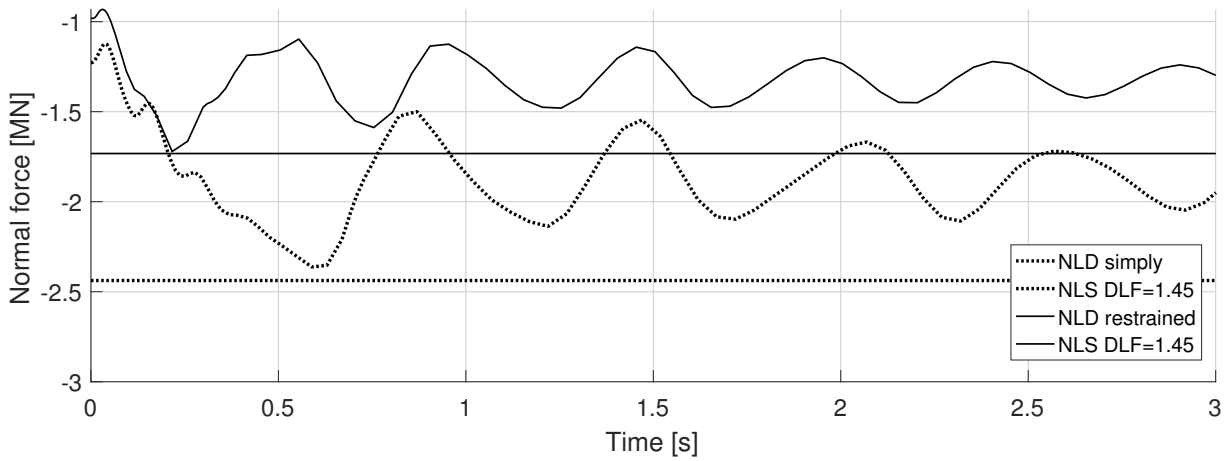


Figure 7.26: Normal force in adjacent column 4, comparison of the results of the NLS and NLD analysis.

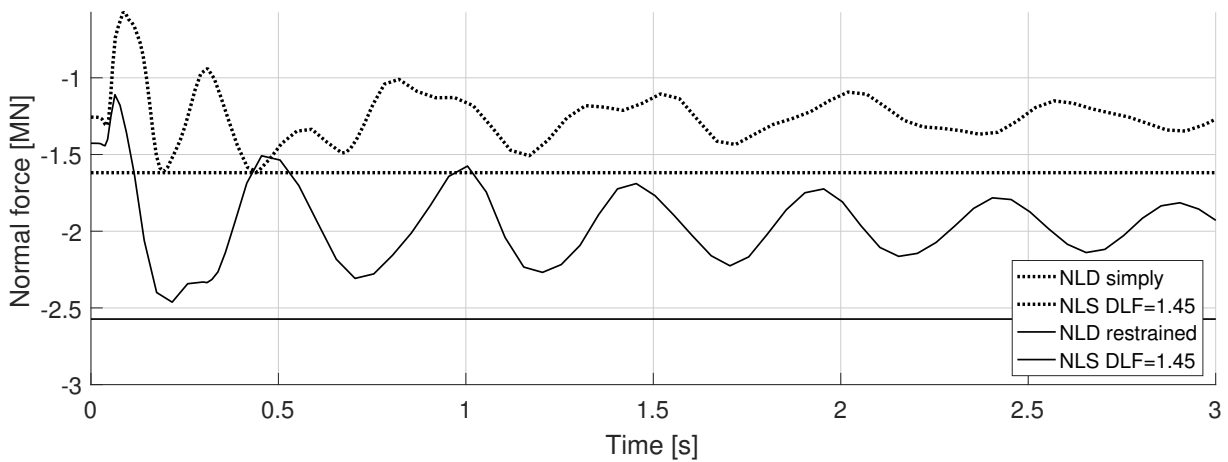


Figure 7.27: Normal force in adjacent column 13, comparison of the results of the NLS and NLD analysis.

7.4 Column 1 removal

In the following section, results are presented from the removal of column 1. Both an NLS and NLD analysis were performed with the two different connection types of the hollow-core units, namely simply and restrained.

The first-floor beam connected to column 1 is referred to as Beam 1. The point in Beam 1 located at the connection of Beam 1 to column 2 is referred to as point Edge. The point in Beam 1 located at the location of the removed column is referred to as point Middle, see Figure 7.28.

The overall ability of the model to develop alternate load paths was studied. It was done by extracting internal forces developed in Beam 1, which has to transfer parts of the load carried by the removed column to adjacent elements. The developed normal force in adjacent columns was also extracted.

The Load transferring from Beam 1 through the slab, and which effect the connection types had on it, was also studied. In the NLD analysis, the dynamic effects were studied and the result from the NLS analysis was compared to estimate the dynamic load factors and if they could represent the overall dynamic effects.

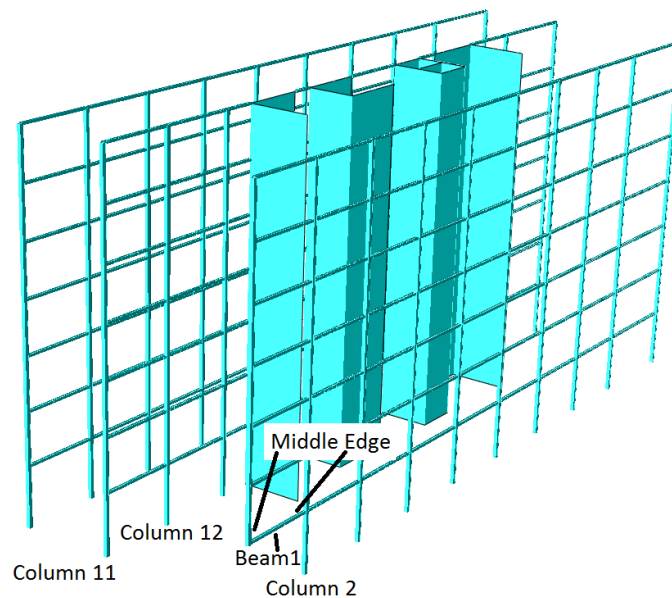


Figure 7.28: Locations in the model where results were extracted.

7.4.1 NLS analysis

In Figures 7.29 and 7.30 the deformation of the model with the two connection types is shown. There was a remarkable capacity increase compared to the 2D analysis. With the connection type, restrained, the capacity increase is not surprising due to cantilever action of the hollow-core units.

However, for the analysis with connection type simply, it was not so obvious that there would be an increase of the capacity. The reason for the increased capacity is most likely due to cable action of the hollow-core units. Due to that the normal forces in the hollow-core units and in the facade beams were perpendicular, there must have been a resisting diagonal force, this is shown in Figure 2.12 in Section 2.4. In the studied model it was achieved by bending resistance of the hollow-core units. Even if they are connected only in the displacement degrees of freedom, the connection along a line to the inner beam will allow them to rotate due to vertical displacement but they will resist rotation due to horizontal displacement.

Figures 7.31 and 7.32 show the moments and normal forces developed in Beam 1. Figure 7.33 shows the displacement of point Middle in Beam 1.

For the analysis with the connection type simply, the load carrying mechanism was achieved through bending stiffness of Beam 1–7, up to about 70% of the load. Up to this load, the result was similar to the 2D analysis, cf. Figure 6.26. After 70% load, the bending capacity of the beam was reached and the displacement increased dramatically. Cable action of the beam and hollow-core units enables an increased load.

No suspension mechanism to upper intact floors was achieved most likely due to an equal displacement of all the floors. The normal force in the remaining parts of column 1 was negligible.

There is no sign that the normal force in Beam 1 was close to a maximum, see 7.31a, which indicates a high capacity in the structure to support horizontal forces if a corner column is removed. Failure would most likely occur due to a high normal force in adjacent columns.

For the analysis with connection type restrained, there were no cable action in Beam 1, the load carrying mechanism was dominated by cantilever action of the hollow-core units.

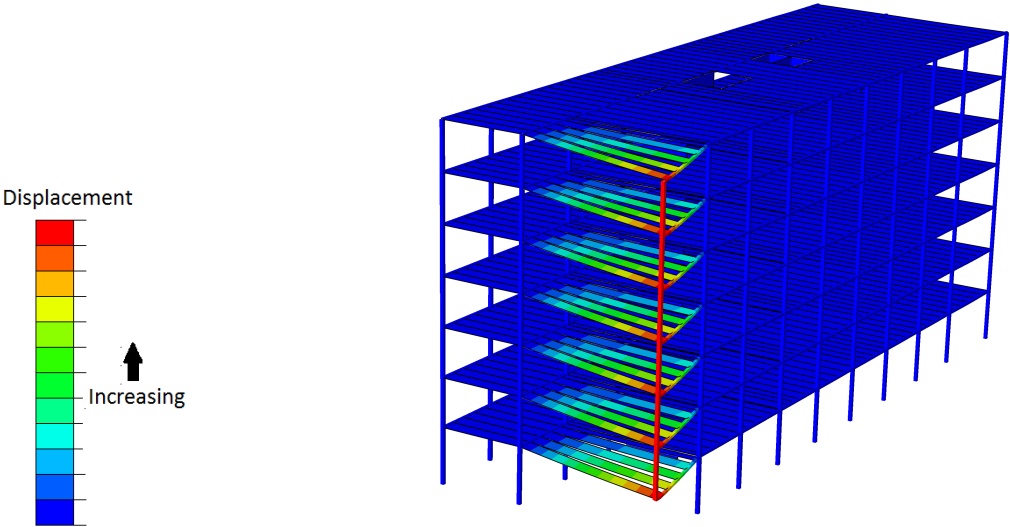


Figure 7.29: Deformation of the model at a dynamic load factor of 2, with connection type simply.

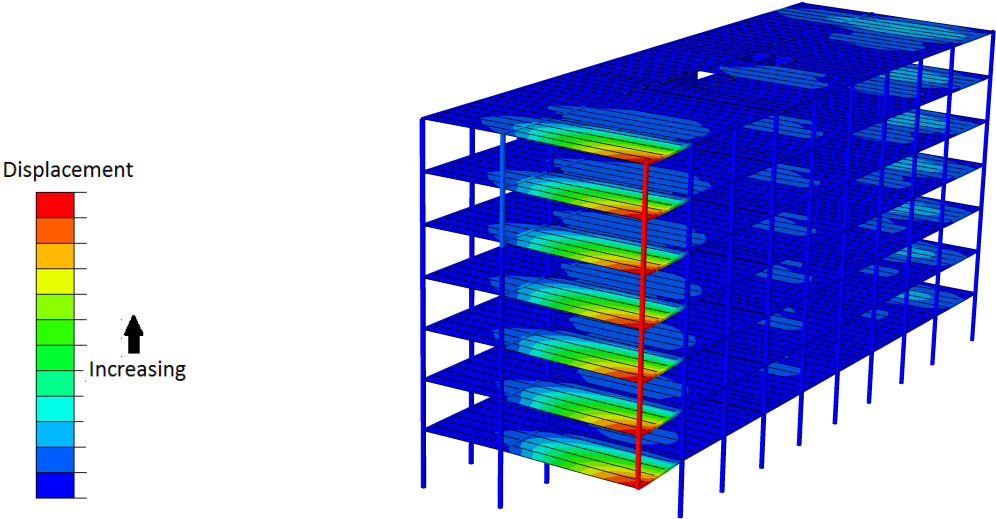


Figure 7.30: Deformation of the model at a dynamic load factor of 2, with connection type restrained.

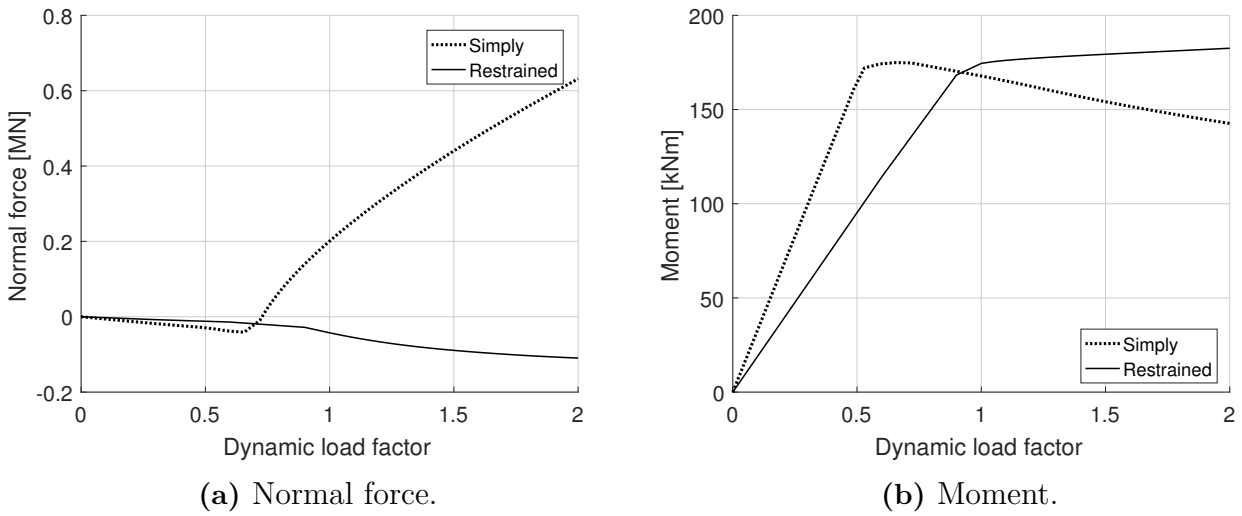


Figure 7.31: Moment and normal force in Beam 1 at point Edge.

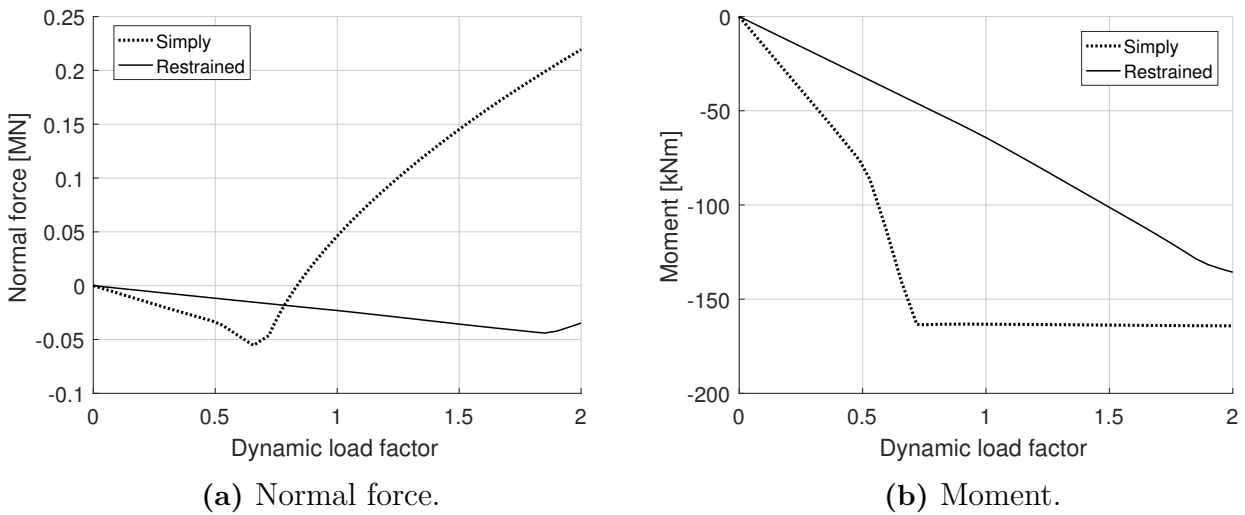


Figure 7.32: Moment and normal force in Beam 1 at point Middle.

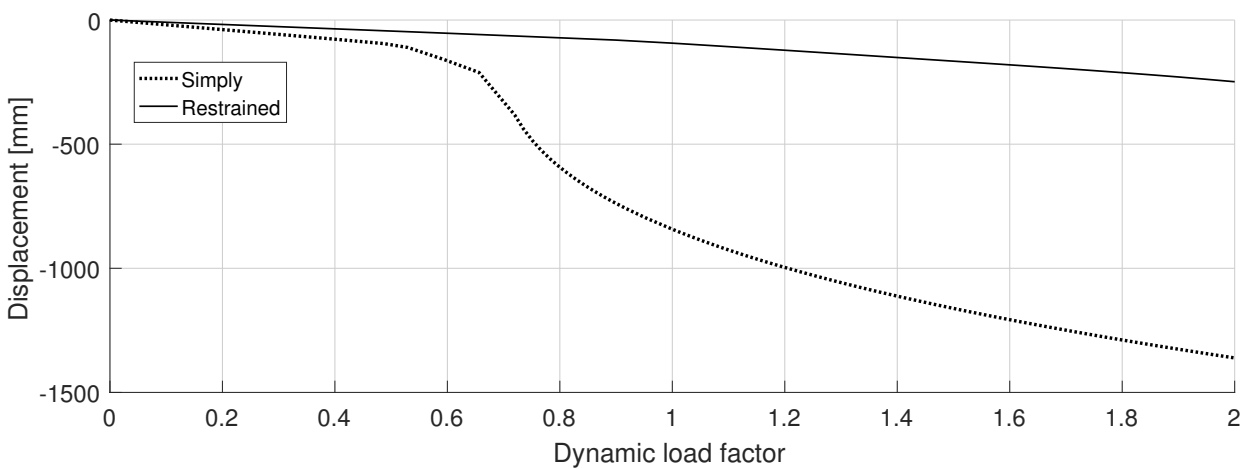


Figure 7.33: Vertical displacement of point Middle in Beam 1.

Figure 7.34 shows that the effective plastic strain becomes high in the analysis with connection type simply. Without the dynamic effects included (a dynamic load factor equal to 1) the effective plastic strain was about 20% and it seems that for the corner column removal the effective plastic strain becomes high because the beam is highly utilised.

The sum of the normal forces in all hollow-core units, that was applied with a dynamic load factor, is shown in Figure 7.35. There was not much cable action developed with the connection type restrained. Up to a dynamic load factor of 0.7, the normal force was equal between the models, above 0.7 the normal force in the slab dramatically increased in the analysis with connection type simply.

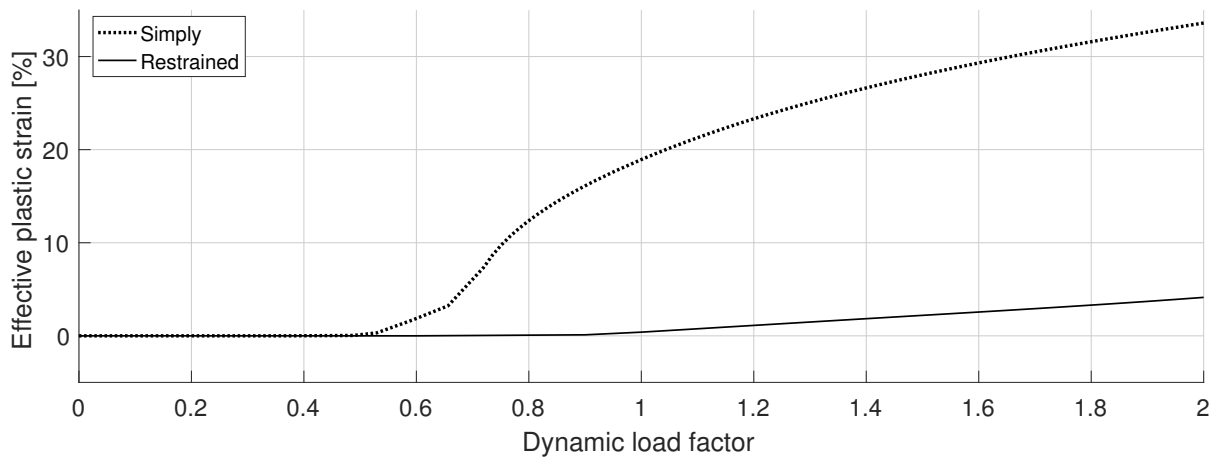


Figure 7.34: Maximum effective plastic strain Beam 1.

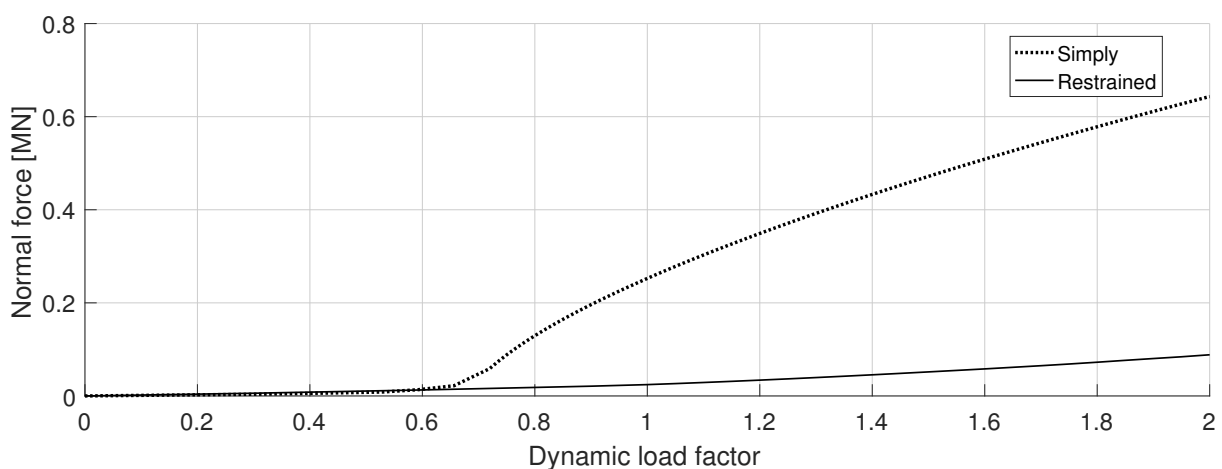


Figure 7.35: The sum of the normal forces in all hollow-core units that were applied with a dynamic load factor.

Figures 7.36–7.38 show the normal forces in three adjacent columns, namely 2, 11 and 12. Legend "Not removed" refers to an analysis in which the column was not removed. It was done to see how the adjacent columns were affected by the column removal.

For column 2 the load increase was much higher with connection type simply due to an inferior ability to transfer the load from the facade to inner parts of the building.

The analysis with connection type simply shows that up to a dynamic load factor of 0.7, the force in column 11 was not affected by the corner column removal. However, when cable action began to develop in the slab, the load was transferred from the facade to column 11. For the analysis with connection type restrained, there was an immediate redistribution of load to column 11.

Column 12 was actually unloaded when the column was removed and connection type simply was used. The hollow-core units close to column 12 were most likely not transferring much load into the structure because their deformation was limited. With the connection type restrained, a small increase of normal force in column 12 was obtained.

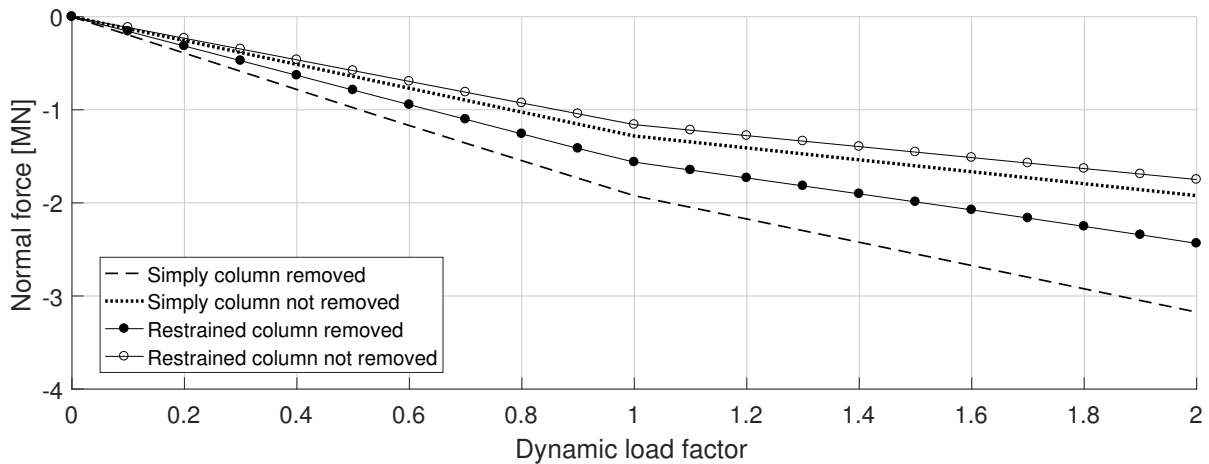


Figure 7.36: Normal force in adjacent column 2. Legend not removed is referring to an analysis where the column was not removed.

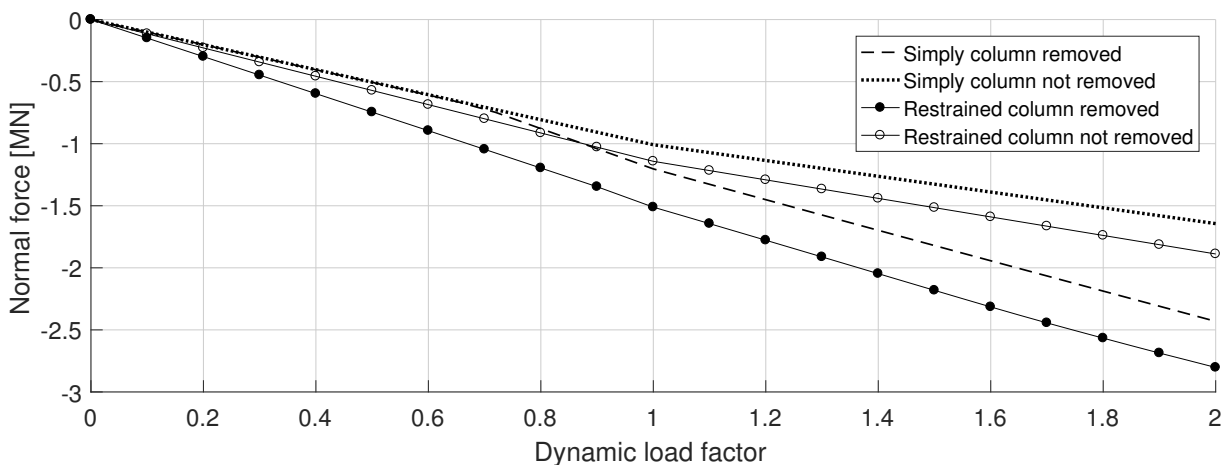


Figure 7.37: Normal force in adjacent column 11. Legend not removed is referring to an analysis where the column was not removed.

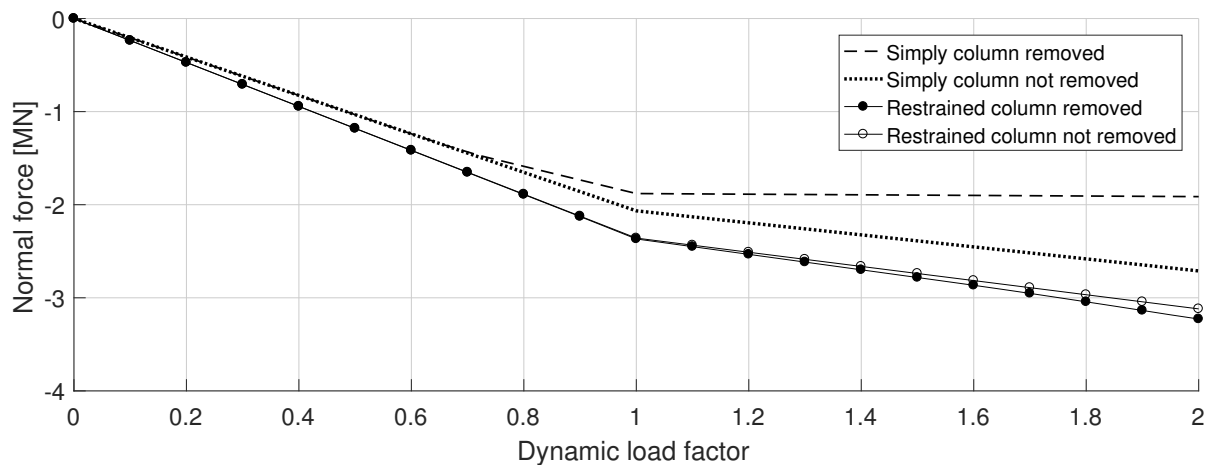


Figure 7.38: Normal force in adjacent column 12. Legend not removed is referring to an analysis where the column was not removed.

7.4.2 NLD analysis

The following section presents the results from an NLD analysis when column 1 was removed. The displacement of point Middle in Beam 1 was used to estimate the dynamic load factor needed in the static analysis to account for the dynamic effects. Figure 7.39 shows the displacement of point Middle in Beam 1 for both slab connection types. A Dynamic load factor of 1.37 gave a good estimation of the dynamic effects in the NLS analysis with connection type simply. A dynamic load factor of 1.45 gave a good estimation of the dynamic effects in the NLS analysis with connection type restrained.

Moments and normal forces in Beam 1, at point Edge and at point Middle are shown in Figures 7.40 and 7.41.

The normal force at point Edge was well estimated with the dynamic load factors 1.37 and 1.45 in the NLS analysis. Note that the moment at point Edge was larger than the capacity of the beam due to damping.

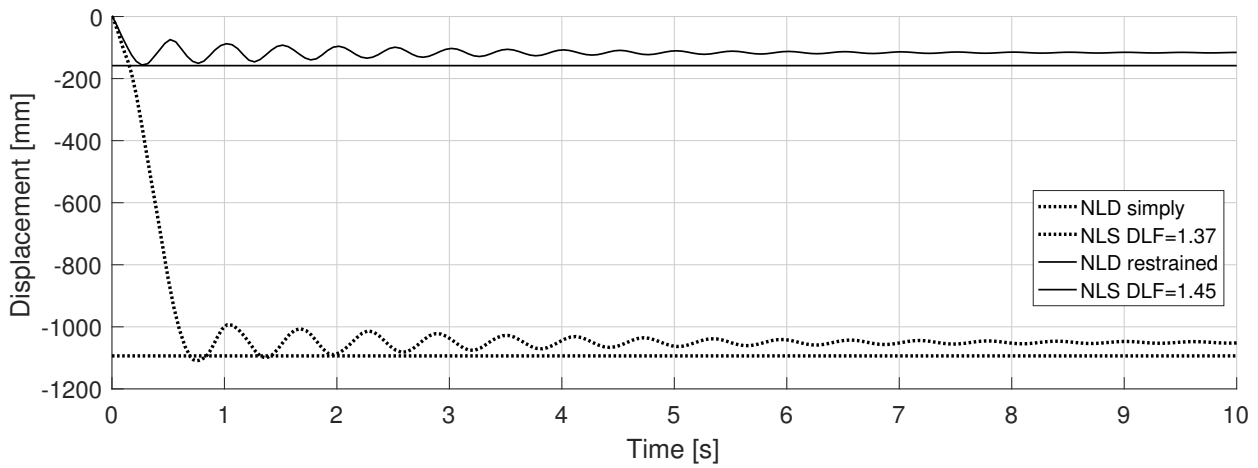
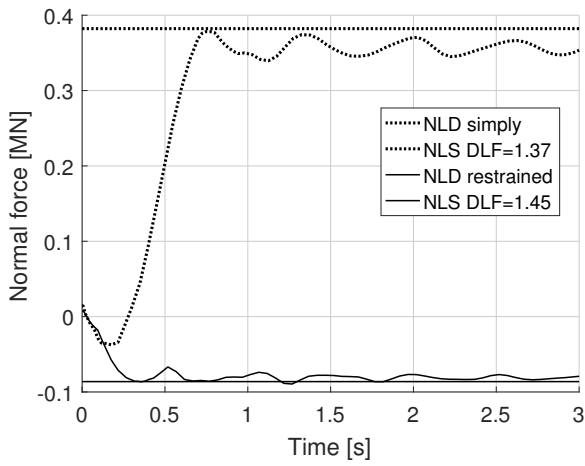
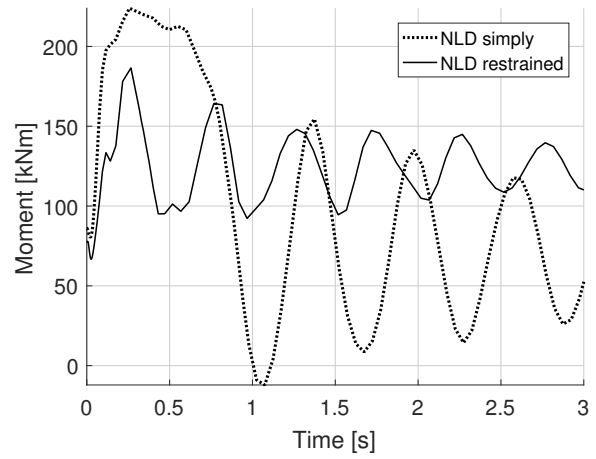


Figure 7.39: Vertical displacement of point Middle in Beam 1, comparison of the results of the NLS and NLD analysis.

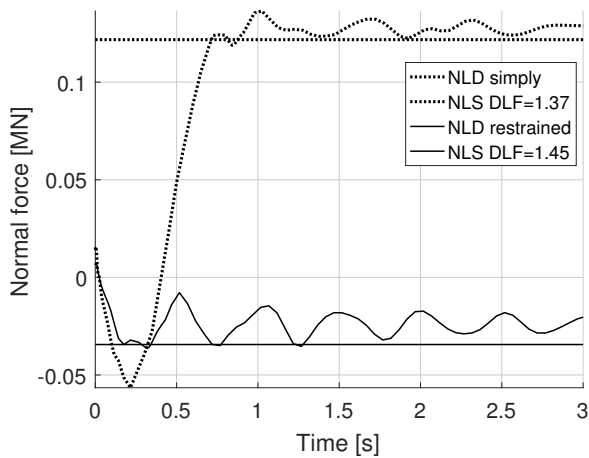


(a) Normal force, comparison of the results of the NLS and NLD analysis.

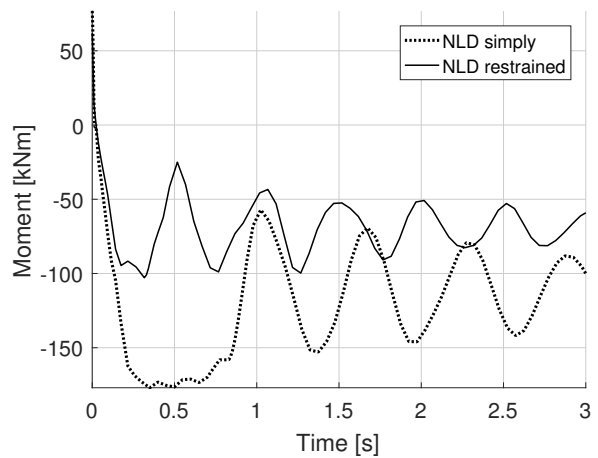


(b) Moment, result of the NLD analysis.

Figure 7.40: Moment and normal force in Beam 1 at point Edge.



(a) Normal force, comparison of the results of the NLS and NLD analysis.



(b) Moment, result of the NLD analysis.

Figure 7.41: Moment and normal force in Beam 1 at point Middle.

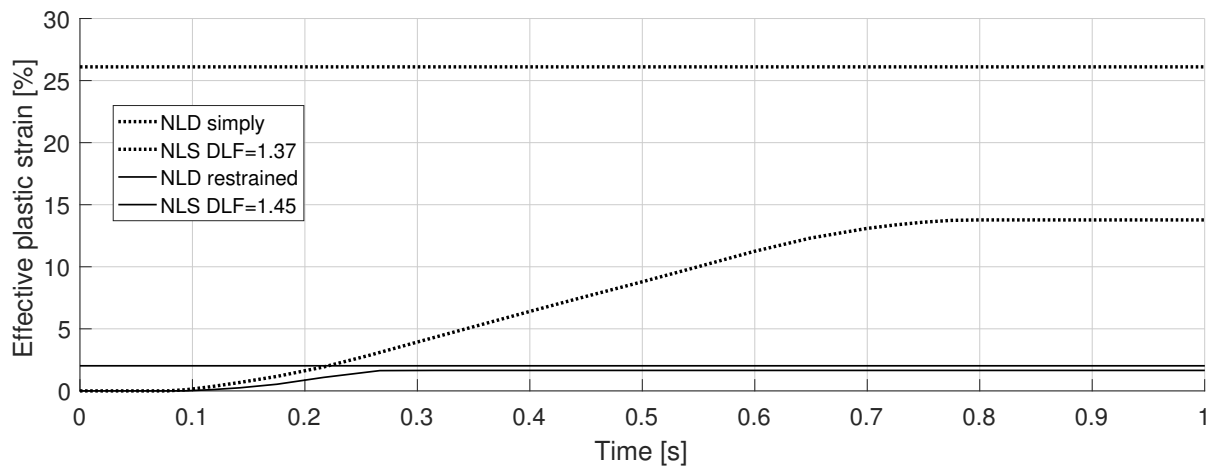


Figure 7.42: Effective plastic strain in Beam 1, comparison of the results of the NLS and NLD analysis.

The effective plastic strain is shown in Figure 7.42. The effective plastic strain was low in comparison with the static analysis due to damping, especially with connection type simply. With both connection types, it was below the limit of 15%. Although, with a dynamic load factor of 1.37, it indicates that large strain could cause a fracture in the material due to the dynamic effects, if connection type simply is assumed.

In Figures 7.43–7.45 the normal forces in adjacent columns 2, 11 and 12 are shown. The dynamic load factors gave a good estimation of the maximum normal force due to the dynamic effects, except for column 12 with connection type simply. However, the dynamic load factor is not applicable for column 12 because it was actually unloaded with connection type simply.

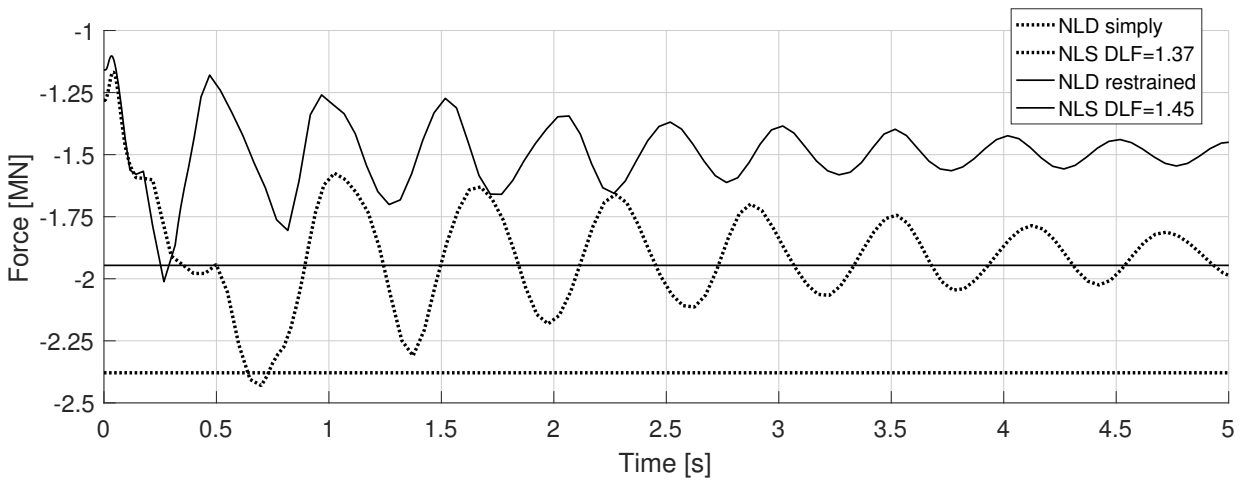


Figure 7.43: Normal force in adjacent column 2, comparison of the results of the NLS and NLD analysis.

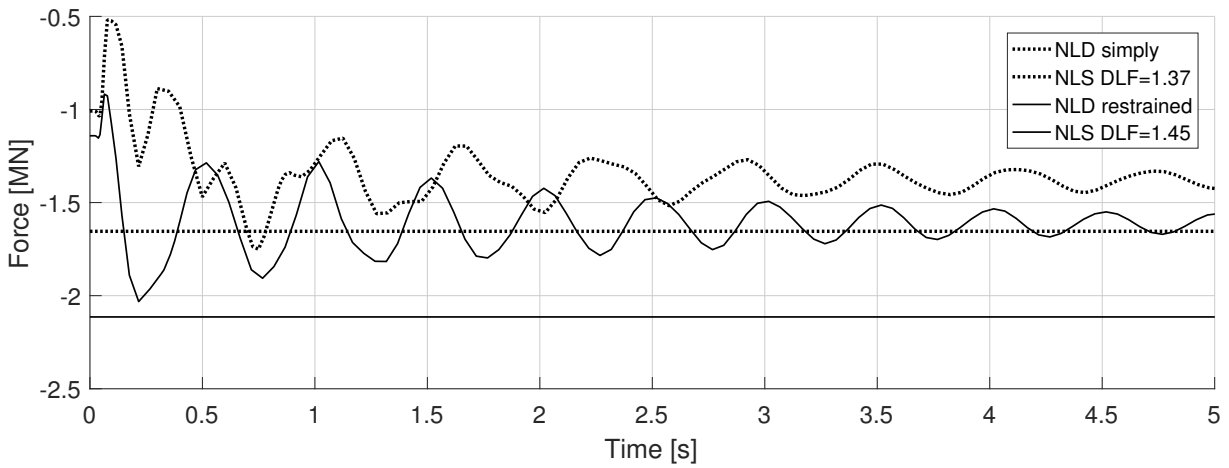


Figure 7.44: Normal force in adjacent column 11, comparison of the results of the NLS and NLD analysis.

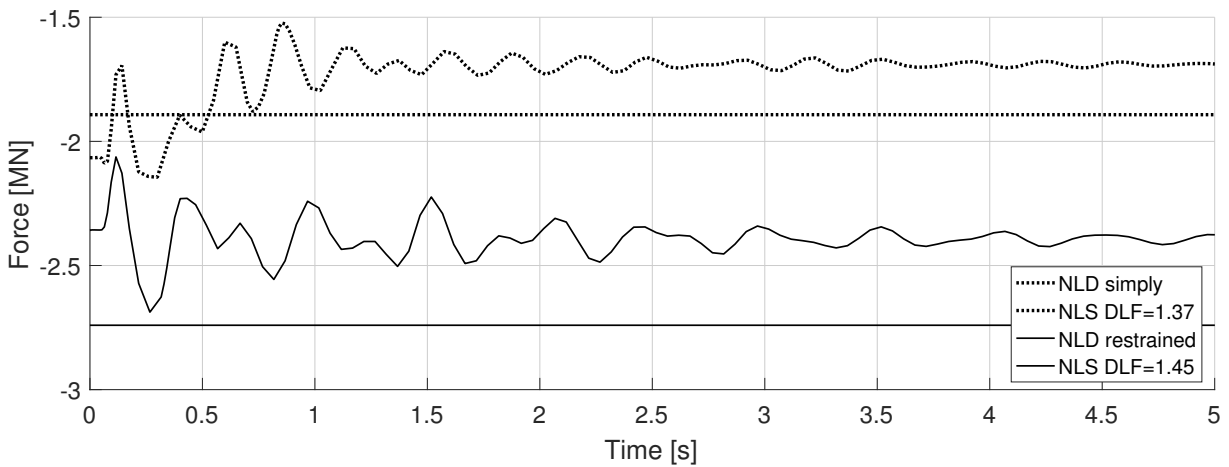


Figure 7.45: Normal force in adjacent column 12, comparison of the results of the NLS and NLD analysis.

7.5 Column 12 removal

In the following section, results are presented from the removal of column 12. Both an NLS and NLD analysis were performed with the two different connection types of the hollow-core units, namely simply and restrained.

The first-floor beam connected to columns 11 and 13 is referred to as Beam 1. Both points in Beam 1 located at the connection to columns 11 and 13 are referred to as point Edge. The point in Beam 1 located at the location of the removed column is referred to as point Middle, cf. Figure 7.46.

The overall ability of the model to develop alternate load paths was studied. It was done by extracting internal forces developed in Beam 1, which has to transfer parts of the load carried by the removed column to adjacent elements. The developed normal force in adjacent columns was also extracted.

The Load transferring from Beam 1 through the slab, and which effect the connection type had on it, was also studied. In the NLD analysis, the dynamic effects were studied and the result from the NLS analysis was compared to estimate the dynamic load factors and if they could represent the overall dynamic effects.

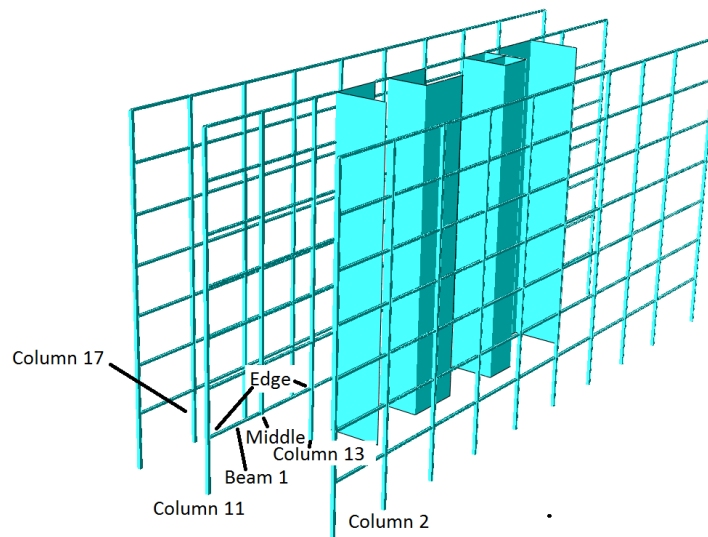


Figure 7.46: Locations in the model where results were extracted.

7.5.1 NLS analysis

For the removal of column 12, the analysis failed at a higher load with connection type simply than connection type restrained. A dynamic load factor of 1.83 compared to 1.81 resulted in a failure. Most likely, a large normal force in combination with a large moment in column 11 was the reason to why it failed. The deformation of the structure before failure is shown in Figures 7.47 and 7.48.

Figures 7.49–7.50 show the developed moments and normal forces in Beam 1 at point Edge, at the connection to columns 11 and 13, and at point Middle.

In the analysis with connection type simply, there was a large difference between the normal force at the different points in Beam 1. The normal force was low at point Edge,

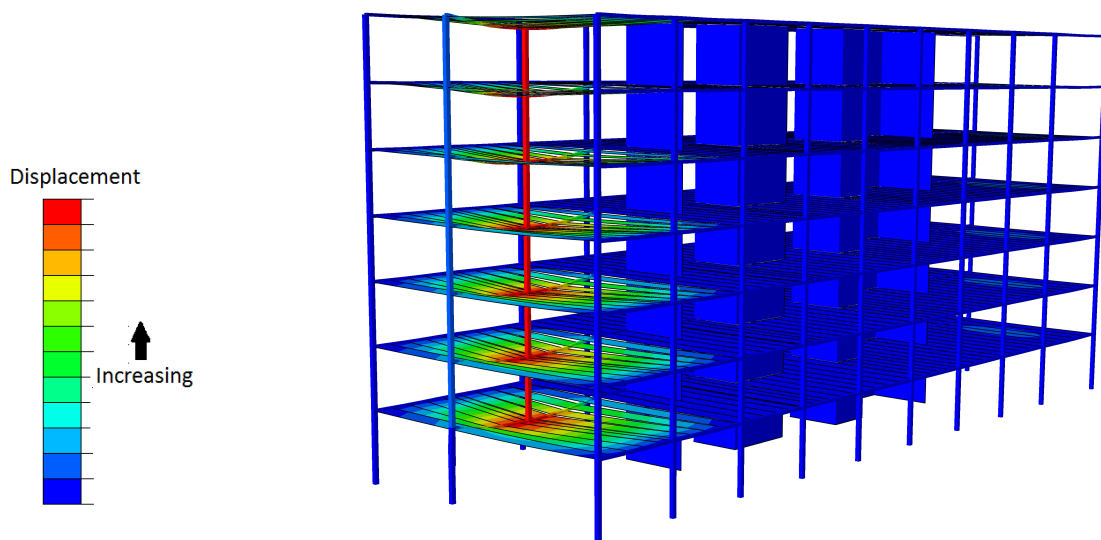


Figure 7.47: Deformation of the model just before failure with connection type simply.

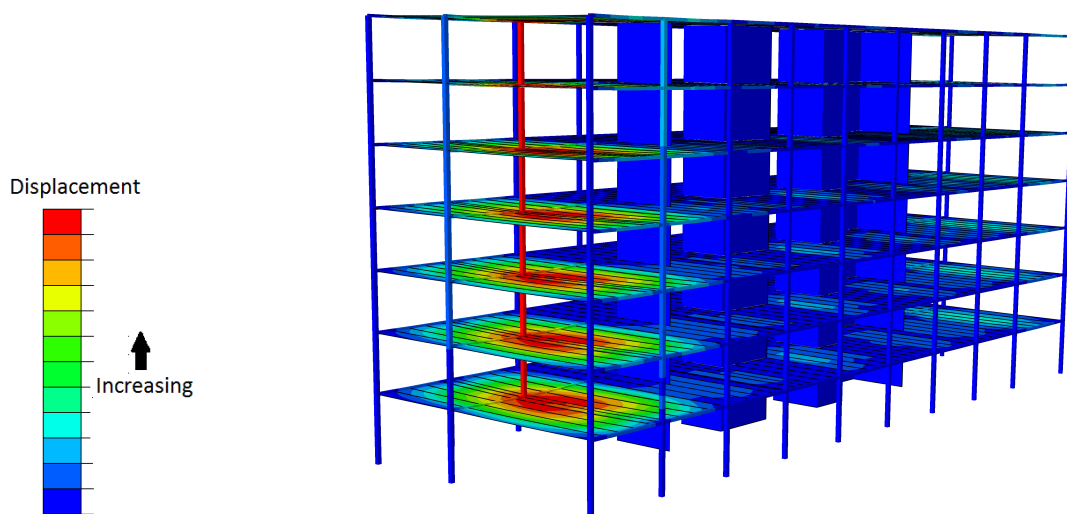


Figure 7.48: Deformation of the model just before failure with connection type restrained.

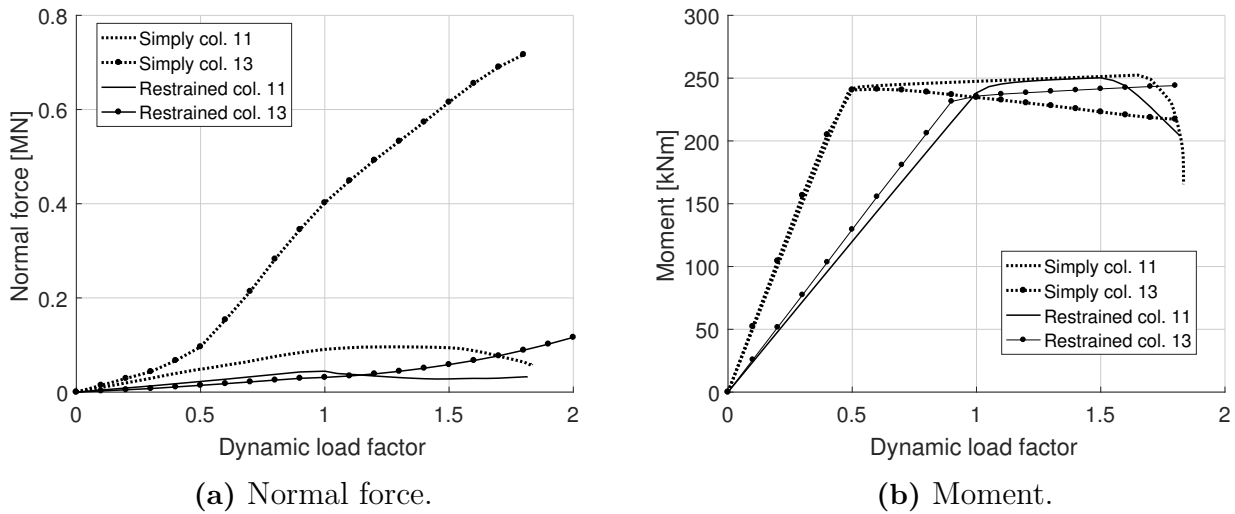


Figure 7.49: Moment and normal force in Beam 1 at point Edge, at the connection to adjacent columns 11 and 13.

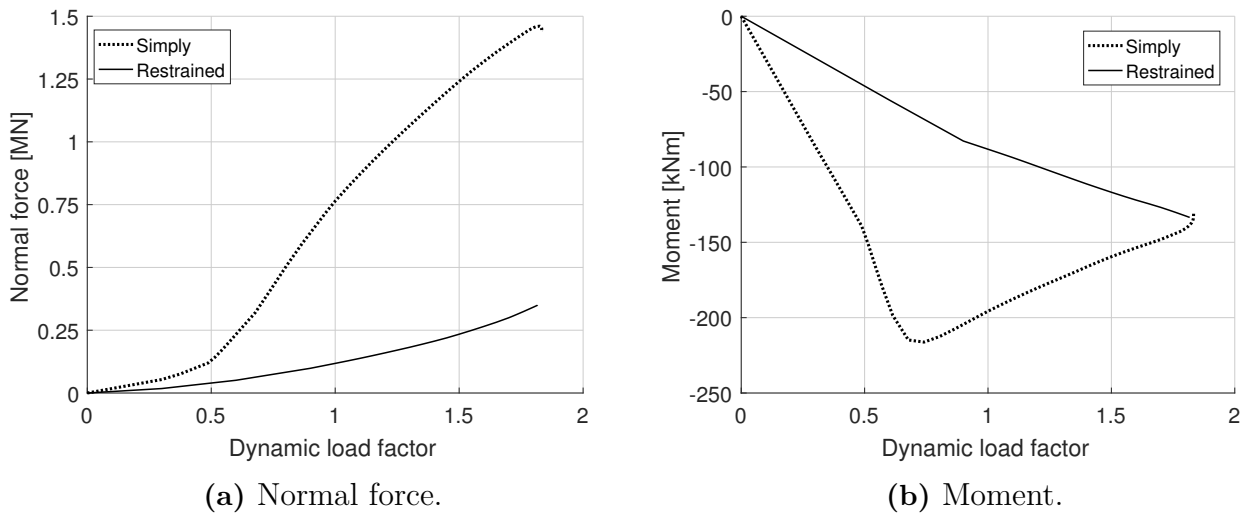


Figure 7.50: Moment and normal force in Beam 1 at point Middle.

at the connection to column 11, in comparison to the other points in the beam. It is not surprising because the normal force at this point was taken up by bending of column 11, which had a limited ability to support the horizontal force.

In the 2D analysis, the force was exactly the same at point Edge at both connections to adjacent columns, if it would not have been equal, the beam would not have been in static equilibrium. The reason that it was not equal when column 12 was removed, must be that a large horizontal force was taken up by a resistance of the hollow-core units along the beam. It would explain the large difference in the developed normal force in Beam 1 at the connection to column 11 and 13.

Figure 7.51 shows the displacement of point Middle in Beam 1. It is not surprising that there was a large difference in the vertical displacement of point Middle in Beam 1 between the models. Note that the displacement was not as high as when columns 1 and

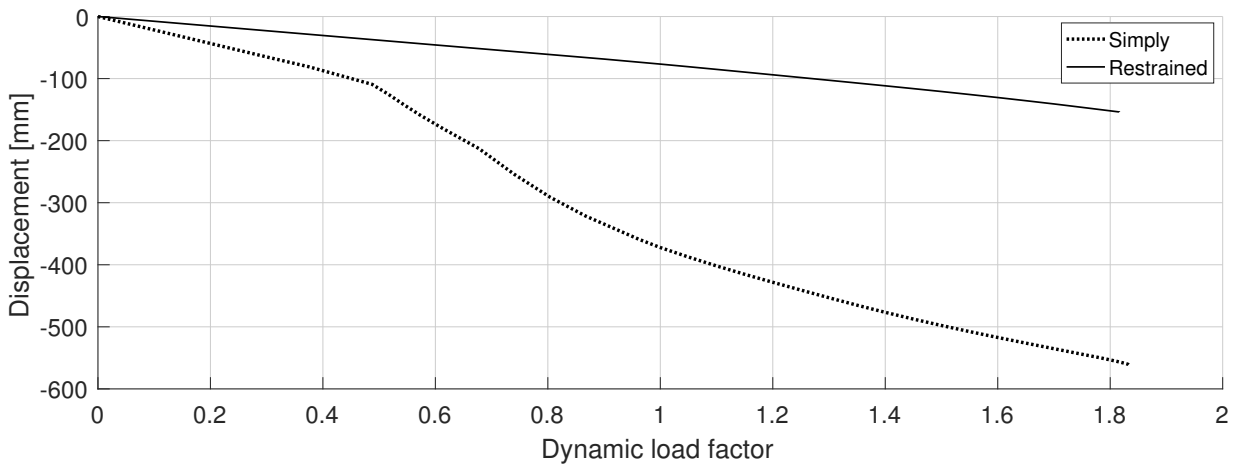


Figure 7.51: Vertical displacement of point Middle in Beam 1.

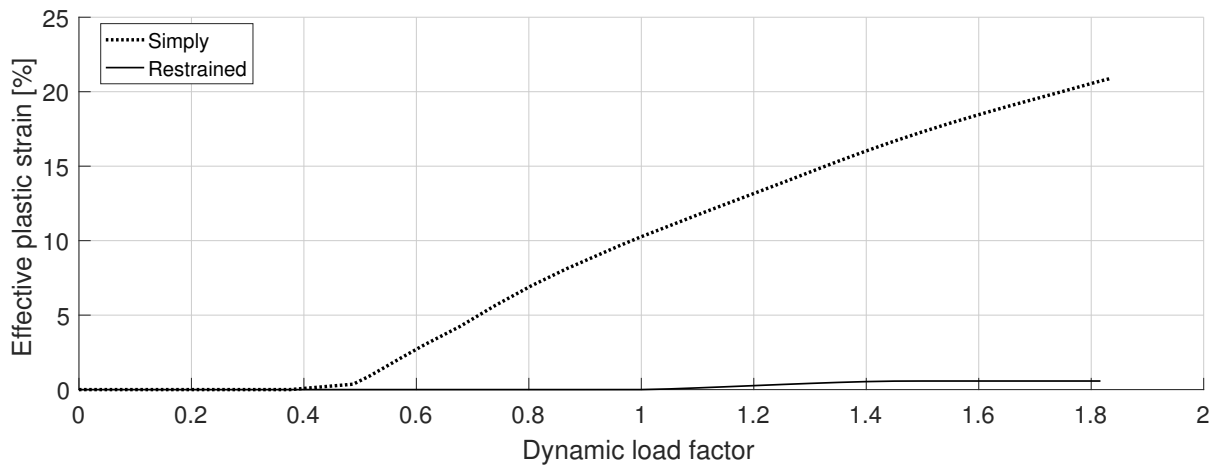


Figure 7.52: Maximum effective plastic strain in Beam 1.

3 was removed.

The effective plastic strain in Beam 1 is shown in Figure 7.52. With the connection type restrained, the effective plastic strain was very low, probably due to that cantilever action of the hollow-core units transferred the load effectively from Beam 1. With connection type simply, the effective plastic strain was not as high as in previous analyses (column 1 and column 3 removal), which indicates that Beam 1 was not as highly utilised. Probably due to an effective transferring of the load through cable action of the slab. A minimum limit of 15% strain, specified in Eurocode for steel S355 [22], would allow a dynamic load factor of about 1.3. The more reasonable strain limit 20–25%, see Appendix D, was barely reached in the beam before the structure failed.

Figure 7.53 shows the sum of the normal forces, in all hollow-core units that were applied with a dynamic load factor. Legend short refers to the shorter hollow-core units with a length of 6.216 m and long refers to the longer hollow-core units with a length of 10.516 m, see Figure 1.3. The large developed normal force, with the connection type simply, indicates that the slab contributes allot to the capacity of the structure by cable

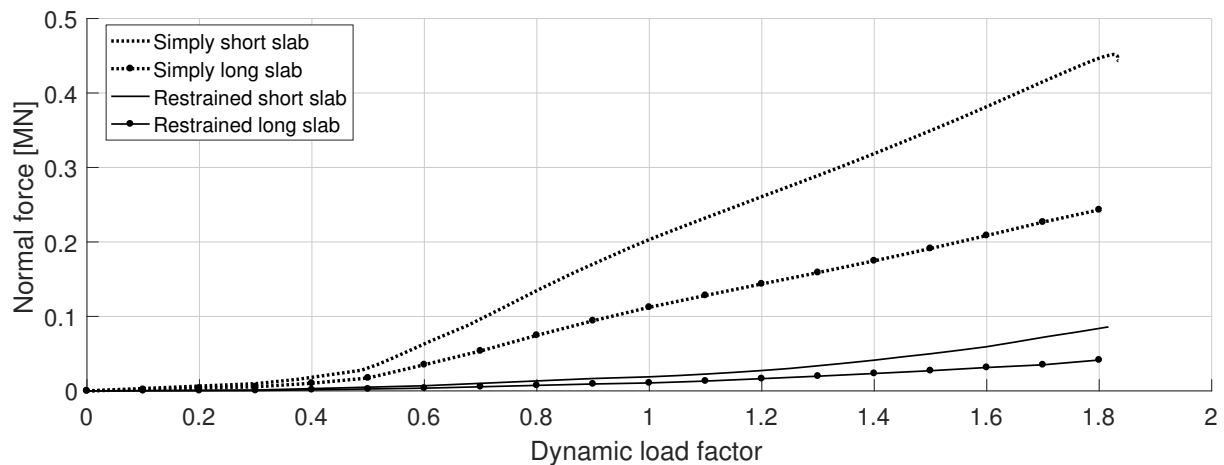


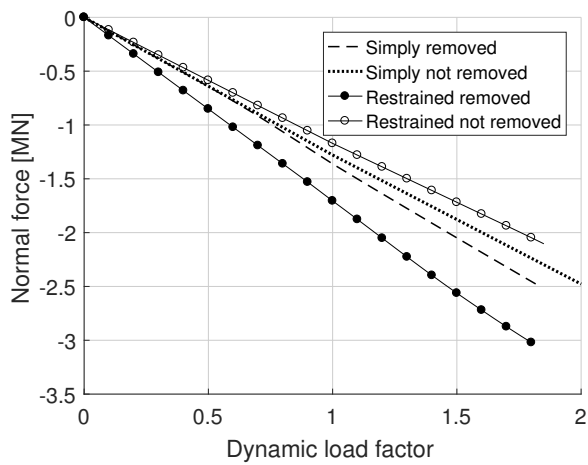
Figure 7.53: The sum of the normal forces in all hollow-core units that were applied with a dynamic load factor. Long is referring to the hollow-core units with a length of 10.516 m and short is referring to the hollow core units with a length of 6.216 m, see Figure 1.3.

action. It was probably the reason to why the capacity of the structure, when column 12 was removed, was almost equal with the two connection types.

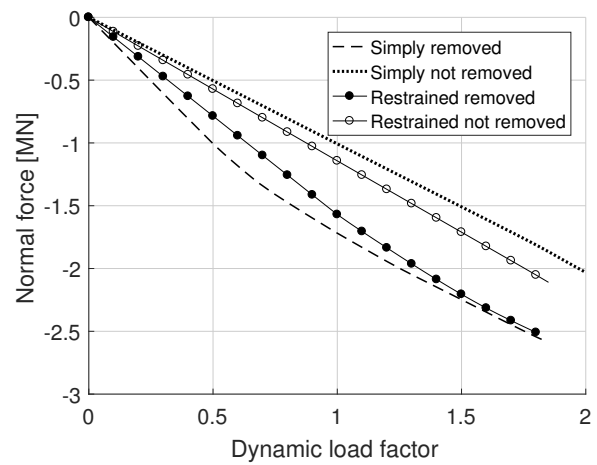
The normal forces in four adjacent columns, namely 2, 11, 13 and 17, were extracted and the results are shown in Figure 7.54. As in previous analyses, the results are compared with the results from an analysis where the column was not removed to investigate how the adjacent columns were affected by the column removal.

For the facade columns 2 and 17, there was a larger increase of normal force with the connection type restrained in comparison to the analysis with the connection type simply. It is due to that the cantilever action of the slab is more effective in transferring the load from Beam 1 to the facade.

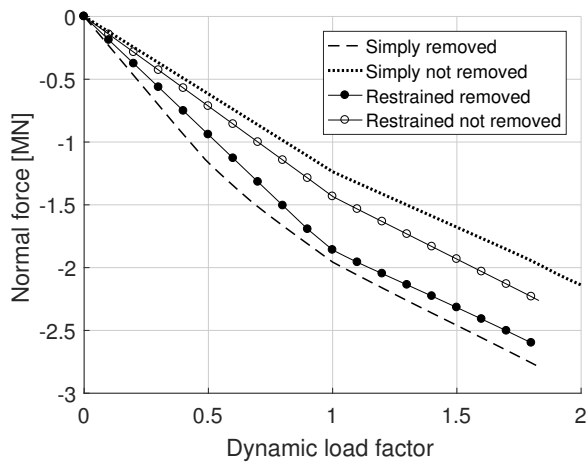
With connection type simply, there was no normal force increase in column 2 and 17 up to a dynamic load factor at about 0.7. This is because, at a lower external load, most of the load was transferred from the beam to column 11 and 13. At a dynamic load factor larger than 0.7, a larger part of the load was transferred to the facade beams instead by cable action of the slabs.



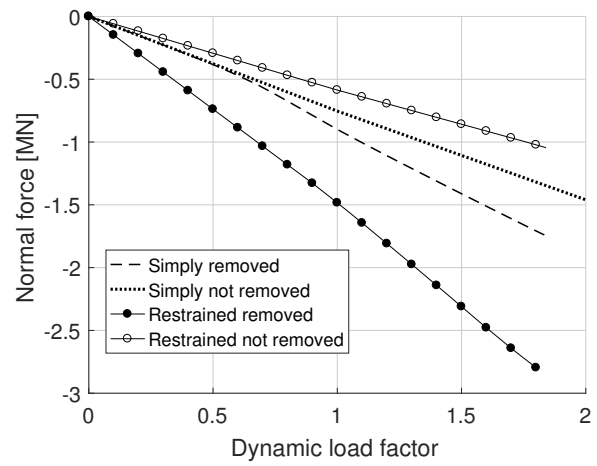
(a) Column 2.



(b) Column 11.



(c) Column 13.



(d) Column 17.

Figure 7.54: Normal force in adjacent columns. Legend not removed is referring to an analysis where column 12 was not removed.

7.5.2 NLD analysis

The following section presents the result from an NLD analysis when column 12 was removed. The displacement was used to estimate the dynamic load factor needed in the static analysis to account for the dynamic effects. Figure 7.55 shows the displacement of point Middle in Beam 1 for both slab connection types. A dynamic load factor of 1.65 was needed in the static analysis to account for the dynamic effects with the connection type simply. A dynamic load factor of 1.45 was needed in the static analysis account for the dynamic effects with the connection type, restrained.

Normal forces and moments developed in Beam 1 at point Edge, at the connection to column 11 and 13, and at point Middle are shown in Figures 7.56–7.57. The chosen dynamic load factors of 1.45 and 1.65 gave a good estimation of the dynamic effects on the developed normal force. Damping caused, as in previous analyses, the moment in Beam 1 at point Edge to be larger than the capacity of the beam, which according to the static analysis was about 250 kNm.

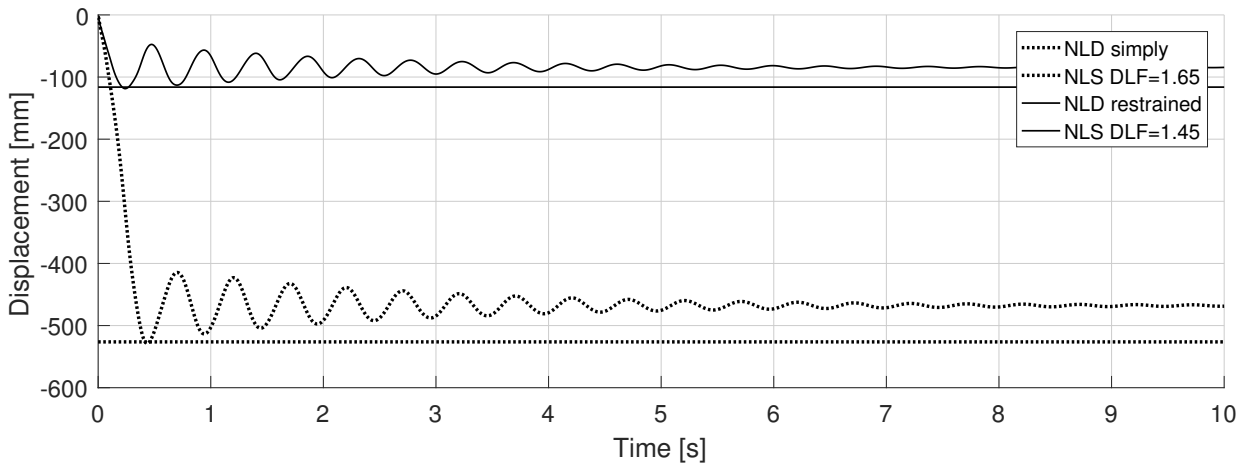
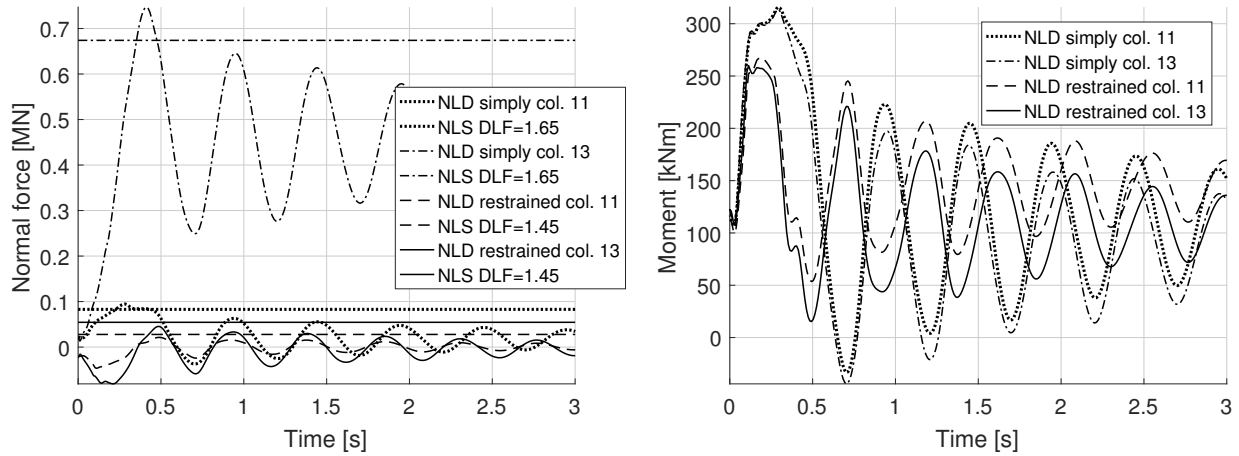


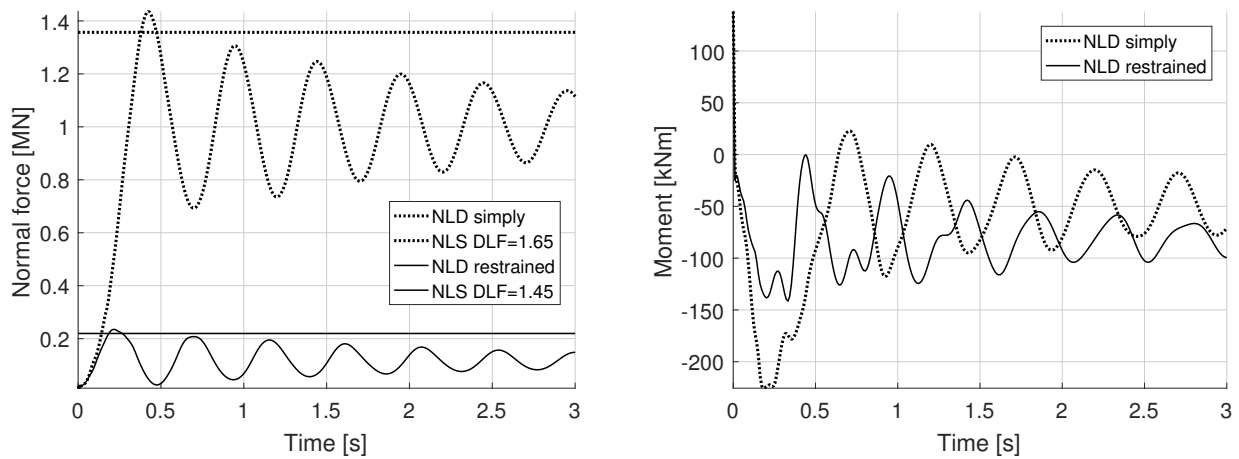
Figure 7.55: Vertical displacement of point Middle in Beam 1, comparison of the results of the NLS and NLD analysis.



(a) Normal force, comparison of the results of the NLS and NLD analysis.

(b) Moment, result of the NLD analysis.

Figure 7.56: Moment and normal force in Beam 1 at point Edge, at the connection to column 11 and 13.



(a) Normal force, comparison of the results of the NLS and NLD analysis.

(b) Moment, result of the NLD analysis.

Figure 7.57: Moment and normal force in Beam 1 at point Middle.

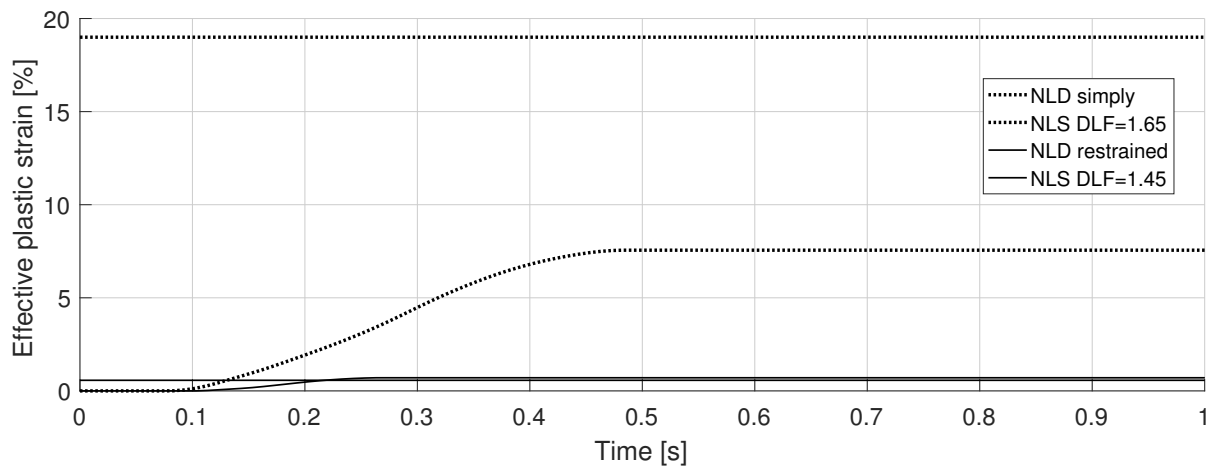
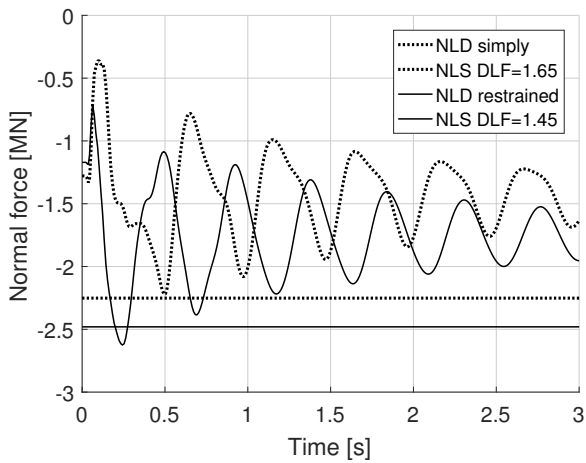


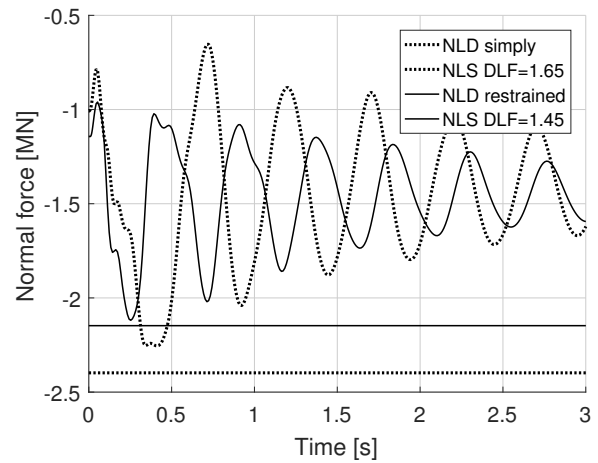
Figure 7.58: Maximum effective plastic strain in Beam 1, comparison of the results of the NLS and NLD analysis.

The maximum effective plastic strain in Beam 1 is shown in Figure 7.58. It was negligible with connection type restrained but well estimated with the dynamic load factor 1.45. With connection type simply, the effective plastic strain was, due to damping, quite low compared to the NLS analysis. It was well below the limit of 15%, specified as a minimum in Eurocode [22]. A dynamic load factor of 1.65 gave an estimation of nearly 20% effective plastic strain in the NLS analysis which still is a reasonable value for steel S355, cf. Appendix D.

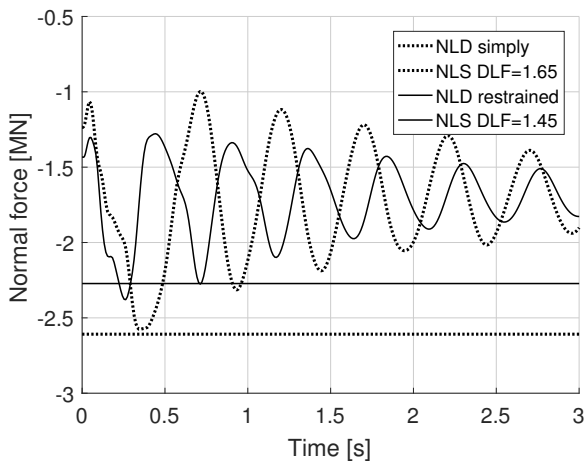
Normal forces in adjacent columns 2, 11, 13 and 17 are shown in Figure 7.59 and they were well estimated with the dynamic load factors.



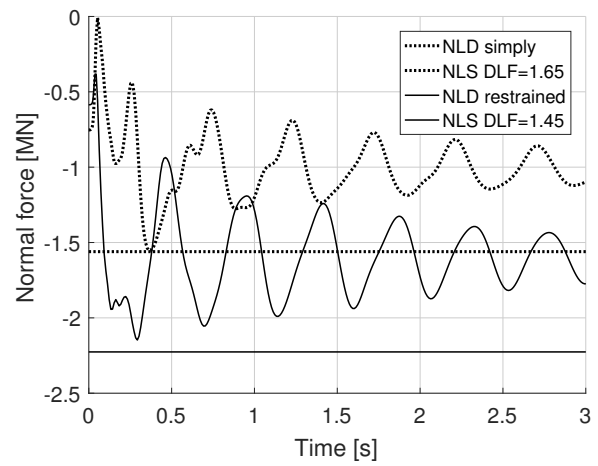
(a) Column 2.



(b) Column 11.



(c) Column 13.



(d) Column 17.

Figure 7.59: Normal forces in adjacent columns, comparison of the results of the NLS and NLD analysis.

7.6 Summary and discussion

Progressive collapse analysis was performed by removing the three columns, namely 1, 3 and 12. Two models were created, one where the hollow-core slab was simply supported by supporting beams and walls, referred to as simply, and one where it was restrained to supporting beams and walls, referred to as restrained.

3D effect – restrained support of the hollow-core units

It was not surprising that a connection type restrained unloaded the studied beams due to cantilever action which transferred the load effectively to other parts of the structure. Cable action in the beams was limited which had a positive effect on the developed strain that was less than 5% for all column removal analyses.

Using fully restrained supports for the hollow-core units might be somewhat unrealistic, especially for the ones directly affected by the column removal (the ones applied with a dynamic load factor). The cantilever action would probably not be as effective in a real structure because of cracks in the concrete. However, the cantilever action would probably be present in the beginning of a dynamic event, when the concrete has not cracked yet, and reduce the acceleration of the masses and limit the dynamic effects.

If it can be assured that the connection of the hollow-core units remains moment stiff, a 2D model would be too conservative and not be representative of the behaviour of the structure in case of a column failure.

3D effect – simply supported hollow-core units

It was not that obvious what to expect from the analysis using simply supported hollow-core units. However, in comparison to the 2D-model, a higher load capacity was obtained in the 3D models. The reason for the increased capacity in the 3D models was most likely due to a better ability to support the horizontal forces at all storeys in the 3D models. It enabled cable action of several beams at different storeys. Another reason for the increased capacity was cable action of the hollow-core units which enabled some load transferring to other parts of the building. This effect is, on the other hand, quite uncertain and should probably not be included if it is beneficial.

The largest difference between 2D and 3D analyses was seen in the corner column removal analysis because of co-action between the hollow-core units and the facade beam. It enabled cable action in the beam, which was not possible in the 2D model. It is doubtful if this effect is realistic in a real building because it was enabled in the model by a horizontal bending resistance of the hollow-core units, an effect which probably was overestimated in the model.

Cable action of the hollow-core units was obtained in all 3D analyses and was most beneficial in the corner-column (column 1) removal and the mid-column (column 3) removal. The normal force was quite large in the slab, for it to apply in a real building, the connection with the in-casted reinforcement needs to hold. Another interesting perspective is that the normal force in the hollow-core units might not always be beneficial. For instance, for the mid-column removal, the normal force in the hollow-core units induced

horizontal forces to the columns in the facade that might not be accounted for only using 2D models.

Both the 2D and 3D analysis showed that the horizontal force capacity of the structure had a major impact on the load capacity in models. It implies that when creating the FE-models, it is very important that the correct horizontal stiffness is achieved in the structure otherwise the result might not be representative of real structure's ability to develop alternate load paths.

The effect of including dynamics

The displacement at the column removal locations, from the NLD analysis, was compared to the NLS analysis to estimate the dynamic load factors. The estimated dynamic load factors represented the overall dynamic effects well, except for the maximum effective plastic strain in the beams, which was overestimated with the dynamic load factors. However, as mentioned in the 2D analysis, damping had a large beneficial effect on the developed effective plastic strain. An uncertain effect that should probably not be accounted for.

The obtained dynamic load factors in the NLS analyses varied from 1.27 in the 2D analysis up to 1.65 in the 3D analysis. It is quite a large increase of the load compared to only applying the accidental action load combination, therefore, dynamic effects must be included somehow if NLS analyses are to be used.

The comparison of the NLS with the NLD analysis showed that the concept of dynamic load factors is a good way to represent the dynamic effects. However, the purpose is to replace the NLD analysis and perform NLS analysis which does not result in such a high computational cost. The method used in these analyses was to first perform an NLD analysis and then determine the necessary dynamic load factor, that approach does not eliminate the NLD analysis. It is desirable that the dynamic load factors could be estimated in some other way, as is done in the UFC, but the resulting dynamic load factors varied quite much which indicates that they could be difficult to estimate.

8 Concluding remarks

A main focus of the thesis has been to examine the level of details that are needed in the model and which type of analysis that can be used to validate the robustness of a structure. The most important conclusions have been summarised in the present chapter.

8.1 Conclusions

Type of analysis

If non-linear effects were accounted for in the analyses, it resulted in a major increase of the load capacity of the beams. As the applied load was increased the load carrying mechanism changed from bending resistance to development of normal force and cable action, which was very beneficial for the beam capacity.

A 2D LS analysis of column removals in the facade resulted in a rejection of the LS approach due to conservative results, even if a non-linear material model (ideal-elastic-plastic) was used. The model failed at about 70% of the applied accidental action load combination. Progressive collapse design is based on the advantage of large deformations and displacements, which are effects that could not be utilised in an FE-model using LS analyses.

By including non-linear effects, a large increase of the capacity was achieved in most of the analyses that were performed. However, the ability of the model to support the horizontal force turned out to have a large impact on how beneficial the non-linear effects were.

Dynamic load factors were applied in the NLS analysis to account for dynamic effects. When comparing results from the NLD analysis and the NLS analysis, respectively, the dynamic load factors varied between 1.27–1.65 dependent on which column that was removed, how the hollow-core units were attached to the beams, and it also varied between the 2D and 3D analysis. Such varying results indicates that an estimation of the dynamic load factor might be complicated but necessary if dynamic analyses should be avoided. The dynamic load factor did, however, estimate the dynamic effects well. The difficult part is to determine the correct dynamic load factor without first performing a dynamic analysis.

The NLD analysis resulted in a high computational cost and it is beneficial if it could be avoided. The NLS analyses with dynamic load factors are suitable for replacing the NLD analyses.

Modelling details

Details in the beam models are important if a correct strain should be estimated. A finer mesh results in larger strain for both solid and beam elements. Small elements might overestimate the strain while large elements might underestimate it. A fracture in the material could be the cause of failure, which implies that a correct estimation of the strain is important. A proper element size was not determined and it remains an uncertainty. However, the beam analyses showed that beam elements as compared to solid elements estimated a similar effective plastic strain rate in the beams at reasonable strain rates below 30%. It is positive because beam elements will most often be used in progressive collapse analyses.

A 2D model is simpler to create and reduces the computational cost compared to a complex 3D model. It is, however, questionable if a 2D model could represent the structural behaviour in the event of a column failure. The horizontal stiffness had, as mentioned in the previous section, a large impact on the results when non-linear effects were included. It is therefore difficult to use a 2D model because some stiffness should be added to represent the horizontal stiffness of the real structure.

In the 2D analysis, diagonals were added in the model to represent the resistance to horizontal forces from the slabs. Without these diagonals, cable action of the beams would be limited due to an inability of the model to support the horizontal forces. The diagonals did not correspond to the horizontal stiffness of the 3D model. The effect of this was that the results from using the 2D analysis did not comply with the results from the 3D analysis, which would be desirable if the 2D model should replace the 3D model.

The feasibility of using a 2D model is also dependent on which column that is removed. Removal of a column in the middle of the facade gave quite similar results between the 2D and 3D model and could be appropriate to use if a correct horizontal stiffness could be modelled. On the other hand, for a corner column removal, a large capacity increase in the 3D model was achieved due to coaction between the facade beam and the hollow-core units. To model a corner column removal requires a more detailed model if the effect of using ties around corners should be included. No 2D analysis for an inner column removal was performed, although, the 3D analysis showed a large effect on the results due to load transferring of the hollow-core units, an effect that would not be seen using a simpler 2D model.

A higher load capacity was obtained in all analyses using a 3D model, for the simply supported hollow-core units the increased capacity was mainly due to a better ability in the 3D model to support the horizontal forces, which enabled cable action of the beams. Another important factor is how to model the connection of the hollow-core slab to beams and walls in the 3D model. It is important because a restrained connection resulted in a very high capacity due to cantilever action of the hollow-core units. The model with simply supported hollow-core units did not have as high load capacity, even if some load transferring was achieved through cable action in the hollow-core units.

In the NLD analysis, plasticity and damping had a large effect on the results. Especially the damping was beneficial due to damping forces at the beam supports, it resulted in a reduction of the strain compared to the static analysis. Both plasticity and damping was beneficial and should be modelled thoroughly if they are included in the NLD analysis.

8.2 Further studies

Some uncertainties in the progressive collapse analysis remain. For instance, predicting the strain in the beams is very important if cable action should be utilised. It would, therefore, be useful to perform experiments, as described in Chapter 5, on real steel beams or make analytical computations, to verify the result from the numerical beam models. In such beam analysis, another interesting investigation would be to study how the effect of hardening in the plasticity model would affect the results.

Reducing the computational cost by replacing NLD analysis with NLS analysis requires that the dynamic load factors can be predicted. An interesting and useful investigation would be to study how these factors can be determined in an efficient manner.

The results presented in the thesis applies to structures designed with continuous steel beams as ties and moment stiff connections. If it is reasonable to validate, by using the finite element method, a structure's robustness that is constructed with rebar ties embedded in concrete, is an interesting question that remains unanswered.

References

- [1] Tim Verlaan. *The Downfall of British Modernist Architecture*. Apr. 2011. URL: <https://www.failedarchitecture.com/the-downfall-of-british-modernist-architecture/>.
- [2] John D. Oстераas. *Murrah Building Bombing Revisited: A Qualitative Assessment of Blast Damage and Collapse Patterns*. Tech. rep. ASCE, Nov. 2006.
- [3] Structural Engineering Blog. *Remembering, Learning, and Improving: The Oklahoma City Bombing and Prevention of Progressive Collapse*. 2016. URL: <http://www.sturdystructural.com/blog/remembering-learning-and-improving-the-oklahoma-city-bombing-and-prevention-of-progressive-collapse>.
- [4] Jonas Niklewski and Kristoffer Nygårdh. *Krav på robusthet i prefabricerade betongkonstruktioner*. Tech. rep. Lund, Sweden: Lunds Tekniska Högskola – Division of Structural Engineering, 2013.
- [5] Task Group 6.9. *Design of precast concrete structures against accidental actions*. Vol. 63. Lausanne, Switzerland: Fédération internationale du béton, 2012.
- [6] Institution of Structural Engineers. *Practical guide to structural robustness and disproportionate collapse in buildings*. Tech. rep. London, Great Britain, Oct. 2010.
- [7] Bo Westerberg. *Stomstabilisering – kurkompodium*. May 2016.
- [8] SIS. *Eurocode 1 – Actions on structures – Part 1-7: General actions Accidental actions*. Tech. rep. SS-EN-1991-1-7:2006. Swedish Standards Institute, 2006.
- [9] Department of Defence. *Unified facilities criteria (UFC) – Design of buildings to resist progressive collapse*. Tech. rep. UFC 4-023-03. Department of Defence, July 2009.
- [10] SIS. *Eurocode 2: Design of concrete structures – Part 1-1: General rules and rules for buildings*. Tech. rep. SS-EN 1992-1-1. Swedish Standards Institute, 2005.
- [11] Boverket. *Byggnaders robusthet – Vägledning för dimensionering av byggnader med hänsyn till olyckslast och fortskridande ras*. Tech. rep. (unpublished report). Boverket, 2017.
- [12] Boverket. *Boverkets konstruktionsregler, EKS 10*. Tech. rep. BFS 2011:10 med ändringar t.o.m. BFS 2015:6. Boverket, 2016.
- [13] Department of Defence. *Unified facilities criteria (UFC) – Structural engineering*. Tech. rep. UFC 3-301-01. Department of Defence, June 2013.
- [14] K. Marchand A. McKay and D. Stevens. *Dynamic Increase Factors (DIF) and Load Increase Factors (LIF) for Alternate Path Procedures*. Tech. rep. Protection Engineering Consultants, Jan. 2008.
- [15] Niels Saabye Ottosen and Hans Petersson. *Introduction to the finite element method*. Prentice Hall, 1992.

-
- [16] Niels Saabye Ottosen and Matti Ristinmaa. *The Mechanics of Constitutive Modelling*. Elsevier Ltd, 2005.
- [17] Steen Krenk. *Non-linear modeling and analysis of solids and structures*. Cambridge University Press, 2009.
- [18] Austrell P-E. et al. *CALFEM – a finite element toolbox*. Vol. 3.4. Lund, Sweden: Division of Structural Mechanics at Lund University, 2004.
- [19] Matti Ristinmaa. *Introduction to non-linear finite element method*. Tech. rep. (unpublished report). Lund, Sweden: Lunds Tekniska Högskola – Division of Solid Mechanics, May 2016.
- [20] Anil.K Chopra. *Dynamics of Structures, Theory and Applications to Earthquake Engineering*. Englewood Cliffs, New Jersey: Prentice Hall, 1995.
- [21] SIMULIA. *Abaqus 2016 Online Documentation*. Dassault Systèmes, 2015.
- [22] SIS. *Eurocode 3: Design of steel structures – Part 1-1: General rules and rules for buildings*. Tech. rep. SS-EN-1993-1-1. Swedish Standards Institute, 2008.
- [23] Nancy Baddoo and David Brown. *High Strength Steel*. 2005. URL: <http://www.newsteelconstruction.com/wp/wp-content/uploads/TechPaper/TechNSCSept15.pdf> (visited on 05/23/2017).
- [24] SIS. *Eurocode – Basis of structural design*. Tech. rep. SS-EN 1990. Swedish Standards Institute, 2010.
- [25] SIS. *Eurocode 1: Actions on structures Part 1-1: General actions – Densities, self-weight, imposed loads for buildings*. Tech. rep. SS-EN 1991-1-1. Swedish Standards Institute, 2009.
- [26] Pia Johansson. *Vibration of Hollow Core Concrete Elements Induced by Walking*. Tech. rep. Lund, Sweden: Lunds Tekniska Högskola – Division of Structural Engineering and Division of Engineering Acoustics, 2009.
- [27] Strängbetong. *Håldäck*. URL: <https://www.strangbetong.se/produkter/bjalklag/haldack/> (visited on 06/01/2017).

A VKR profile

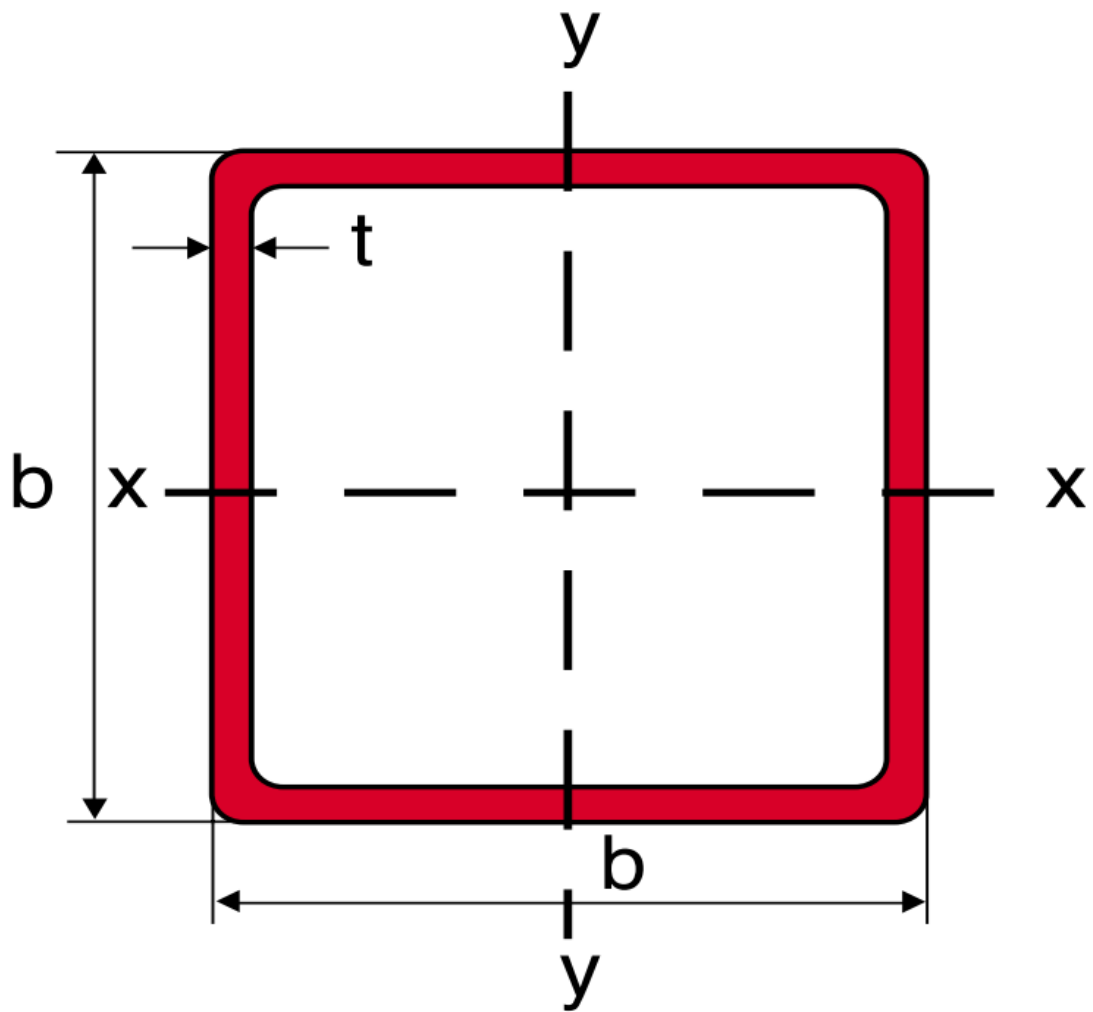


Figure A.1: Cross-section of a VKR-profile

B Example of a column-to-beam connection

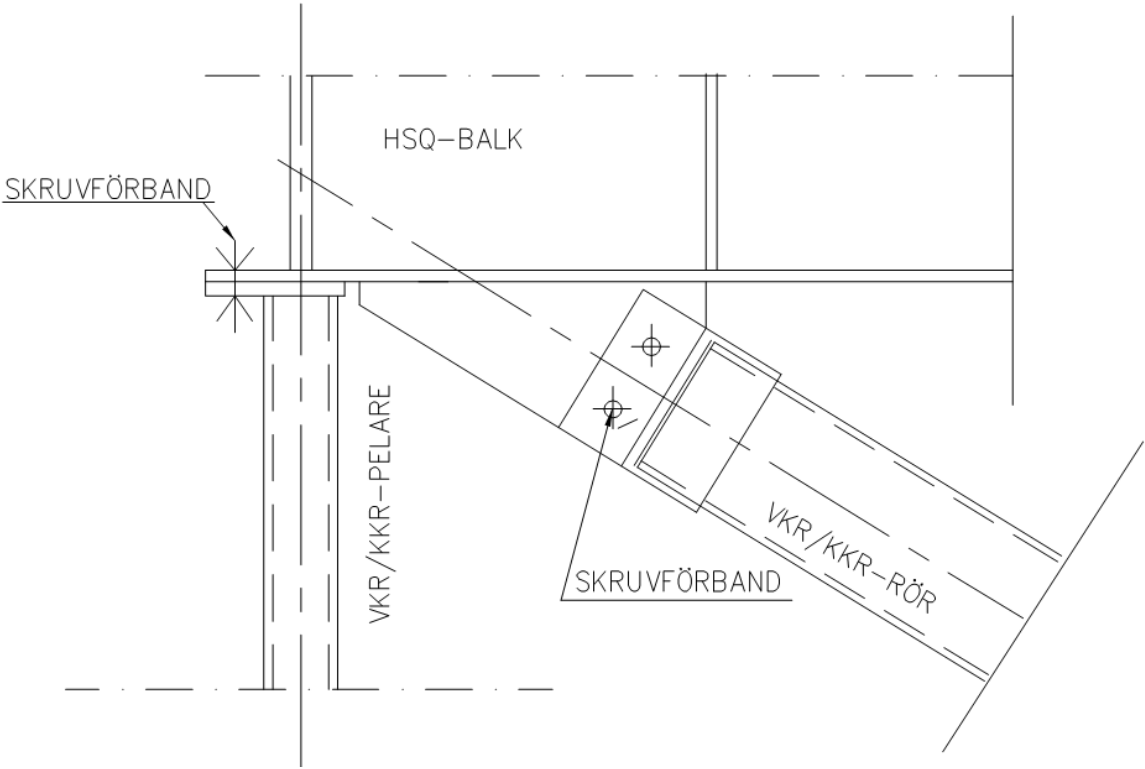


Figure B.1: Connection of a VKR-column to an HSQ-beam.

C Example of a hollow-core beam

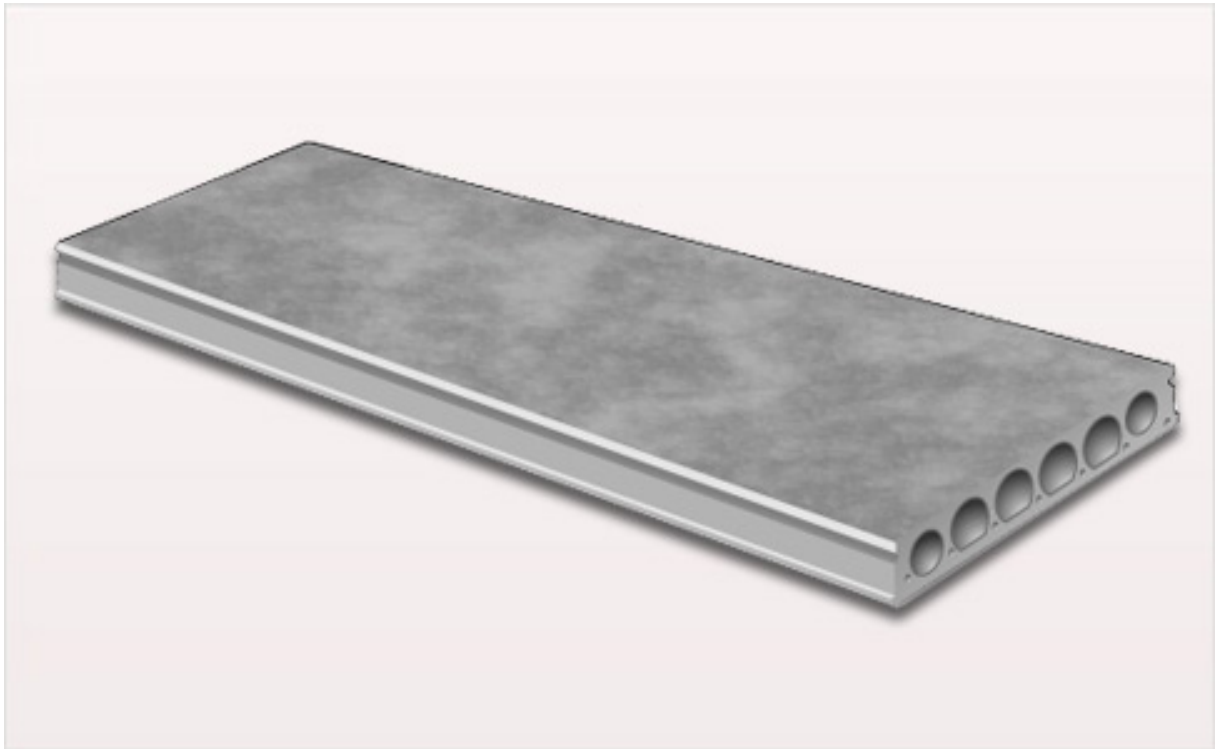


Figure C.1: Hollow-core beam, retrieved from [27].

D Strain limits for different steel classes

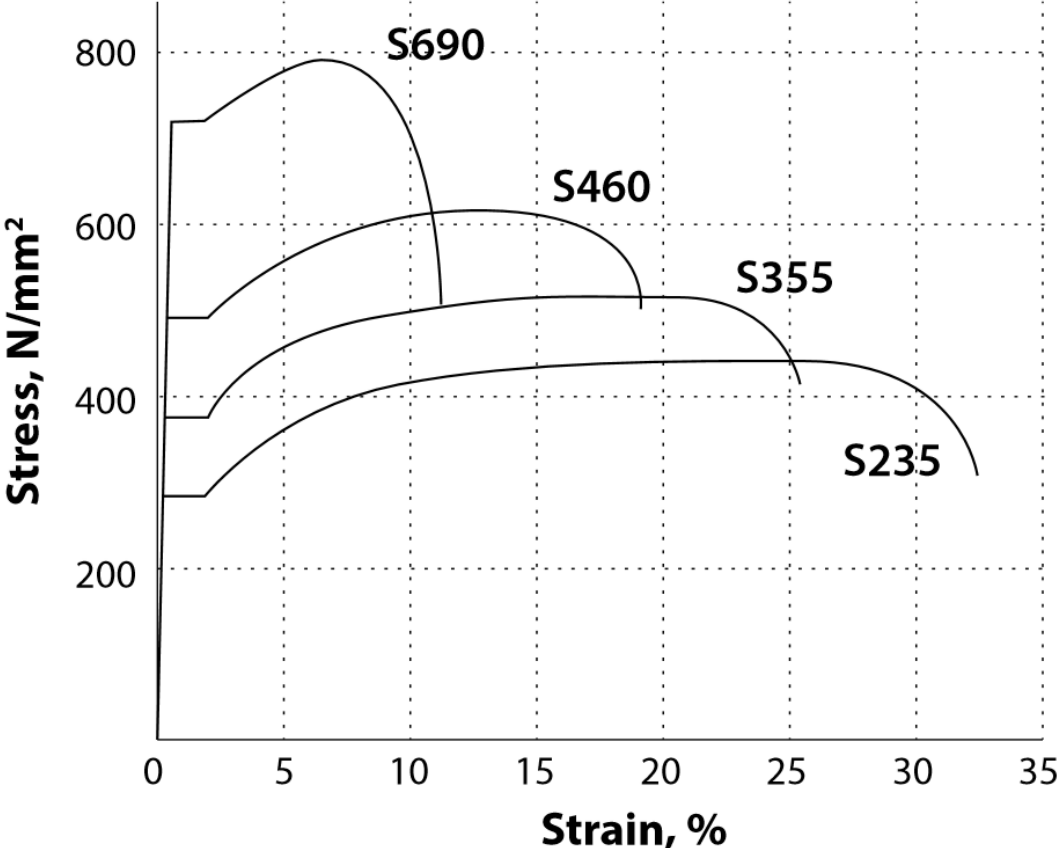


Figure D.1: Stress strain curve for different steel classes, retrieved from [23].

E UFC – risk category of buildings and other structures

Table E.1: Risk category of buildings and other structures, retrieved from [13].

Risk Category	Nature of Occupancy	Seismic Factor I_E	Snow Factor I_S	Ice Factor I_I
I	<p>Buildings and other structures that represent a low hazard to human life in the event of failure, including, but not limited to:</p> <ul style="list-style-type: none"> • Agricultural facilities • Certain temporary facilities • Minor storage facilities 	1.00	0.8	0.80
II	<p>Buildings and other structures except those listed in Risk Categories I, III, IV and V</p>	1.00	1.00	1.00
III	<p>Buildings and other structures that represent a substantial hazard to human life or represent significant economic loss in the event of failure, including, but not limited to:</p> <ul style="list-style-type: none"> • Buildings and other structures whose primary occupancy is public assembly with an occupant load greater than 300 people • Buildings and other structures containing <i>elementary school, secondary school, or daycare facilities</i> with an occupant load greater than 250 • Buildings and other structures containing <i>adult education facilities, such as colleges and universities</i>, with an occupant load greater than 500 • Group I-2 occupancies with an occupant load of 50 or more resident care recipients but not having surgery or emergency treatment facilities • Group I-3 occupancies • Any other occupancy with an occupant load greater than 5,000^a • Power-generating stations; water treatment facilities for potable water, waste water treatment facilities, and other public utility facilities that are not included in Risk Categories IV and V • Buildings and other structures not included in Risk Categories IV and V containing sufficient quantities of toxic, flammable, or explosive materials that: Exceed maximum allowable quantities per control area as given in Table 307.1(1) or 307.1(2) or per outdoor control area in accordance with <i>NFPA 1: Fire Code</i>; and are sufficient to pose a threat to the public if released.^b • <i>Facilities having high-value equipment, as designated by the AHJ</i> 	1.25	1.10	1.25

Risk Category	Nature of Occupancy	Seismic Factor I_E	Snow Factor I_S	Ice Factor I_I
IV	<p>Buildings and other structures designed as essential facilities, including, but not limited to:</p> <ul style="list-style-type: none"> • Group I-2 occupancies having surgery or emergency treatment facilities • Fire, rescue, and police stations, and emergency vehicle garages • Designated earthquake, hurricane, or other emergency shelters • Designated emergency preparedness, communication, and operation centers, and other facilities required for emergency response • Power-generating stations and other utility facilities required as emergency backup facilities for Risk Category IV structures. • Buildings and other structures containing quantities of highly toxic materials that: <ul style="list-style-type: none"> Exceed maximum allowable quantities per control area as given in Table 307.1(1) or 307.1(2) or per outdoor control area in accordance with NFPA 1, Fire Code; and are sufficient to pose a threat to the public if released.^b • Air traffic control tower (ATCT), Radar Approach Control Facility (RACF) and air traffic control centers unless the AHJ determines that the facility is classified as a non-essential facility and is not required for post-earthquake operations (i.e. minor facility, availability of an alternate temporary control facility, auxiliary outlying field, etc.). Contact the AHJ for additional guidance. • Emergency aircraft hangars that house aircraft required for post-earthquake emergency response; if no suitable back up facilities exist • Buildings and other structures not included in Risk Category V, having DoD mission-essential command, control, primary communications, data handling, and intelligence functions that are not duplicated at geographically separate locations, as designated by the using agency • Water storage facilities and pump stations required to maintain water pressure for fire suppression 	1.50	1.20	1.25
	<ul style="list-style-type: none"> • <i>Facilities having high-value equipment, as designated by the AHJ</i> 			

Risk Category	Nature of Occupancy	Seismic Factor I_E	Snow Factor I_S	Ice Factor I_I
V ^c	<p>Facilities designed as national strategic military assets, including, but not limited to:</p> <ul style="list-style-type: none"> • Key national defense assets (e.g. National Missile Defense facilities), as designated by the AHJ. • Facilities involved in operational missile control, launch, tracking, or other critical defense capabilities • Emergency backup power-generating facilities required for primary power for Category V occupancy • Power-generating stations and other utility facilities required for primary power for Category V occupancy, if emergency backup power generating facilities are not available <p>Facilities involved in storage, handling, or processing of nuclear, chemical, biological, or radiological materials, where structural failure could have widespread catastrophic consequences, as designated by the AHJ.</p>	1.0	1.50	1.50